Cape Peninsula
University of Technology

Variable Stroke Crank Shaft for an Internal Combustion Engine

by

Fareed Ismail

Thesis submitted in fulfilment of the requirements for the degree of

Master of Technology in Mechanical Engineering

in the Faculty of Engineering

at the Cape Peninsula University of Technology

Supervised by: Prof J. Gryzagoridis and Mr S. Saal

Cape Town
April 2012

DECLARATION

I, Fareed Ismail, declare that the contents of this dissertation/thesis represent my own unaided work, and that the dissertation/thesis has not previously been submitted for academic examination towards any qualification. Furthermore, it represents my own opinions and not necessarily those of the Cape Peninsula University of Technology.

Signed **Date**

ABSTRACT

Our planet is continuously being depleted of its natural resources leading to a need to conserve energy and the environment. One of the major energy consumers is the conventional internal combustion engine. Many attempts have been made to make these conventional internal combustion engines more efficient focussing mostly on the combustion side of the engine.

The focus of this study is on the modification of the reciprocating and rotating components of the sub-assembly of a conventional internal combustion engine. An in-depth review was carried out on the fundamentals of spark ignition internal combustion engines and savings on fuel consumptions.

A prototype single piston internal combustion engine was developed that can adjust its stroke length. Lengthening or shortening the stroke and simultaneously extending or retracting the connecting rod's travel distance, allows the internal combustion engine to function very efficiently consequently reducing the free space between the piston and cylinder head at TDC position. This allows the internal combustion engine to alter its power capability on demand whilst maintaining relatively high compression efficiency.

The method of altering the stroke length is achieved by manipulating gears situated internally and externally of the engine sub-assembly. The control of these eccentric gears lowers or lifts the crankshaft in a radial motion. The eccentrics also control the automatic extension or retraction of the connecting rod's travel distance.

The externally concentric gears control the mechanism that allows the internal combustion engine to change its capacity easily as adapted for automation. This study does not extend into the automation issues of the external mechanism.

The prototype engine that was built could not endure vigorous testing and it failed after running for a short while. The primary focus had been on the kinematics of the engine mechanism – and to show whether the idea was feasible. The engine passed the kinematics test but failed possibly due to dynamic loads. Investigating this requires measuring instantaneous temperatures from which peak pressures can be deduced. This was not done because it was outside the scope of the project.

ACKNOWLEDGEMENTS

I wish to thank:

- Prof J. Gryzagoridis, Sheldon Saal, Mark Kilfoil, Vicky Cain, Ian Noble-Jack, lecturing staff, workshop staff and students for their continuous support and assistance.

DEDICATION

I would like to dedicate this thesis to my lovely wife Firoza and children, Aatiqah, Amirah and Uwais.

TABLE OF CONTENTS

CHAPTER TWO: Model

CHAPTER THREE: Prototype detail design and manufacturing

CHAPTER FOUR: Testing and evaluation

LIST OF FIGURES

Chapter 1

Chapter 2

Chapter 3

Chapter 4

LIST OF TABLES

GLOSSARY

Terms/Acronyms/Abbreviations	Definition/Explanation
BDC	**Bottom Dead Center**
CO_2	**Carbon Dioxide**
C_p	**Specific heat capacity at constant pressure**
CPUT	**Cape Peninsula University of Technology**
CR	**Compression Ratio**
C_v	**Specific heat capacity at constant volume**
ECU	**Engine control unit**
FEA	**Finite Element Analysis**
I	**Current (electrical)**
ICE	**Internal Combustion Engine**
n	**Polytropic expansion index**
P	**Pressure**
R	**Resistance (electrical)**
SA	**South Africa**
T	**Temperature**
TDC	**Top Dead Center**
USA	**United States of America**
V	**Voltage (electrical)**
V	**Volume**
VVT	**Variable valve timing**
WOT	**Wide open throttle**

CHAPTER ONE

Introduction

1.1 Problem statement

There is a growing need to conserve energy and the environment. This has led to numerous design attempts to improve the fuel consumption and efficiencies of internal combustion engines. Many automotive manufacturers are looking at alternate fuels or Hybrids to stay abreast of the market for the future. Hybrid vehicles can reduce fuel consumption and green house gas emissions by 30 to 50 % without any change in vehicle class (Romm, 2005).

Litman (2005) stated that various incentives or transport regulations can be used to encourage the production, sale and use of alternative fuel vehicles, including diesel, liquid petroleum gas, methanol, ethanol, hydrogen and electricity. These fuels reduce per-km energy consumption and emissions.

Using alternate fuels such as hydrogen presents us with the greater risk of its storage needing to be kept safe during collision or accidents. A viable method of storing hydrogen onboard motor vehicles is still under development (Ross, 2006).

The main dangers with electric vehicles are electrocution, battery chemicals and accidents with pedestrians and cyclists due to their quietness. Electric vehicles have no tailpipe emissions but the overall emission impact on the electrical generation fuel has a detrimental effect to the environment as most power stations use fossil fuels. Most of these alternate fuelled vehicles are higher priced with low operating cost. The reduction in performance attributes such as speed, range and load carrying capacity still poses problems (Litman, 2005).

Turrentine and Kurani (2006) listed in their research the following reasons for buyers in the USA to pay more attention to fuel economy:

- Rising and volatile fuel prices over the past few years.
- New fuel economy instrumentation, which make users aware of their fuel consumption. The end user can now also properly budget for fuel consumption.
- Obvious effects of global climate change due in part to CO_2 vehicle emissions.

- Increased national dependence on imported oil. Some conservatives have recently embraced the idea of oil independence in the USA and therefore higher automotive fuel economy is a strategic national policy.

The research carried-out by Turrentine and Kurani (2006) found that in the USA most middle and upper middle-income households with children preferred to have at least one large enough vehicle to accommodate their children, friends, dogs, vacation baggage and large shopping items.

The South African Department of Transport research survey, 'Moving South Africa' **(**www.transport.gov.za/projects/msa/), shows that urban end users buy vehicles to commute between home and work and travel on average 20 km per trip. For such usage a low powered vehicle would suffice, as driving through heavy traffic only requires slow speeds and perhaps the use of an air-conditioner during summer. However what happens over weekends or holidays when people want to take the open road to their holiday destinations or simply to do end of month shopping? These low powered vehicles are normally small and do not have enough space to load a full months worth of groceries let alone children and friends. These vehicles are also not normally powerful enough to pull a caravan, trailer or carry lots of passengers. For this reason the average middle to upper middle-income family tend to purchase higher powered vehicles. These high powered vehicles are then often under utilised for daily commuting at higher operating costs to the detriment of the owner's finances and the environment.

This study will attempt to develop a prototype sub assembly of an internal combustion engine. This ICE will be able to vary the stroke length of the crankshaft as well as adjust the travelling length of the connecting rod simultaneously, so that the free space volume between the piston and cylinder head (clearance volume) when top dead center is reached remains constant. This concept will enable users to purchase a single vehicle which could switch over between a low powered or high powered vehicle, whilst in motion. This concept is in a nutshell a variable stroke engine.

1.2 Background to the research proposal

During January of 2007 an inventor, Mr C le Roux, approached CPUT with a sketch based on his patent (SA Patent Number 2006/06391) of how one can control the stroke and swept volume of a single cylinder spark ignition internal combustion engine.

The purpose of the invention was to change the throw of the crank shaft whilst the engine was in motion. This would alter the stroke. All conventional internal combustion engines have a fixed stroke crank shaft.

The intention of this design was also for the piston to maintain as far as possible its original top dead center position irrespective of the stroke variance being selected. For this to be made possible the connecting rod length must change as the crankshaft throw is varied. These changes will allow the power output to be varied.

The aim of Le Roux's (2007) design was not only to control a change in the stroke length of the crankshaft, but also to maintain the compression ratio by allowing the piston to travel closest to its original top dead center position. If one is to only shift the crankshaft down or up the pressure in the combustion chamber will drop and rise respectively. These would result in changes to compression ratio and everything else which depends on compression ratio, including fuel consumption.

In order to maintain constant compression ratio with the engine in continuous operation one would need to match the lowering or lifting of the crankshaft by simultaneously lengthening or shortening the connecting rod respectively.

1.2.1 Explanation of how the proposed design works

By manipulating various gears, a set of eccentrics (indicated as cams in figure 1.1) can control the position of the crankshaft and connecting rod. The ultimate goal is to lift and lower the crankshaft whilst simultaneously retracting or extending the travelling distance of the connecting rod. This process is intended to ensure that the piston reaches its original TDC position with every change in stroke. Being able to achieve this, efficient combustion can be maintained.

The stroke set worm gears control the lifting and lowering of the crankshaft by rotating gear set 3 which is fixed to the eccentric (cam 2) (see figure 1.1). The connecting gear (set gear 3) is fixed to an eccentric (cam 2) through which the crankshaft rotates. The second set of gear drives (gear drive 1X and 2X) controls the extending or retracting of the connecting rod via the eccentric (cam 1). This enables the two eccentrics (cam 1 and 2) to control the position of the crankshaft and piston head during stroke changes.

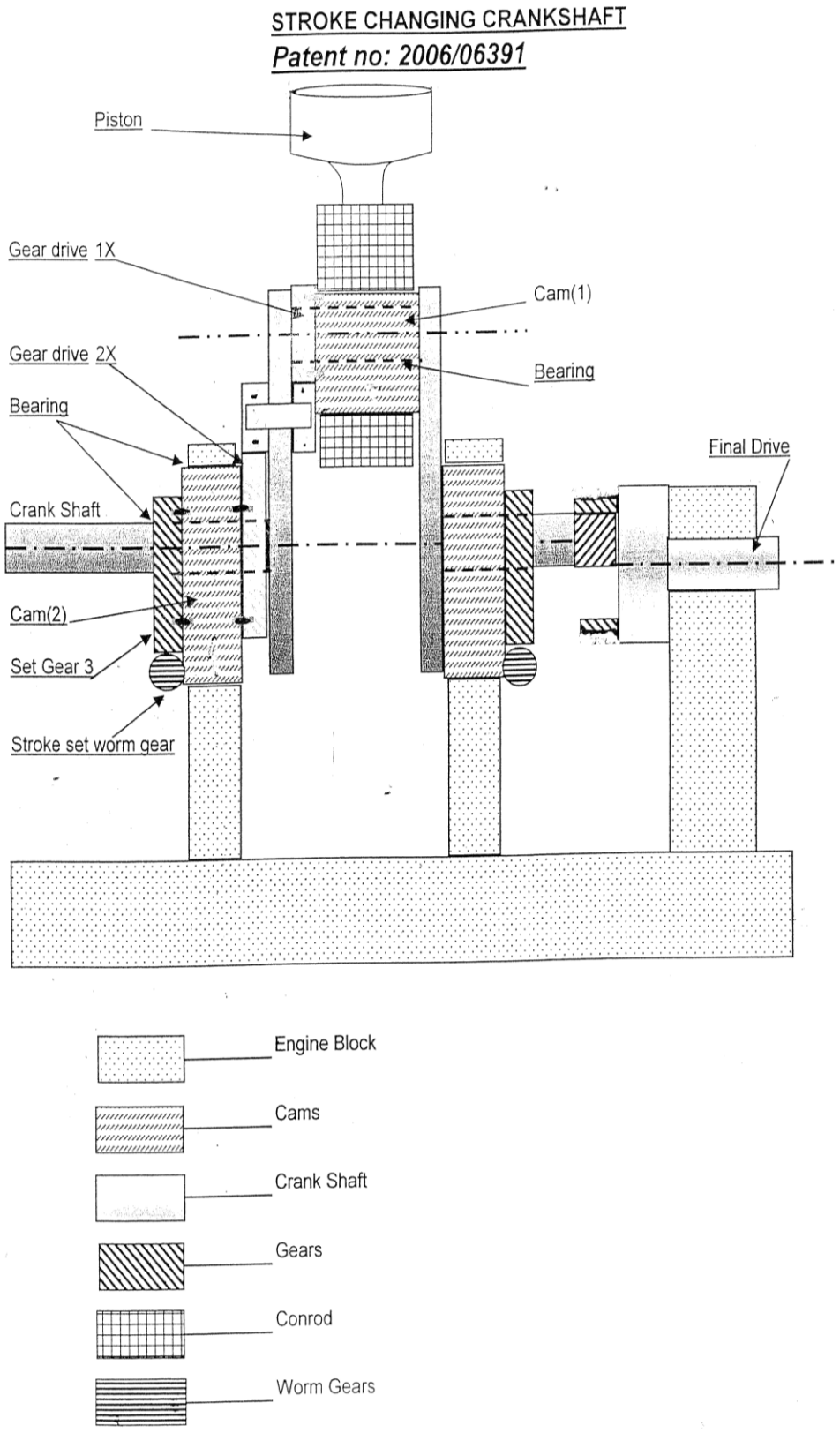

Figure 12.1: Proposed variable stroke engine

(Le Roux, 2007)

1.3 Aims and objectives

The aim of this project is to determine whether or not the proposed patented design will work, and if so, whether more power can be produced on demand from the same internal combustion engine. For the development to be successful it will be necessary to investigate various key objectives.

- Internal combustion engine basics.
    - In order to tackle this type of project it is important to understand the basics of a normally spark ignition single cylinder internal combustion engine. As this project aims to reduce the use of fuel consumption by developing smart stroke length controls it is also necessary to investigate different types of fuel saving devices.

- Design, computer aided simulation and build a physical model.
    - Modelling the design concept with the aid of CAD, different scenarios can be analysed.
    - Building a physical model based on the sketch will allow the basic concept of the design to be analysed. By understanding the working of the model interventions to facilitate or improve on the design can be included in the prototype.

- Modify a prototype engine.
    - It will be a modified spark ignition single cylinder internal combustion engine.

- Testing of the prototype.
    - Compare the vibration of a standard engine to that of the modified engine. This can be achieved by attaching an external drive mechanism such as a variable speed electric motor. The electric motor can be attached to the engine by means of sprockets and chain.
    - Measuring the amount of power drawn for the stroke range losses due to friction and imbalance can be determined.
    - Compression ratio will need to be measured and compared for the stroke range. Changes in compression ratio will affect the power produced.

1.4 Review of related literature

The literature review revealed that most research carried out on this topic covered only the shifting of the crankshaft and rarely accommodated the drop in pressure caused by the subsequent lowering of the piston head during stroke changes.

1.4.1 Fundamental principles of a spark ignition internal combustion engine

Tobolt et al., (1989) describe various important principles with regards to engine performance such as power, torque, friction, pressure, thermal efficiency etc.

At low engine speeds the engine torque is low but it increases rapidly as the engine speed increases. See figure 1.2.

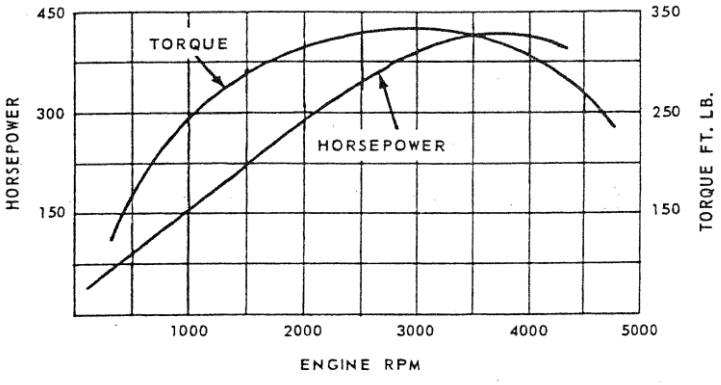

Figure 1.2: Typical power/torque curves
(Tobolt et al., 1989)

Experiments conducted by General Motors showed that with a compression ratio of 17 to 1 the maximum efficiency can be obtained from normal petrol (octane not specified by author). In order to determine a desired compression ratio the following formulae would apply $A = \frac{B}{C-1}$ where A=volume of the combustion chamber, B=displacement of the cylinder and C=desired compression ratio.

Volumetric flow rate is the rate at which a full charge of combustible fuel enters the combustion chamber. A theoretical full charge is practically impossible to achieve due to restrictions in intakes, throttling, valve timing and atmospheric pressure changes etc. The maximum volumetric efficiency is achieved when the internal combustion engine reaches its maximum torque (Tobolt et al., 1989).

The spark plug initiates fuel ignition normally just before the piston reaches TDC position during the compression stroke. Early ignition results in better efficiency reducing exhaust gas temperatures but increasing the level of oxides of nitrogen. Premature ignition is normally caused by high ignition advance, high compression ratio, high air density, insufficient engine cooling or high thermal load in the combustion chamber. The above can cause ignition even before the spark plug acts. This is known as knocking or pinging and can cause damage to the engine e.g. piston and valve burning and crankshaft failure (Van Bashuysen and Schafer 2006). The four stroke (spark ignition engine) is also known as the Otto cycle. (Figure 1.3 shows the basic operation.)

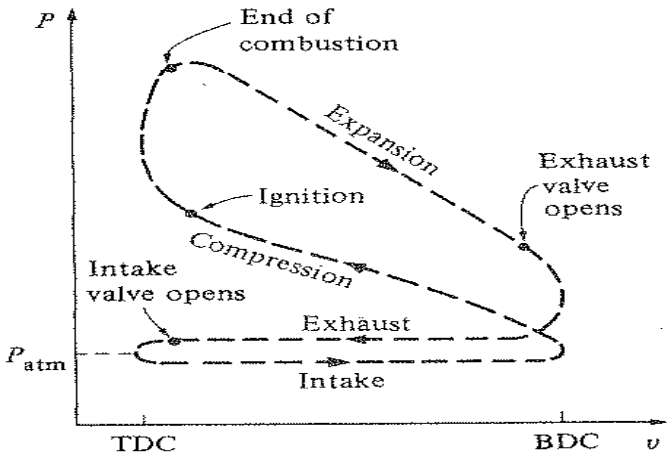

Figure 1.3: Typical four stroke curve
(Cengel and Boles)

1.4.2 Performance simulation of a four-stroke engine with variable stroke-length and compression ratio

Yamin and Dado (2003) published results from a performance simulation of a four-stroke engine with variable stroke-length and compression ratio. Experimental data was used for verification. The engine was based on a slider crank and inverted slider crank mechanism. Stroke length and compression ratio were controlled by shifting of a pivot point (O_2) mounted to a four-bar rocker arm which controls the starting and ending points of the two pistons (see figure 1.4). Several pivot point locations were considered.

A long stroke length is normally required for high engine loads. With longer stroke engines the speed of the engine is significantly lower. More torque can be produced with such engines. The components are normally heavier in design thus forcing the

engine speed to a minimum, in order to reduce centrifugal and out of balance forces. These types of engines are normally used in larger vehicles for transporting goods etc. With the shorter stroke engines the power to weight ratio of the vehicle and engine components are normally lower. This allows for quicker acceleration to obtain higher speeds in a shorter time period.

Once the stroke length is increased a drop in the compression is indicated. This drop in compression is desired in preventing engine knocking at high engine loads. If the compression is too high pre-ignition might occur. The problem with the compression being too low can cause unburnt fuel to expel through the exhaust valve thus making the engine less efficient and polluting the environment. At low power levels high compression ratio is aimed for good fuel combustion.

Normal fixed stroke internal combustion engines require the user to throttle the intake fuel-air mixture in order to vary the load capacity of the internal combustion engine. At full throttle the internal combustion engine is most efficient.

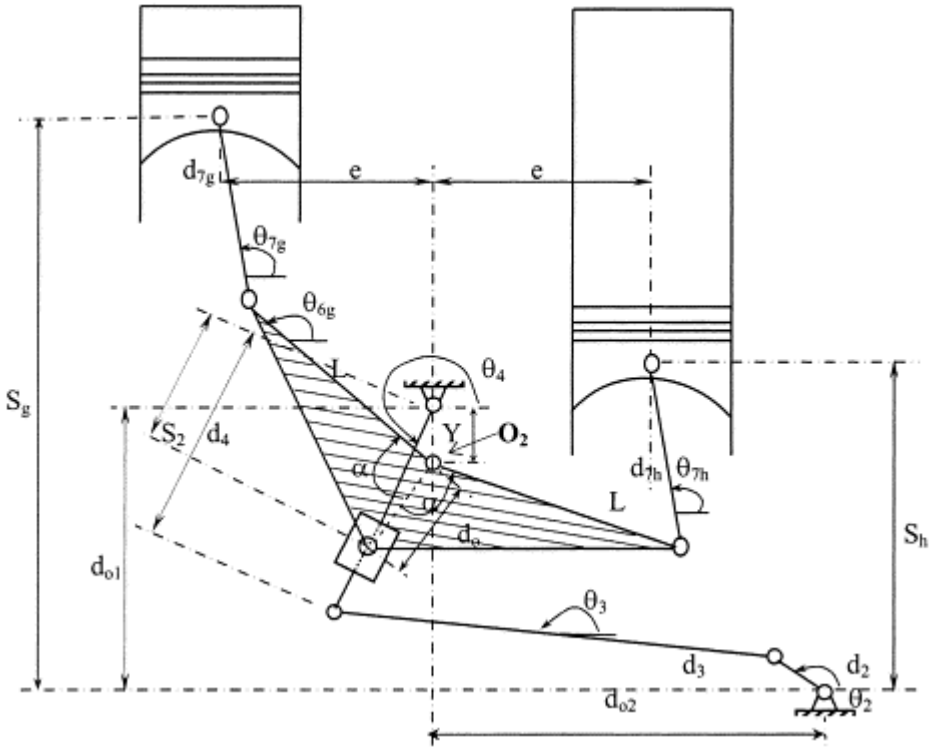

Figure 1.4: The variable-stroke mechanism
(Yamin and Dado 2003)

Yamin and Dado (2003) found that with a variable stroke engine an increase of 62 % in power was achieved over that of the ordinary constant stroke engine. Fuel consumption was improved but harmful emissions increased. The harmful emissions were more noticeable during long engine strokes with the lower engine compression ratios.

From the proposed design of Le Roux (2007) these harmful emissions can be taken care of as the high compression ratio can be constantly maintained throughout different crankshaft stroke variations.

1.4.3 Methods to improve efficiency of four stroke, spark ignition engines at part load

It is well known that four stroke spark ignition internal combustion engines have very poor part load efficiency caused by the flow restriction at the cross sectional area of the intake manifold due to throttling – see, for example Kutlar et al., 2005.

It is important to understand the various methods of improving fuel consumption and their effects. The ideal Otto air cycle has a thermodynamic efficiency of approximately 60 %. These values are based on a standard spark ignition internal combustion engine with a typical compression ratio of 9:1 or 10:1. This efficiency is a function of the compression ratio and specific heat ratio of air (C_p/C_v) (Stone and Ball 2004). This ideal Otto air cycle efficiency is higher than the ideal Otto fuel air cycle which is approximately 45-50 % efficient. The ideal Otto fuel air cycle is based on the function of the compression ratio and fuel/air ratio. Due to heat losses, incomplete combustion and leakages this efficiency drops by another 20% leaving the actual spark ignition internal combustion engine with a typical thermodynamic efficiency of approximately 35-40%. See Figure 1.5. These calculations of the actual spark ignition internal combustion engine are done with the engine at full load and the throttle wide open. Mechanical effects cause a 10% power reduction, resulting in 30-35% efficiency at the fly wheel.

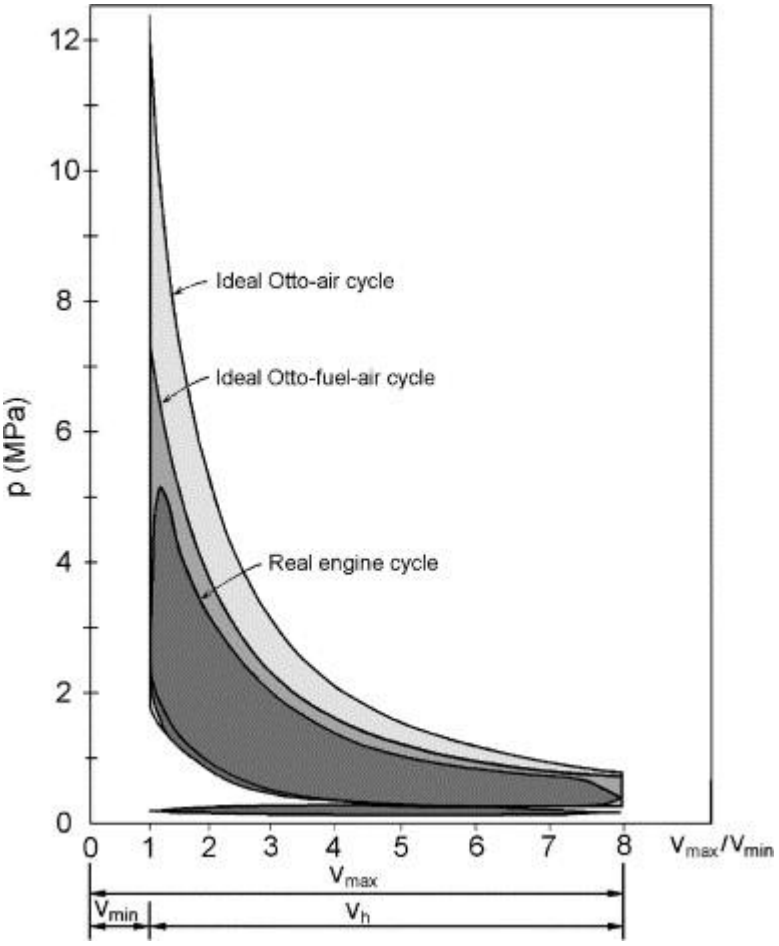

Figure 1.5: Comparative pressure–volume (*p–V*) diagram of standard ideal Otto air cycle, ideal Otto fuel–air cycle and real engine cycle.
(Kutlar et al., 2005)

Lower combustion speeds and cycle to cycle variations caused by partially closing the throttling valve leads to an increase in pumping losses. All fixed stroke length engines run most efficiently when they are moving at the vehicle designed cruising speed (WOT). When travelling slower the piston still has to travel the full length of the stroke even though a shorter stroke would have sufficed. Stratified charging and variable displacement engines show the most promise in decreasing fuel consumption.

The pumping loop from the p-V diagram is depicted on the lower part (see figure 1.6) showing the induction and exhaust strokes. The pumping loss effect at full load (WOT) condition shows that it is relatively substantially smaller when compared to a part load condition. The pumping losses increase relative to the upper part of the diagram, as seen in figure 1.6.

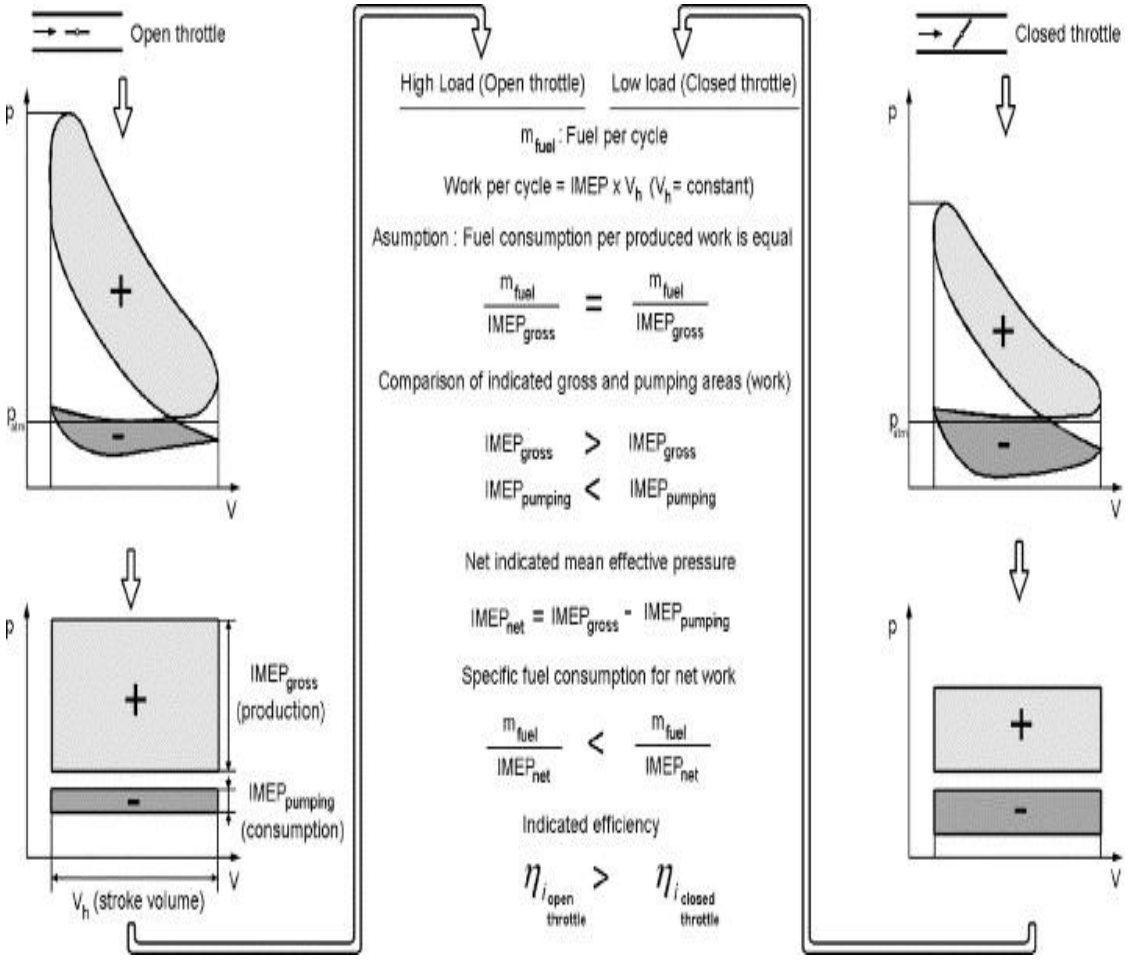

Figure 1.6: Schematic comparison of gross, pumping, net IMEP and their effect on indicated efficiency in high and low load conditions in SI engines.
(Kutlar et al., 2005)

It is suggested hence that if one can maintain the WOT condition and control the stroke of the crankshaft to compensate for the load variations, maximum engine efficiency can be maintained.

1.4.3.1 Variable valve timing

Variable valve timing can control the operation of the inlet or/and exhaust valves by allowing the lift or duration or timing to be changed while the engine is in operation. The camshaft controls the manipulation of the opening and closing of the valve action. The profile and position of the cam lobes can be optimised for a specific engine speed in a trade off which normally limits low-end torque or high-end power. Efficiency or power can be maximised by changing the cam profile.

At high engine speeds more air is required and therefore the inlet valves have to remain open for longer period during the duration of the stroke. At lower engine speeds the intake valve is required to be open at a lesser interval so that just enough fuel passes through for efficient internal combustion. This can be obtained by switching between different cam lobes and valve rocker arms. These additional rocker arms can normally be locked in place by a hydraulically operated pin forcing the corresponding cam lobe to further depress the valve during high load demands. This operation is controlled by the electronic control unit. Less energy is wasted during lower load demands thus minimising valve spring compression as the valve springs do not have to be compressed completely by the rocker arms. Variable valve timing provides the opportunity to reduce pollution and waste of un-burnt fuel at low engine speeds.

It can be seen clearly in figure 1.7 that the amount of work done is greatly reduced at part load compared to full load conditions. Less fuel is admitted into the cylinder at part load conditions therefore reducing pumping losses. Fluid friction can also be minimised by making the intake manifold surfaces smoother, reducing sharp edges and increasing flow area at valves by introducing multiple valve systems (Pulkrabek 2004).

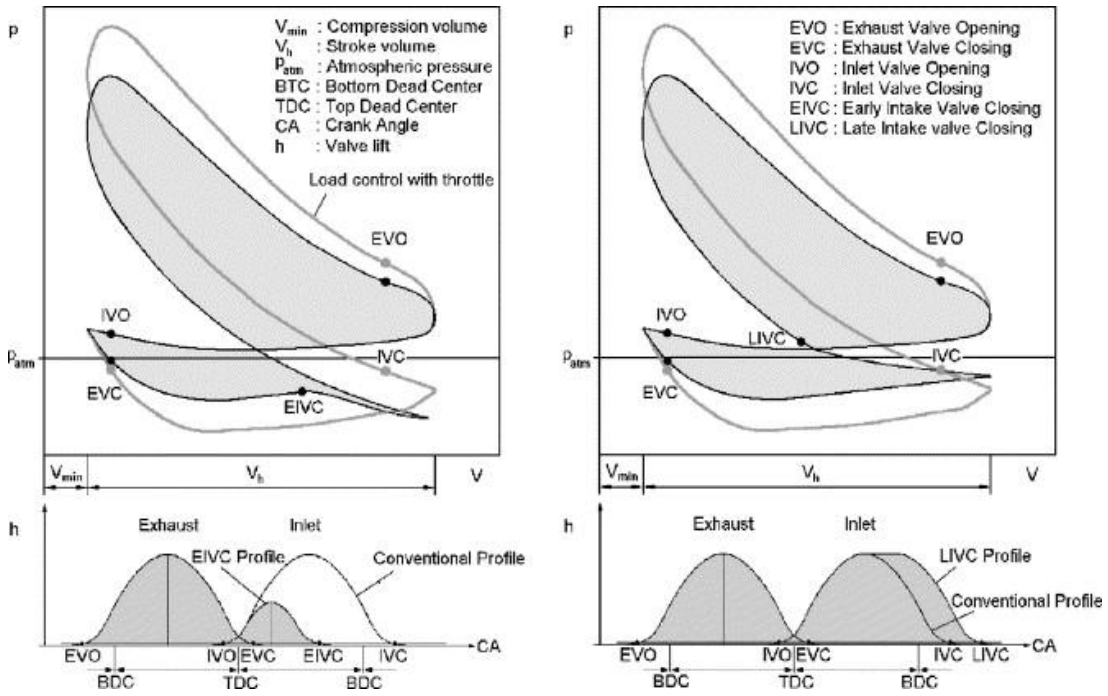

Figure 1.7: Comparison of load controls with and without VVT and Lift (early or late intake valve closing on p-V diagram)

(Kutlar et al., 2005)

1.4.3.2 Variable compression ratio

Variable compression ratio is the ability whereby one can vary the compression ratio while the engine is in operation. The car manufacturer Saab experimented and produced a promising prototype engine during 1990 which allowed the user to change the compression ratio while the engine was running (Pulkrabek, W.W. 2004). The increase or decrease in volume above the piston when at TDC can be achieved by lifting or lowering the cylinder head by means of a hydraulic system which is connected to the crankshaft. Petrol engines are limited to the amount of pressure the fuel/air mixture can handle before it detonates opposed to burning during the compression stroke. Knocking is normally experienced when the compression ratio is too high.

During part load conditions throttling causes a significant decrease in the intake pressure. This decrease in fuel/air mass flow causes a lower effective compression ratio leading to poor combustion conditions. Chances of creating the knocking effect are low due to the lower compression. The low compression caused by throttling is therefore ideally suited for variable compression ratios whereby the compression can

be increased for better fuel combustion. See figure 1.8. High engine loads require lower compression ratio while light engine loads require a higher compression ratio in order to burn the fuel more efficiently. A turbocharger or supercharger can be introduced to increase the inlet pressure.

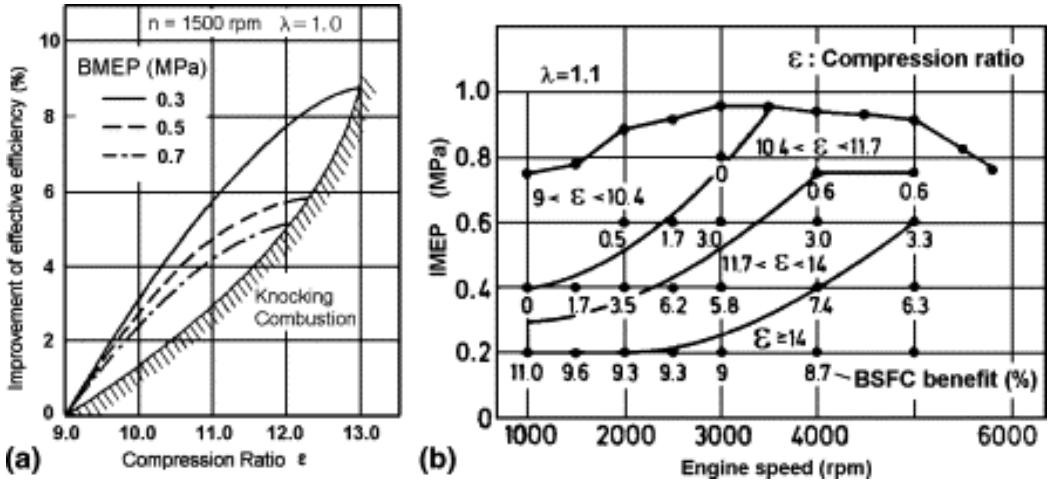

Figure 1.8: Increasing compression ratio with combustion knocking limit
(Kutlar, O.A., Arslan, H. and Calik, A.T. 2005)

1.4.3.3 Supercharging

A naturally aspirated internal combustion engine draws in air at atmospheric pressure and by introducing a supercharger or turbocharger increases the mass of charge in the cylinder at intake, resulting in increased volumetric efficiency. A supercharger compresses intake air which is forced into the combustion chamber. The increase in mass flow of oxygen combined with the fuel/air mixture creates an increase in the specific work cycle which in turn increases the power output of the engine. The compressed air to the engine is controlled by means of by-pass valves which are set to operate at different pressures as required by different engine loads. A supercharger or compressor is normally powered by the crank shaft of the ICE by means of belt, gear and shaft or chain-drive. The supercharger can also be powered by the exhaust gases which drive a centrifugal turbine, more commonly known as a turbocharger.

1.4.3.4 Variable displacement (Cylinder deactivation or cut off)

Variable displacement engines work on the principle of deactivating certain cylinders by stopping the fuel and controlling the valve lifters. In simple terms when full power is required at acceleration all cylinders are functioning but at cruising speed certain cylinders can be deactivated reducing the need to down throttle. The Mercedes S500

V8 was the first European vehicle on the market that made use of this type of technology as an optional extra (SAE, nd).

1.4.4 Experimental data of an internal combustion engine with variable stroke and compression ratio

Romano et al., (1990) published experimental data of an internal combustion engine with variable stroke and compression ratio. The experimental data was gathered from a modified Fiat 126 A10000-650 spark ignition internal combustion engine. The modification consisted of an eccentric fitted to the crankpin around which the big end section of the connecting rod rotates. With the rotation of the eccentric the stroke can be increased or decreased resulting in a drop or rise in the compression ratio respectively.

The results of the tests carried out consisted of P-V (pressure vs volume) diagrams, torque and power diagrams plotted against angular velocity at various positions of the eccentric. The tests were conducted at various speeds of between 1500 rpm and 3000 rpm. Throttle position was also varied. It was noted that the stroke lengths for the inlet, exhaust, compression and expansion parts of the cycle changed for each scenario. For example:

Case1: placing the eccentric at angle of 180° the inlet and exhaust strokes were longer than the compression and expansion strokes. The compression ratio was 7.5 and the displacement was 321 cm^3.

Case2: placing the eccentric at angle of 150° the inlet and exhaust strokes decreased with an increase in the compression and expansion strokes. The compression ratio was 7.63 and the displacement was 330 cm^3.

Case3: placing the eccentric at angle of 120° the inlet and exhaust strokes were smaller than the compression and expansion strokes. The compression ratio was 8.3 and the displacement was 341 cm^3.

Case4: placing the eccentric at angle of 210° the inlet and exhaust strokes were greatly increased reaching a maximum pressure of 4.2 MPa. The compression ratio was 7.88 and the displacement was 340 cm^3.

It was noted that there was a definite increase in power and torque through each preceding angle of placement of the eccentric. These changes indicate that the working condition of the internal combustion engine can be optimised by adapting each stroke to the load demands.

1.4.5 Balancing small engines

Hannah and Stephens (1975) state that a shaft carrying several eccentric masses will only be in static balance if the centre of gravity of the system lies on the axis of the shaft. If the shaft is rotated it should remain still in any position. When the parts start to rotate the off centre masses create centrifugal forces. The faster the shaft rotates the bigger the centrifugal forces become. Centrifugal forces acting out of balance can cause premature bearing failure or even shaft fatigue.

Wesbury (1951) published notes on how to balance small engines. In a conventional single cylinder internal combustion engine the piston head is linked to the crankshaft by means of a connecting rod. The connecting rod consists of a small end which is connected to the piston head by means of a gudgeon pin. The big end of the connecting rod is connected to the crankpin of the crankshaft. The small end, gudgeon pin and piston travel in a reciprocating motion within the piston sleeve. The big end, crankpin and counterweight crankshaft lobes move in a rotational manner about the main bearings of the crankshaft.

In an attempt to balance such an engine the types of motion described need to be separated as far as possible. The mass of counterweight required (opposing the crankpin) needs to be established in order to balance all the rotating parts. The following method can be utilised for balancing the crankshaft assembly.

- Weigh the piston complete with rings, gudgeon pin and retainers.
- Weigh the two ends of the connecting rod simultaneously. This can be achieved by using two spring balances and suspending the connecting rod horizontally. The small end can be taken as a reciprocating mass and the big end as rotating mass.
- The total reciprocating mass must be halved and added to the rotating mass.
- By placing the crankshaft between bearings on the main journals and suspending half the reciprocating mass from the crankpin it can be determined whether extra mass needs to be added or subtracted from the counter mass on the crankshaft (see figure 1.9).

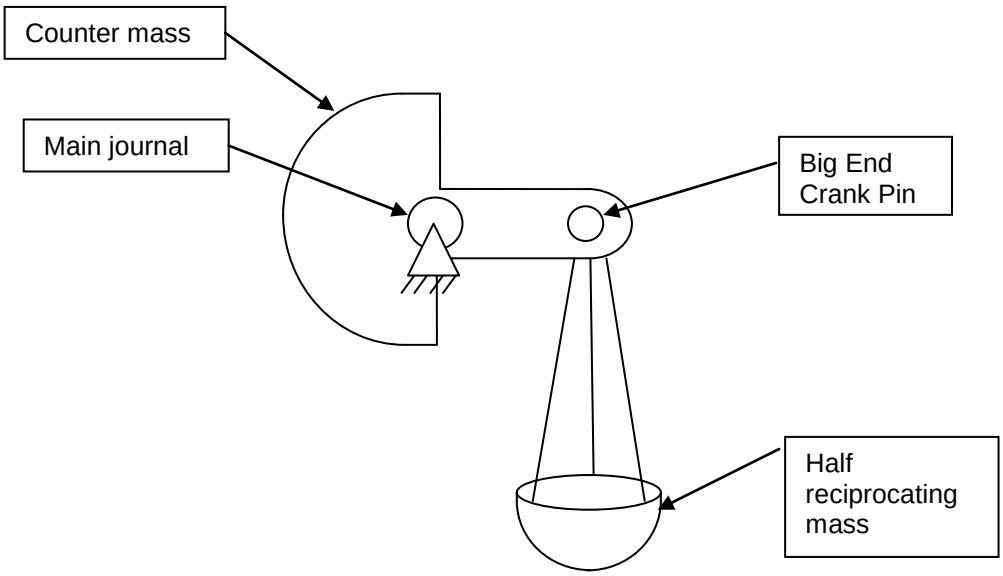

Figure 1.9: Crankshaft balancing

(Author's impression)

1.4.6 Internal combustion engine with variable ratio crankshaft

Moore (2002) patented an invention whereby the dwell point of a piston can be controlled thus improving connecting rod leverage. An eccentric is located on the crankpin which is controlled by a 1:1 gear ratio. The eccentric is set at a position perpendicular to the piston at TDC (see figure 1.10). During the combustion stroke the piston is forced downwards and the rotation of the eccentric tends to extend the crankpin lever in line with the central horizontal axis of the crankpin and main journals of the crankshaft. This extension thus grants extra leverage to the crankshaft (see figure 1.11).

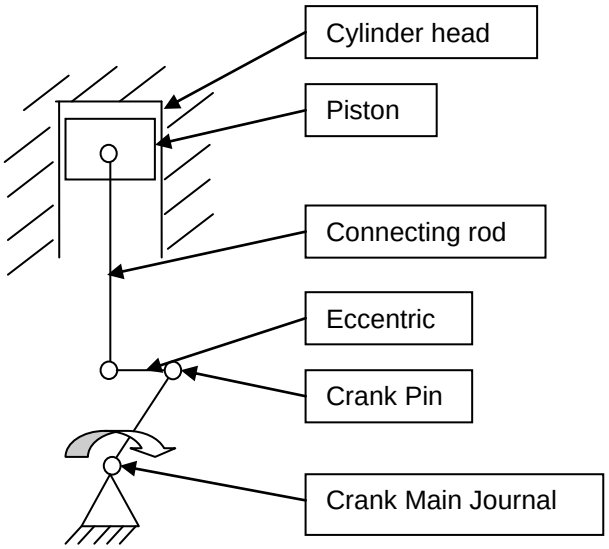

Figure 1.10: Piston at TDC

(Author's impression)

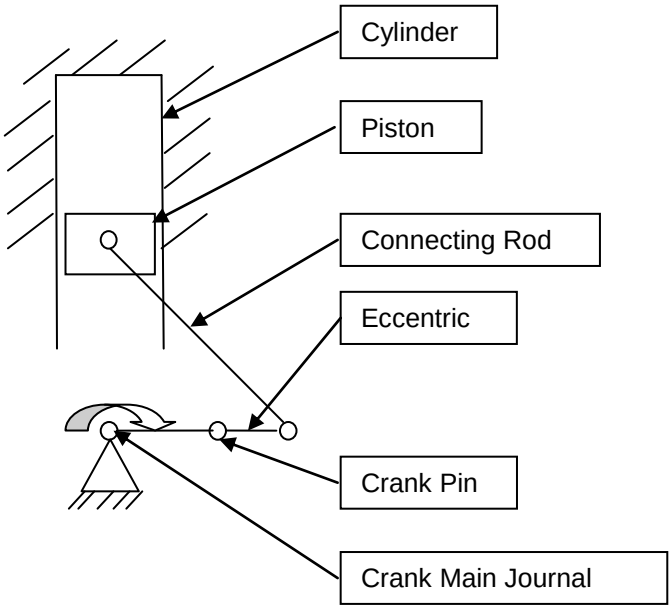

Figure 1.11: Piston halfway through combustion stroke

(Author's impression)

CHAPTER TWO

The physical model to achieve variable stroke

2.1 Model development

To understand the concept of variable stroke in an internal combustion engine it was necessary to build an affordable and effective model which could be manipulated in order to give an overview of the motion of the parts.

The model based on the initial design proposal of Le Roux (2007) was built using clear plastic for the main structure so as to allow the observation of all the parts when they are in motion. Steel gears were purchased from a local supplier and fitted to the two eccentrics to simulate the effect of the drive–mechanism. By controlling the lift and lowering the crankshaft (using the rack coupled to the gears connected to the eccentrics) the mechanism demonstrated the function of variable stroke (See Figure 2.1). The initial design proposal was to double the stroke length. To achieve this, the connecting rod had to be long and slender in order to avoid scraping on the bottom edge of the piston sleeve.

2.2 Explanation of how the model works.

The physical model of the Variable Crankshaft Mechanism is illustrated in figure 2.1. The eccentric 1 is allowed to rotate about its own center axis within the housing. The crankshaft main journal is located at an off-set within the eccentric 1. The crankshaft is allowed to rotate freely about its center axis within the eccentric 1. By controlling the rotation and fixing position of eccentric 1, the position of the crankshaft main journal can be determined. This will allow for the crankshaft to be placed lower or higher by the radial movement of the eccentric 1.

To control the position of the eccentric 1, the spur gear 1 is fixed to the eccentric 1. The spur gear 1 is driven by the rack which can be controlled externally from the engine block. When the eccentric 1 has been placed in its desired location it will remain fixed in that position until such a time as it is desired to change the stroke length.

Gear 1 is fixed to eccentric 1 with its axis located on the same axis of the crankshaft main journal. Meshing with gear 1 is an idler gear which transmits motion to gear 2. Gear 2 is fixed to eccentric 2. The axis of eccentric 2 rotates about the axis of the

connecting rod's big end. This allows the connecting rod to rotate at an off-set about the connecting rod's big end. The piston TDC and stroke length can now be set by the gear train ratio (1:2) and off-set position of the connecting rod big end and crankshaft main journal on the eccentrics.

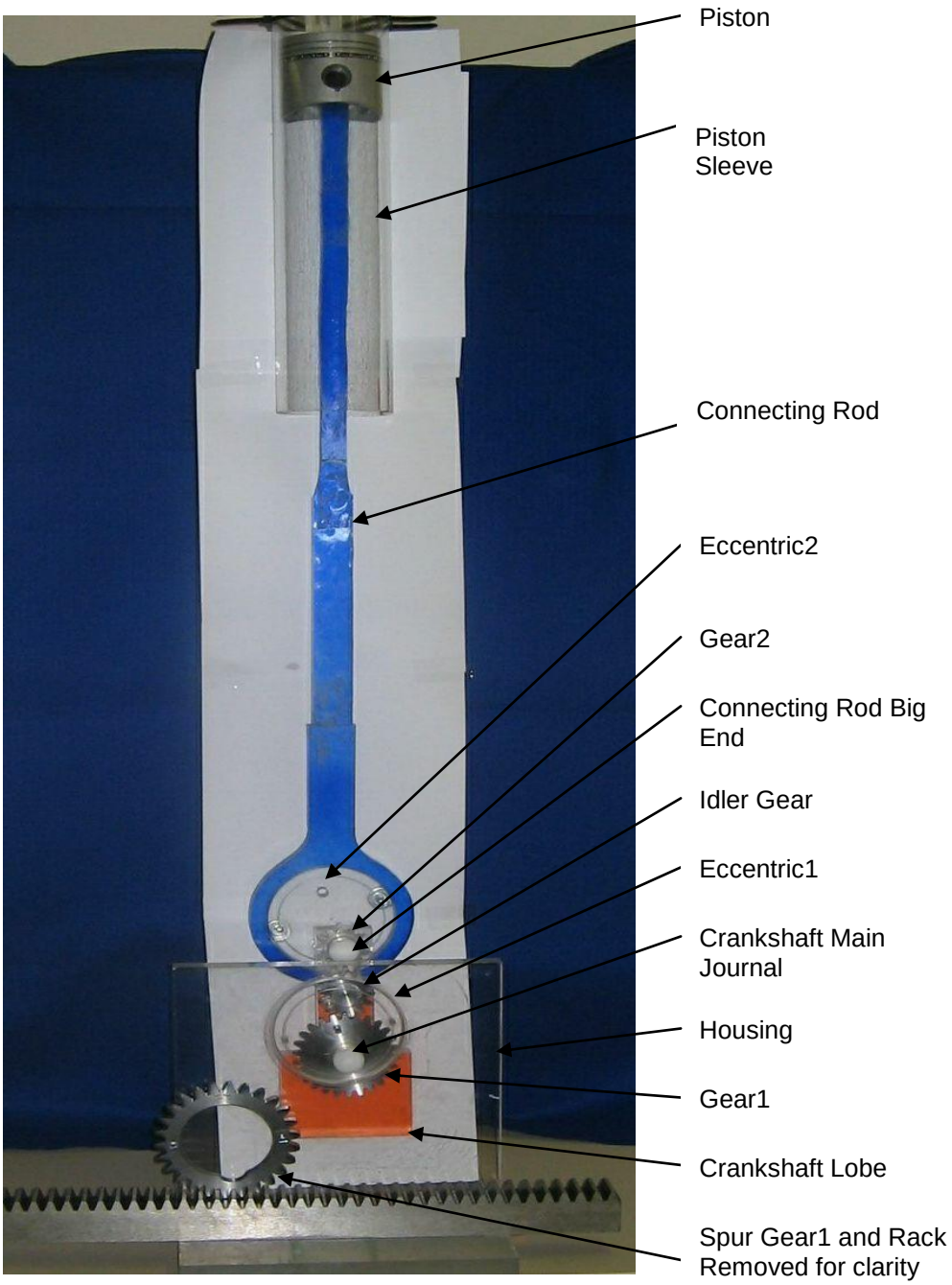

Figure 2.1: Physical Model of Variable Crankshaft Mechanism

2.3 Analysis of model

For the analysis of the model, three scenarios of crankshaft off-set positions were simulated, namely 0°, 90° and 180°. What would be of particular interest is to see if it is possible to maintain the original TDC position after moving through different stroke ranges. The original piston TDC should be maintained in order to supply sufficient high pressure for combustion.

2.3.1 Basic operation of model at eccentric off-set of 0°

With the eccentric 1 positioned and fixed at its uppermost 0° position the total stroke length attainable was 137mm. This determined the shortest stroke available from this model. In this position the crankshaft is at its highest position and the connecting rod at its lowest position when the piston is at TDC. This position was considered as the datum to which all other crankshaft off-set positions were compared to (see figure 2.2).

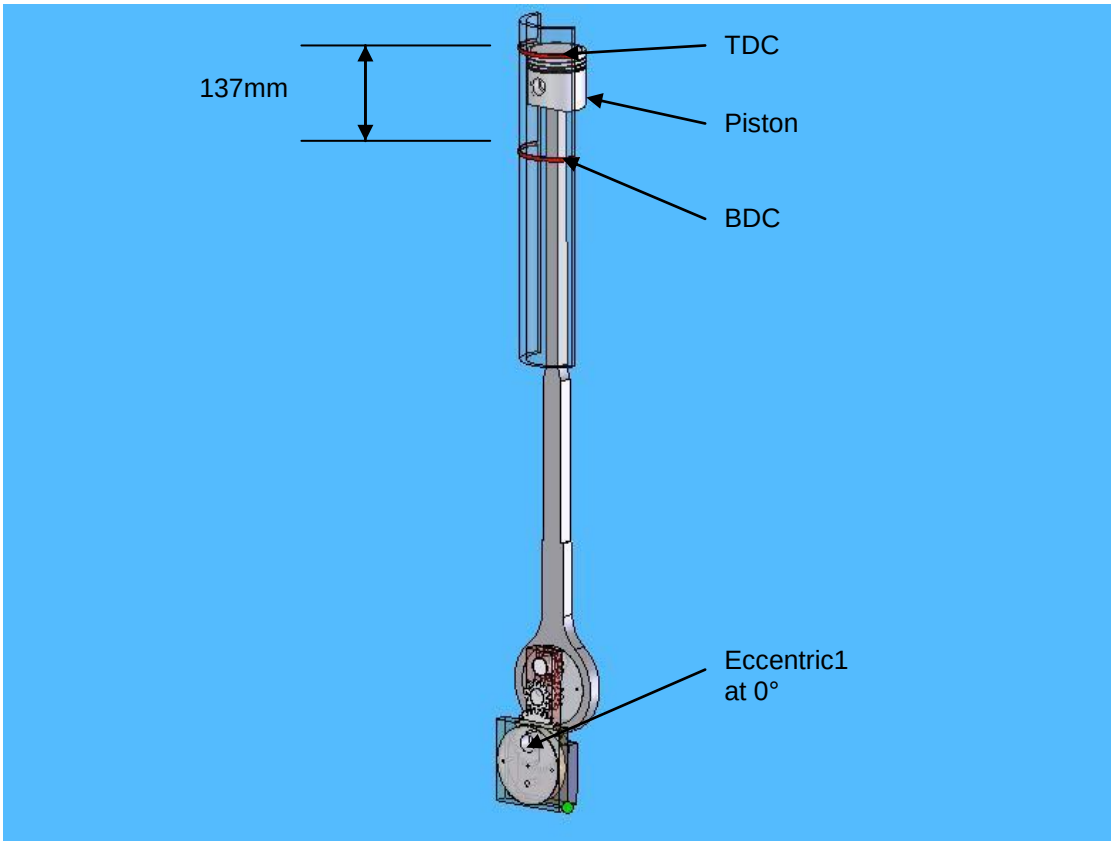

Figure 2.2: Model at 0° off-set

2.3.2 Basic operation of model at eccentric off-set of 90°

With the eccentric 1 positioned at its outermost 90° position the total stroke length attainable was 253mm. This is almost double the original stroke length of the base line (the original stroke length - i.e. that of the datum position). The piston has pushed up passed the original base line TDC at the 0° off-set position by 28,4mm (see figure 2.3).

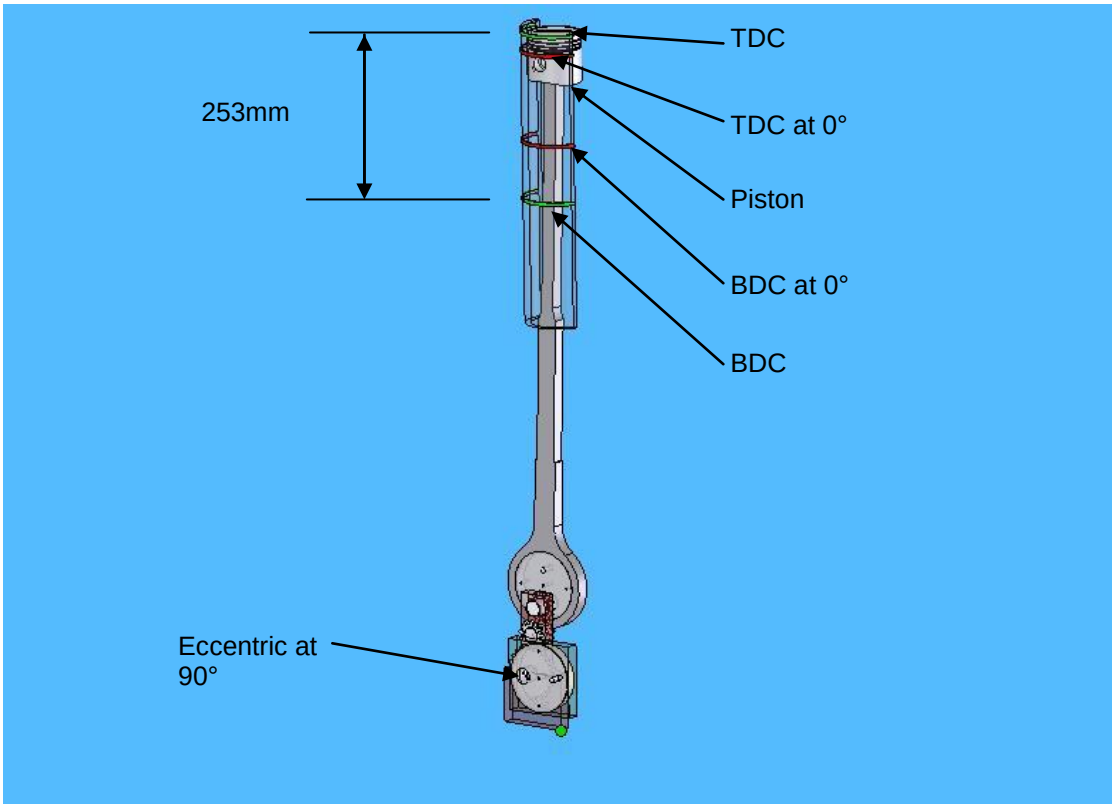

Figure 2.3: Model at 90° off-set

2.3.3 Basic operation of model at eccentric off-set of 180°

With the eccentric 1 positioned at its lowest position the total stroke length attainable was back to 137mm. The piston drop from the original TDC (0° position) was too great for this position to work. The compression ratio was too small for effective combustion (see figure 2.4).

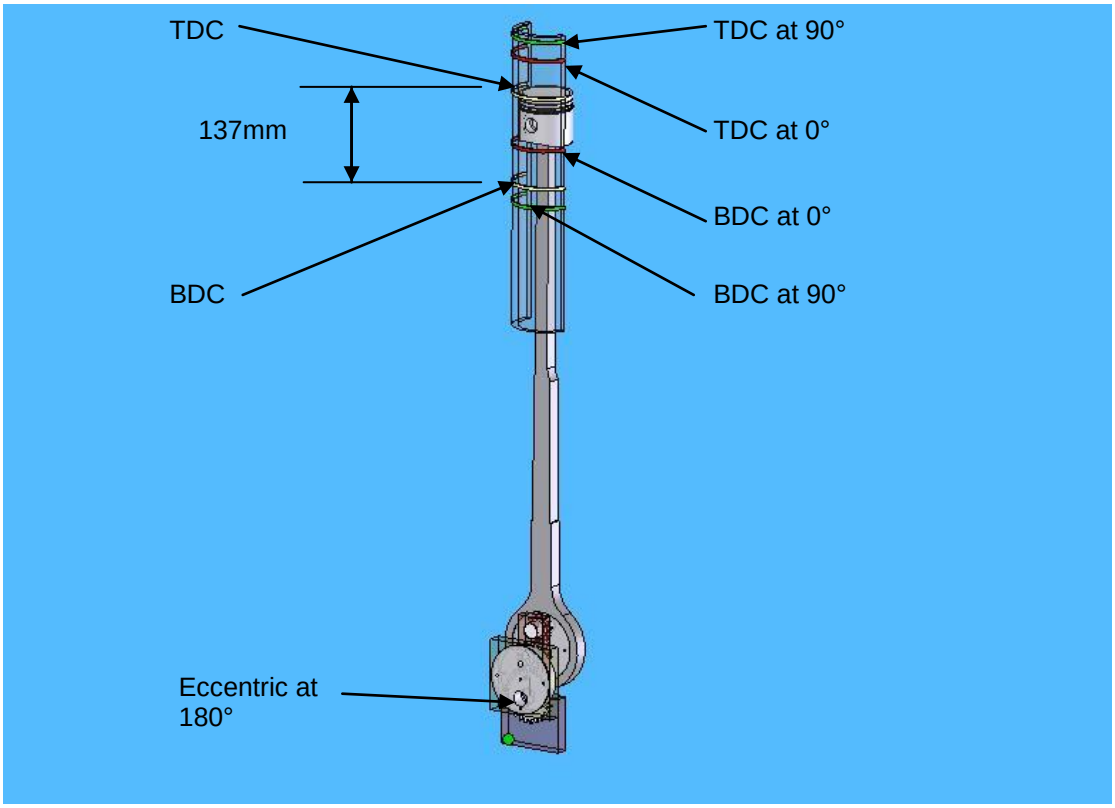

Figure 2.4: Model at 180° off-set

2.3.4 Crankshaft displacement at 5° Intervals from 0° through to 90°

During the analysis of the model it was found that the most favourable working condition would be to displace the crank shaft through a 90° rotational displacement. The graph below illustrates the increase in stroke length and piston position at 5° intervals. The 0-0 line represents the datum line. This would be the ideal TDC position for the piston to return to after every stroke. It is clear that there is an increase in the stroke length (SL) but the TDC position is not desirable as it moved above the horizontal datum (0-0 line). The piston in this case would be slamming into the cylinder head of the engine (see figure 2.5).

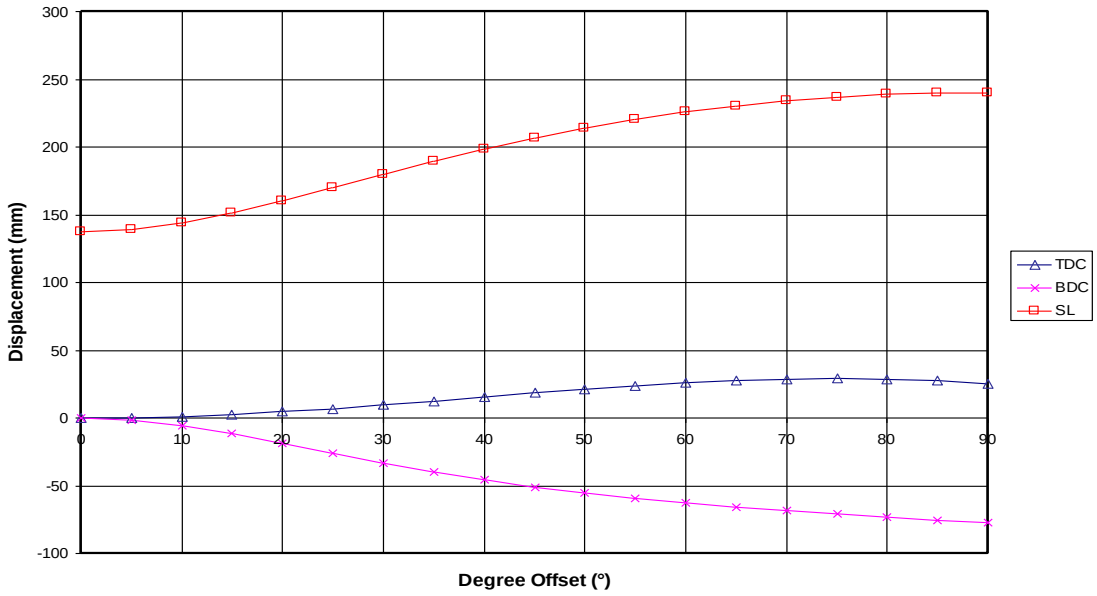

Figure 2.5: TDC and BDC positions, stroke length vs. offset

2.4 Design Shortcomings of the Model

The connecting rod will need to be long and slender to avoid scraping on the bottom edge of the piston sleeve when the crankshaft has been positioned at 90° to its outermost position. Compared to conventional internal combustion engines, with similar capacities, this connecting rod is approximately 4 times longer than normal. Failure caused by buckling could occur.

By rearranging/changing the gear train and eccentrics, the excessive horizontal movement of the big end of the connecting rod can be greatly reduced. Movement of the unbalanced masses through a relatively large distance from the axis of rotation could lead to bearing failure caused by out of balance centrifugal forces. By changing the gear and eccentric design these out of balance forces can be minimised.

The piston TDC varies continuously with the change in crankshaft position. This will cause a reduction in the compression ratio which would lead to a low combustion pressure during ignition. By changing the gear and eccentric ratio this problem can be minimised.

The results from the analysis of the model clearly indicate that to increase the capacity of the internal combustion engine by almost 100% was over ambitious.

CHAPTER THREE

Prototype Detail Design and Manufacturing

3.1 Introduction

The internal combustion engine burns fuel in the volume between the free space of the cylinder head known as the clearance volume and top of the piston head. The combustion process forces the piston to move within the cylinder in a linear motion in a reciprocating engine. The extensity of the combustion is based on the compression ratio of the engine which is caused by the travelling distance of the piston from bottom dead centre to top dead centre. It is important to maintain a high compression ratio at all times. In a conventional internal combustion engine these maximum travel points are fixed; namely bottom and top dead centres. In the prototype internal combustion engine the top dead centre can shift only by a small amount. Most of the variation when changing the length of the stroke takes place at the bottom dead centre. This is desirable in that the maximum compression ratio can be maintained regardless whether the crankshaft stroke length has been extended or shortened.

The model sub assembly unit was designed so that it can be incorporated into an existing Briggs and Stratton 10hp ICE. Considerable changes were introduced to make the prototype a more feasible solution to what was experienced with the model. A stroke variance of 12% was considered for the prototype. This meant that the connecting rod could retain its original standard length without the problem of scraping on the bottom edge of the piston sleeve. The idler gear was also removed by reconfiguring the gear train. This meant that the gears were now spaced closer to one another resulting in a reduction in the magnitude of the centrifugal forces.

3.2 Workings of the Prototype

The eccentric 1 is allowed to rotate about its own axis within the housing (refer to figure 3.1). The crankshaft main journal is located off-set within the eccentric 1. The crankshaft is allowed to rotate freely about its axis within the eccentric 1. By controlling the rotation and fixing the position of eccentric 1, the position of the crankshaft main journal can be determined. This will allow for the crankshaft to be placed lower or higher by the radial movement of the eccentric 1. To control the position of the eccentric 1, gear 1 is fixed to the eccentric 1. Gear 1 can be driven by the rack. The rack is suspended by hangers which move in unison with the eccentric

1 during adjustment. The rack can be controlled externally from the engine block by means of jacking screws, hydraulics, also electrically (for further development). When the eccentric 1 has been placed in its desired location it remains in that position until such a time when it is desired to change the stroke length. Gear 1 is fixed to eccentric 1 and its axis is located on the same center axis of the crankshaft main journal. Gear 1 mesh with gear 2. Gear 2 is fixed to eccentric 2. The eccentric 2 axis rotates about the axis of the connecting rod's big end. This allows the connecting rod to rotate off-set about the connecting rod's big end. The piston's TDC and stroke length can now be determined by the gear train ratio (1:2), the off-set position of the connecting rod's big end and crankshaft's main journal on the eccentrics.

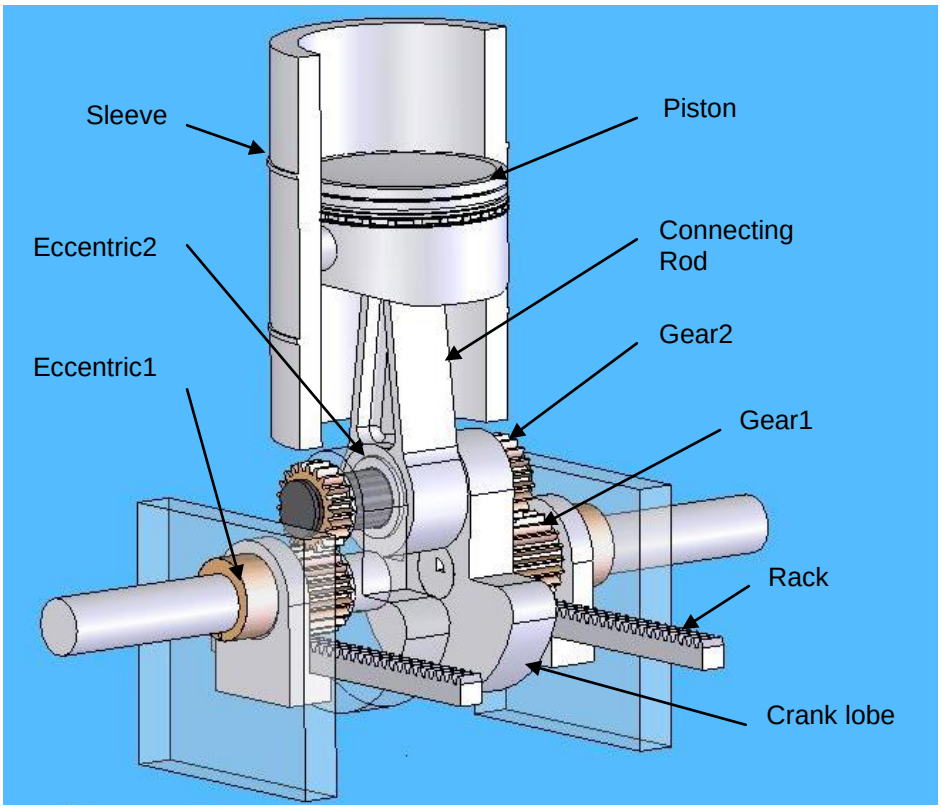

Figure 3.1: Proposed Prototype

3.3 Final Concept of the Prototype

One apparent problem with this proposed prototype was that it would be difficult to seal the rack when it enters the housing of the sub assembly. The rack would also be moving up and down with the rack hanger complicating the idea of having to adequately seal the mechanism. Further complications that could arise is that gear 2 can become worn and start floating on the wider gear 1. This would cause gear 2 to smash into the track with catastrophic results (see figure 3.1).

It became apparent that the rack mechanism had to be removed and placed on the outside of the sub assembly housing. This new challenge was quickly overcome by attaching another gear 3 on either side of the housing externally. This gear 3 would be fixed to the eccentric 1. This set of gears 3 will also rotate concentric with the hole in the housing eliminating the need for a travelling rack hanger. See figures 3.2 and 3.3 for final concept of the prototype.

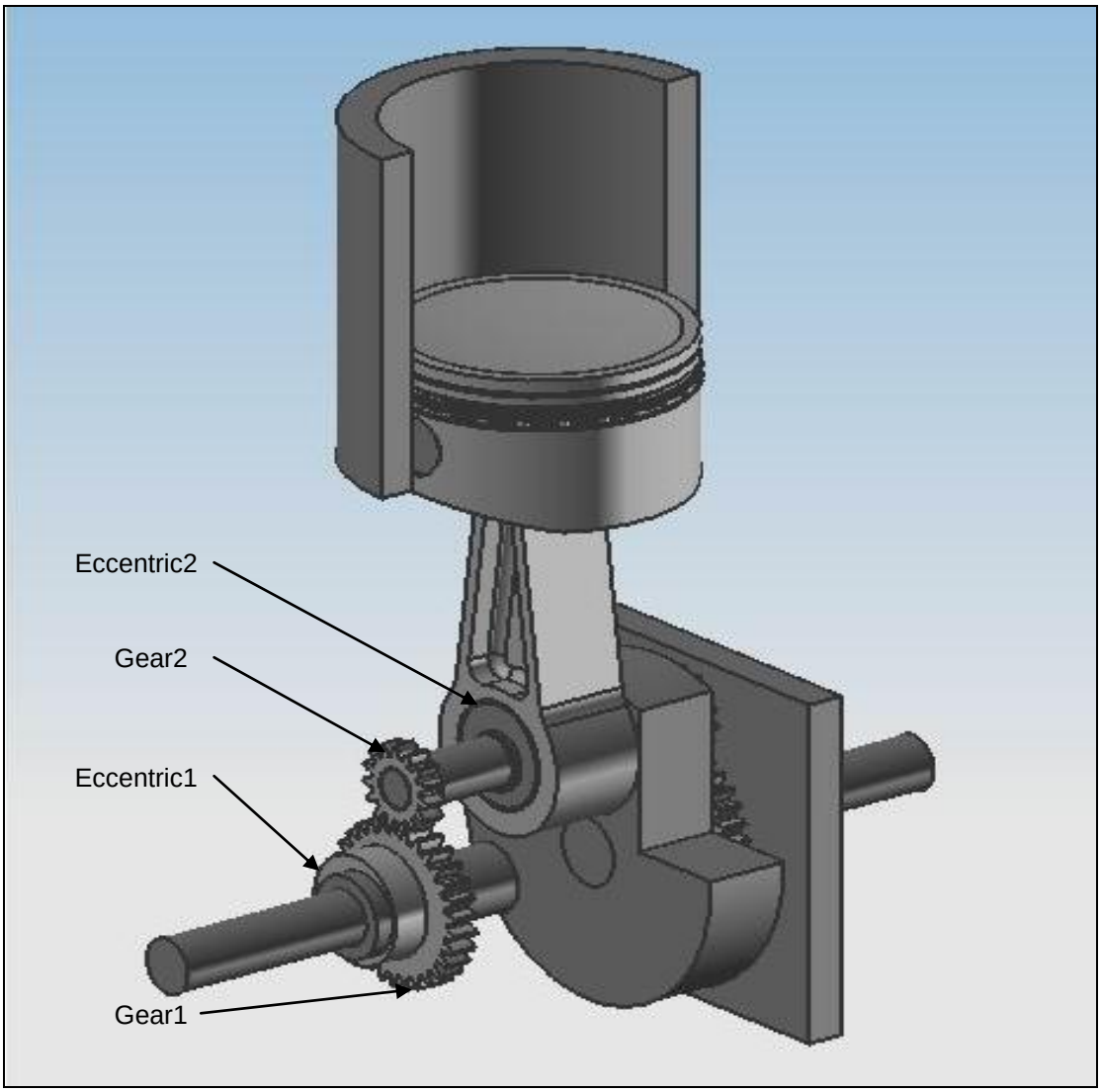

Figure 3.2: Final Concept (housing and gears 3 omitted for clarity)

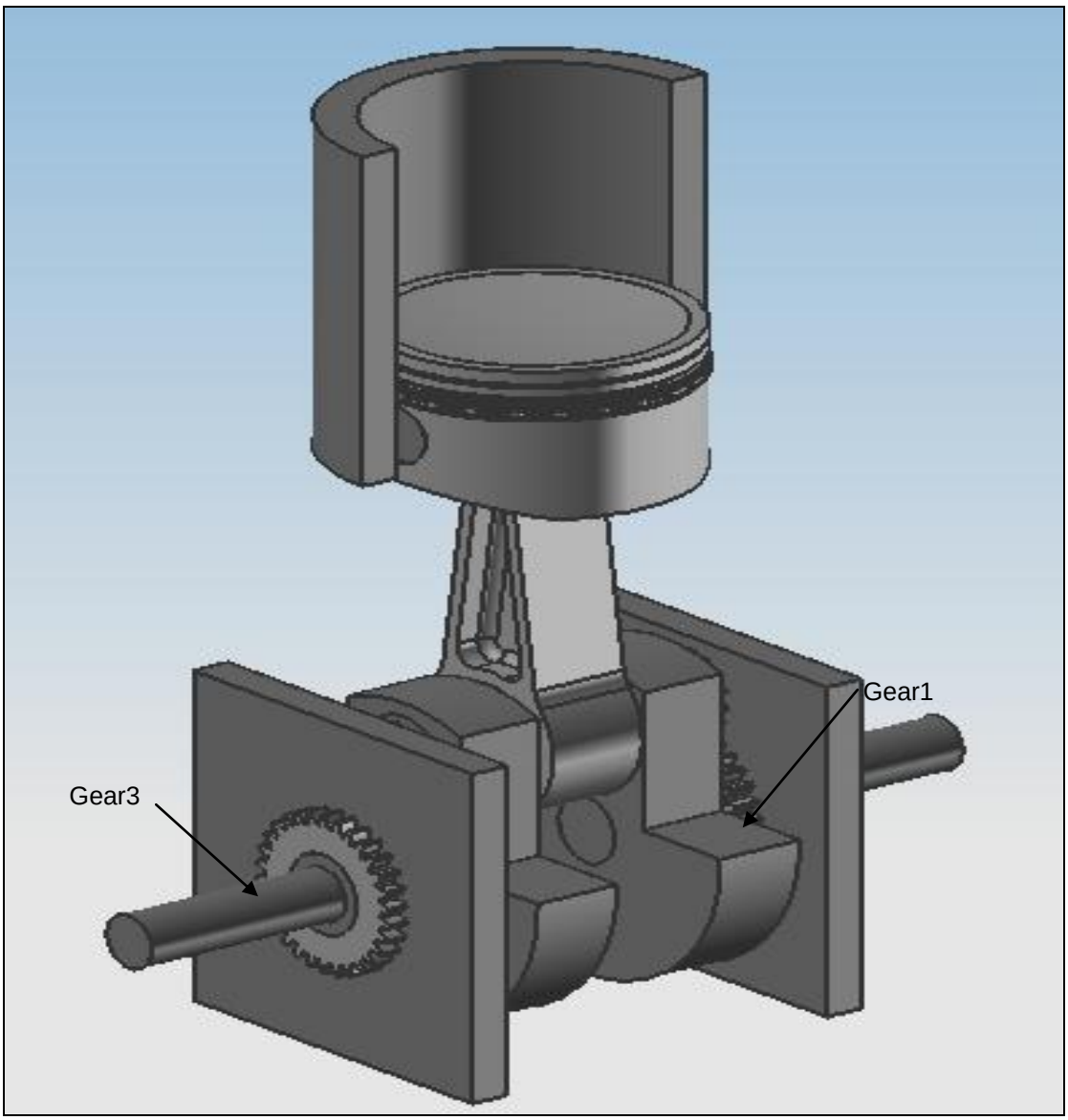

Figure 3.3: Final Concept of the Prototype

3.4 Operation of the Prototype

In order to test the concept a prototype (Briggs and Stratton standard 10HP Intec engine) was employed. The important areas to focus on were the swept volume (V_s) and clearance volume (V_c).

The following dimensions were obtained for this internal combustion engine.

- Original engine capacity, V_S = 305 cm^3
- Bore diameter, d = 7.92 cm
- Original stroke length, L_S = 6.17 cm

$$V_S = \frac{\pi}{4} \times d^2 \times L_S + V_c$$

$$\therefore V_c = V_S - \frac{\pi}{4} \times d^2 \times L_S$$

$$V_c = 305 - \frac{\pi}{4} \times 7.9248^2 \times 6.1722$$

$$V_c = 305 - 304.443$$

$$V_c = 0.55665 cm^3$$

For the prototype engine the swept volume must be added to the clearance volume in order to determine the engine's capacity at different stroke positions. Figures 3.4 and 3.5 depict the variable stroke prototype concept showing the positions of the eccentrics at a 0° off-set for the main journal eccentric 1.

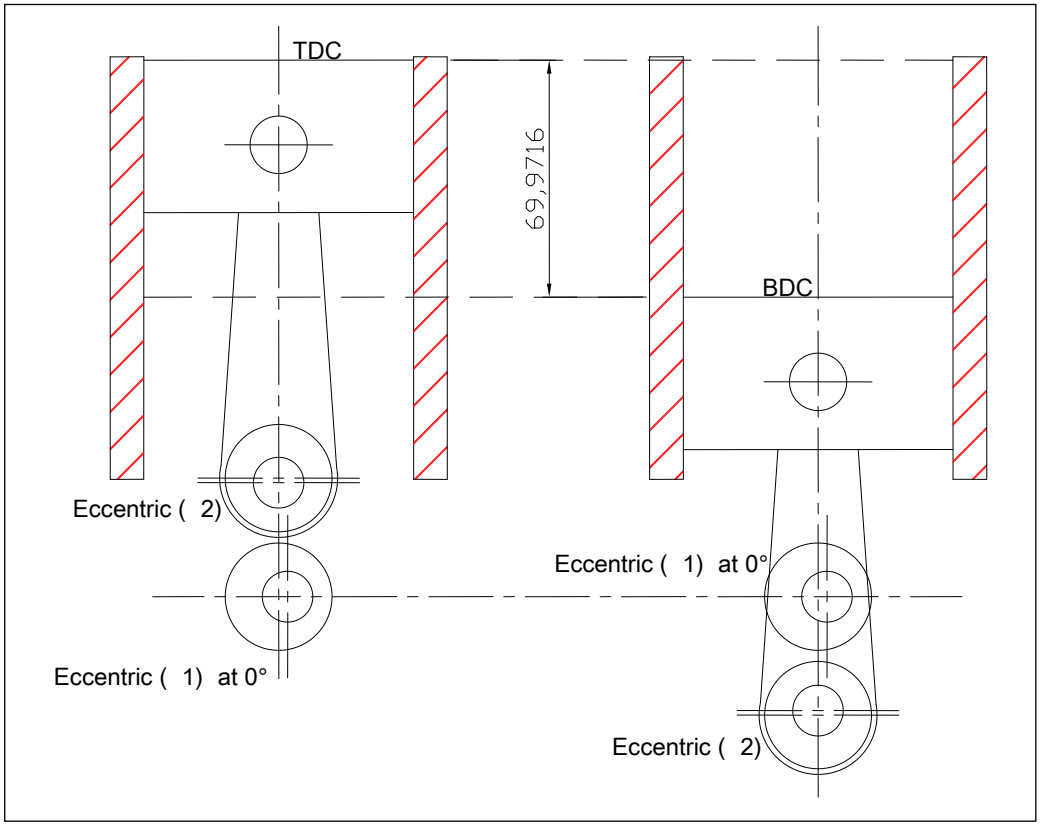

Figure 3.4: TDC and BDC Schematic sub assembly

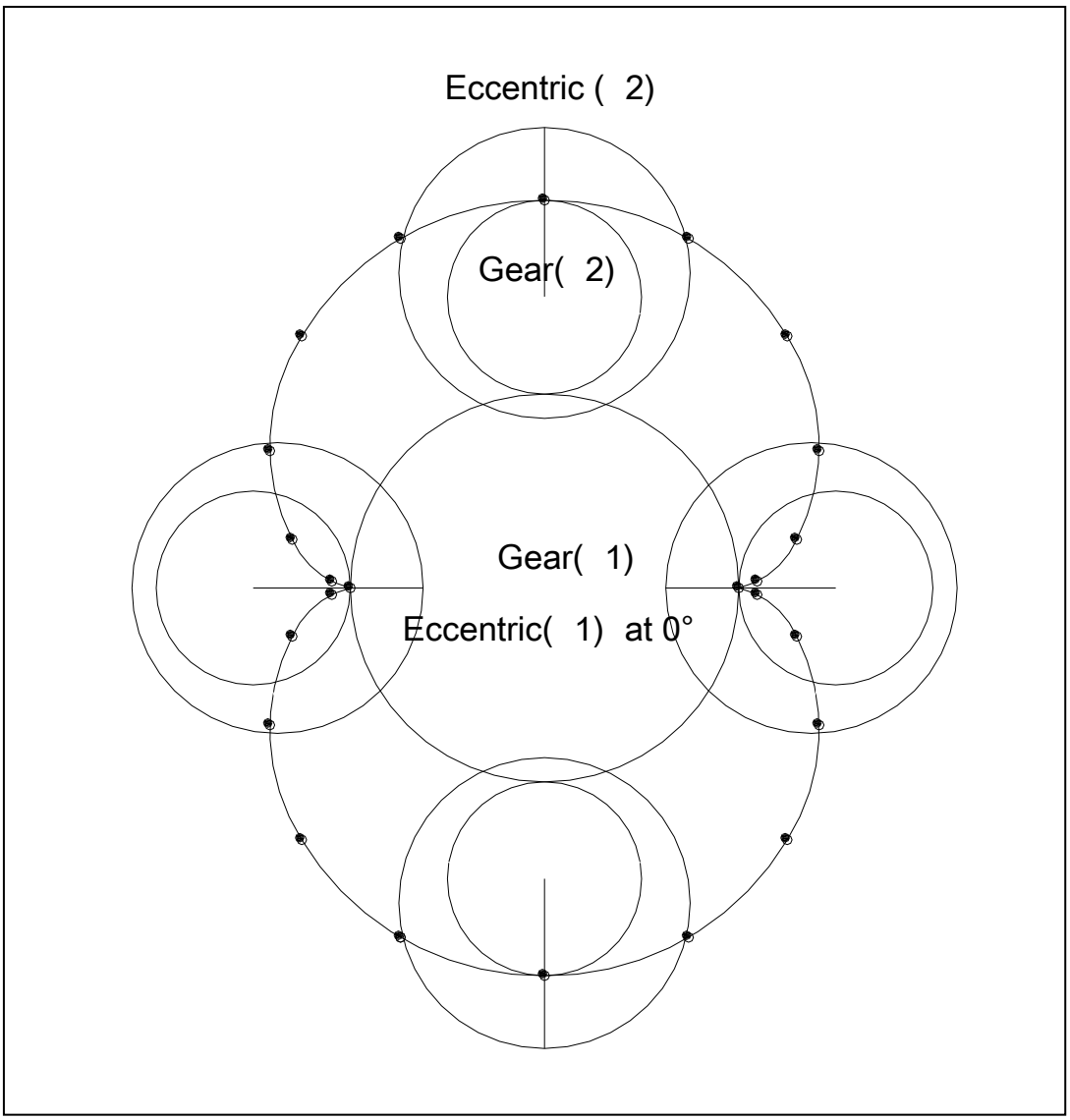

Figure 3.5: TDC and BDC schematic of eccentrics

By adjusting eccentric1 from 0° through 5° intervals to a 90° position and tabulating the respective stroke length a definite variance in the internal combustion engine capacity was noted (see figure 3.6).

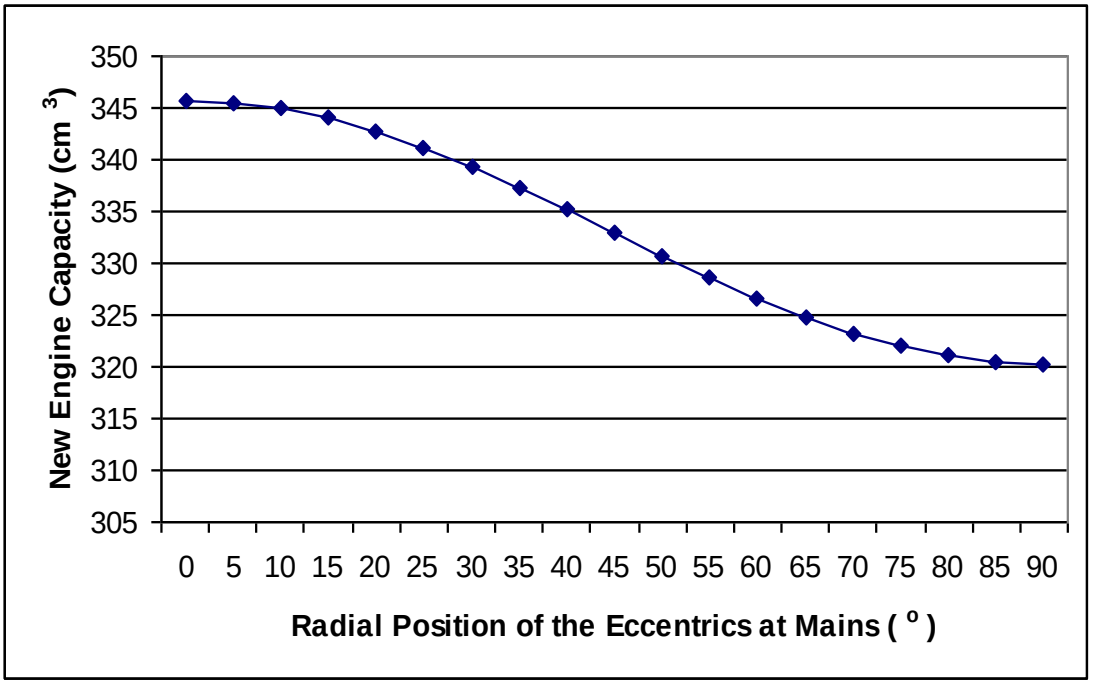

Figure 3.6: Engine capacity vs stroke variance

The graph in figure 3.6 indicates that with an approximate 6.5 mm difference in stroke an additional 25 cm^3 could be obtained resulting in an 8.2 % increase in capacity.

3.5 Crankshaft

One of the major components of an internal combustion engine is the crankshaft. The crankshaft changes the reciprocating motion caused by the piston assembly driven by the combustion processes into rotational motion.

In conventional internal combustion engines the crankshafts are normally forged from steel as one solid piece (see figure 3.7). The main journals are normally mounted in the cylinder block. They rotate within journal bearings which are made of a softer material and lubricated with oil. As these bearings later start wearing it is more cost effective to replace the bearings than the whole crankshaft. The big end journal accommodates the big end of the connecting rod and the same principle of operation applies here as for the main journals. The counter mass lobes facilitate with balancing the forces created by the reciprocating motion of the piston and connecting rod assembly.

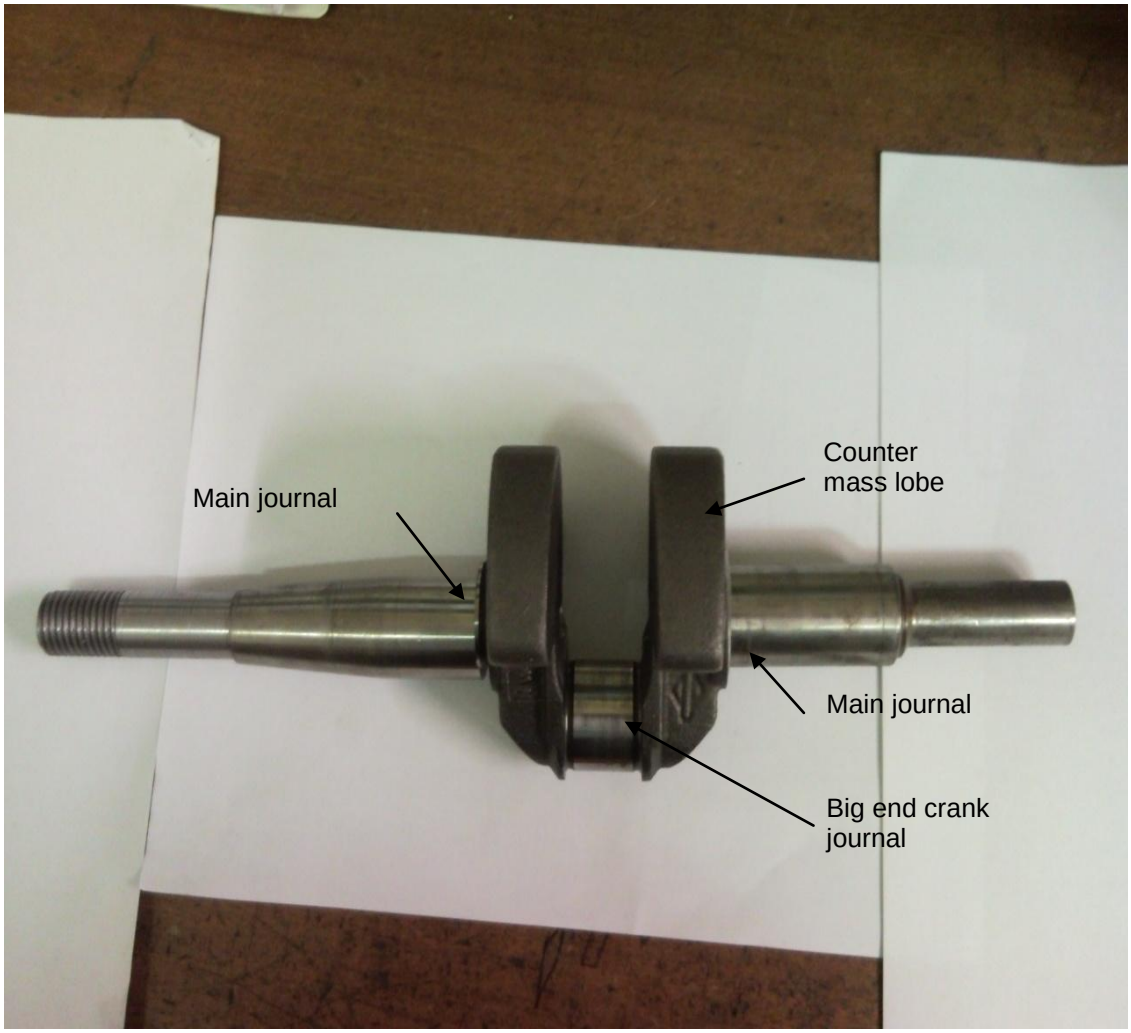

Figure 3.7: Typical Intec Briggs and Stratton internal combustion engine crankshaft

The prototype's crankshaft was made up of two counter mass lobes that can move independently from one another (see figure 3.8). This is not desirable as these two masses are required to move in unison. The reason why these two masses are not rigidly fixed to one another is that it would be impossible to control the eccentric position of the big end crank journal. The big end crank journal is allowed to rotate within the counter mass lobes. This is achieved by making use of needle bearings (OD 28mm x ID 15 x W 23) that are press fitted into the two counter mass lobes. The position and rotation of the eccentric of the big end crank journal will be controlled by gears (control gears 1, 2 and 3). The control gears 2 are press fitted and Tig welded at either ends of the big end crank journal.

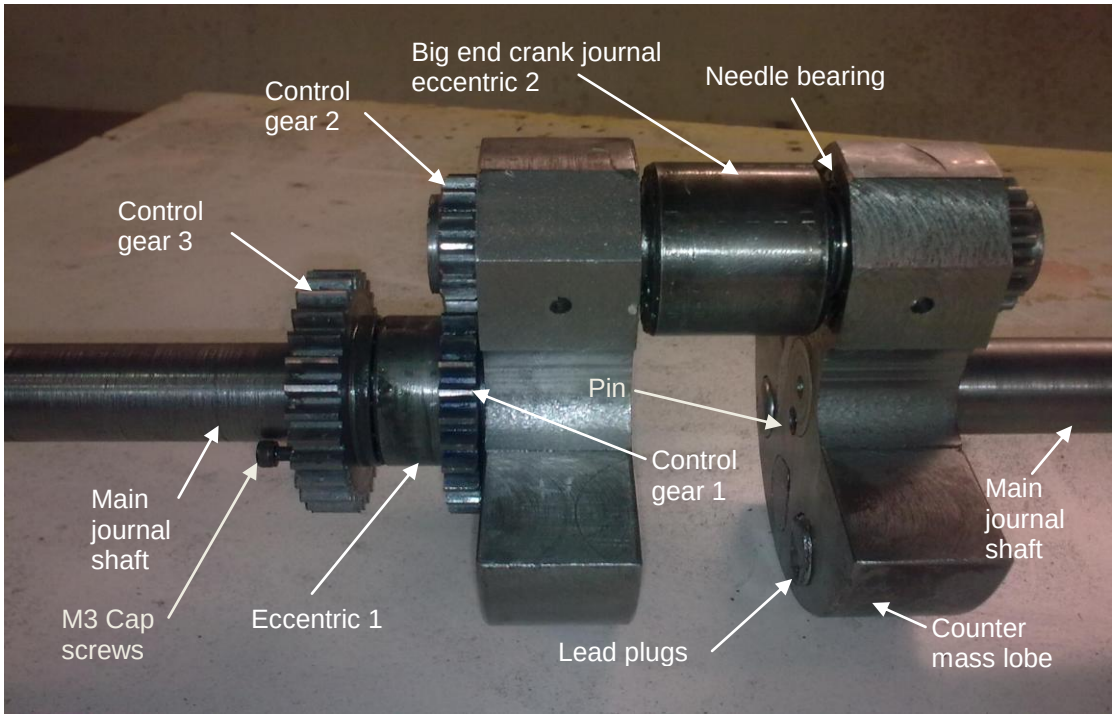

Figure 3.8: Prototype crankshaft (eccentric 1, control gear 1 and 3 are omitted on the right side of the crankshaft)

The control gear 1 and eccentric 1 are machined out of one piece of steel and form a rigid component (see figure 3.9). The control gear 3 is bolted to the eccentric 1 by means of high tensile steel cap screws and has a lip on the control gear and recess on the eccentric for ease of location and centralisation. The control gear 3 is machined in such a manner that the gear teeth rotate concentrically with the eccentric 1's outer surface thus requiring the rack only to move in a forward or backward direction and not up and down (see figure 3.10). The control gear 1 is machined to rotate concentrically with the off set main journal shaft holes of the eccentrics 1.

The crankshaft is held between two bearings within the housing, one in front and one at the rear of the crankshaft lobe section. These bearings are also known as the main bearings. In conventional internal combustion engines these main bearings are stationery within the housing. In the case of the prototype engine the outer bearing surface was allowed to rotate off-set of the actual rotation of the crankshaft. This allowed the crankshaft to lower or lift in a circumferential manner. Control gear 3 and 1 bolts together and the middle section forms the eccentric which will be accommodated inside the housing (see figures 3.9 and 3.10).

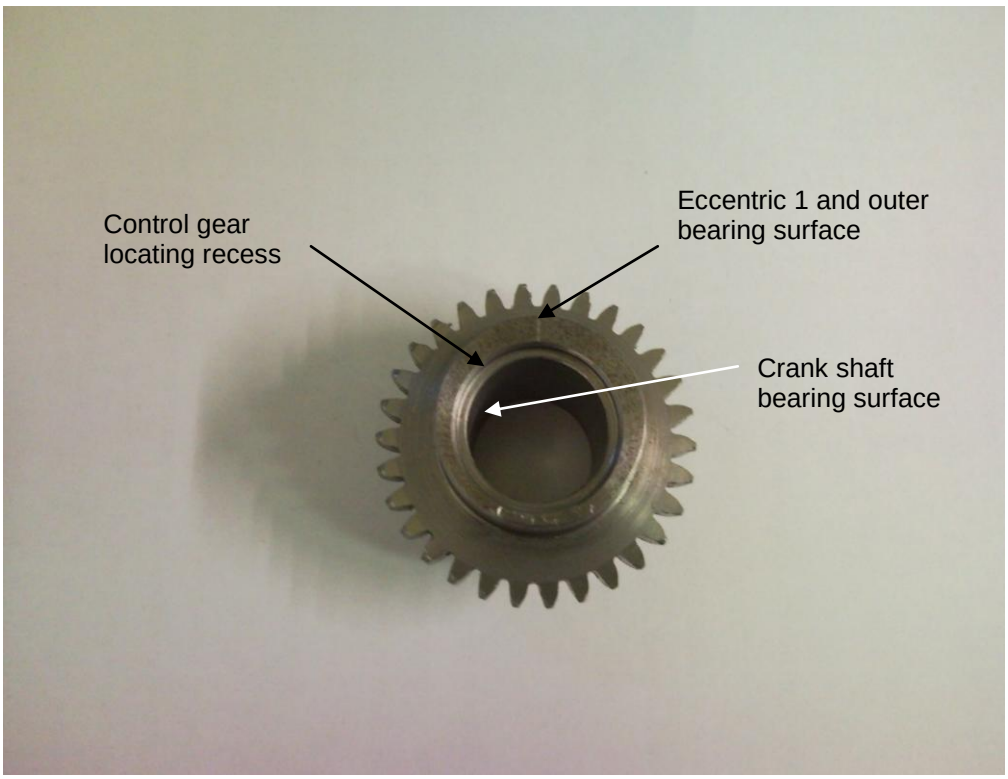

Figure 3.9: Control gear 1

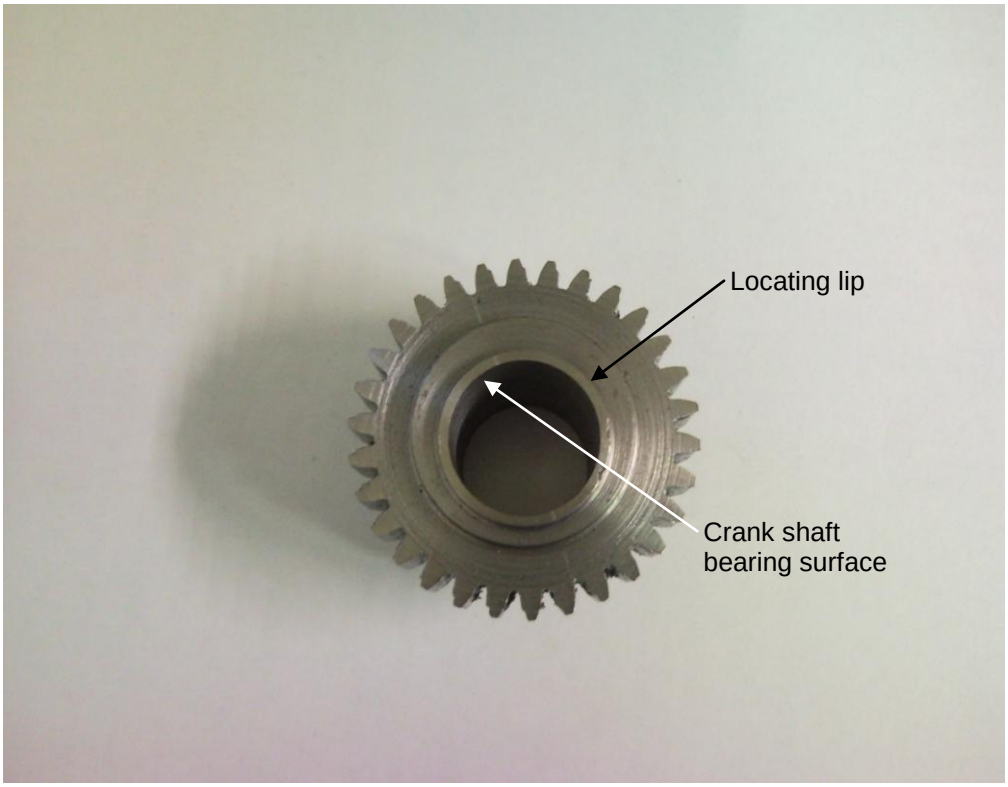

Figure 3.10: Control gear 3

3.5.1 Big end crankshaft journal

The connecting rod is mounted on the big end crankshaft journal. In conventional internal combustion engines the big end journal is normally a rigidly fixed part of the crankshaft (see figure 3.7). The coupling of the connecting rod with the crankshaft journal is known as the big end.

In the case of the prototype the big end crank journal (see figures 3.8 and 3.11) was allowed to rotate eccentrically about its own axis. The control of this rotation and position of the eccentric governed by small gears fixed on either side of the big end journal. This allows the shifting of the connecting rod to extend or shorten its travel when the crankshaft stroke is adjusted (see figure 3.8 gear 2 and eccentric 2). The eccentricity of the big end crank journal can be seen on figure 3.12.

The bearings fitted between the connecting rod big end and big end crank journal are normally made from dissimilar metal to that of the crankshaft, allowing for less wear and friction. In most conventional internal combustion engines these bearings are made from a metal collar lined with a layer of alloys such as copper, lead and tin. To further alleviate frictional problems oil is introduced between the rotating surfaces. It is also cheaper to replace worn bearings than to replace the actual moving component such as the connecting rod, crankshaft, bearing caps or housing.

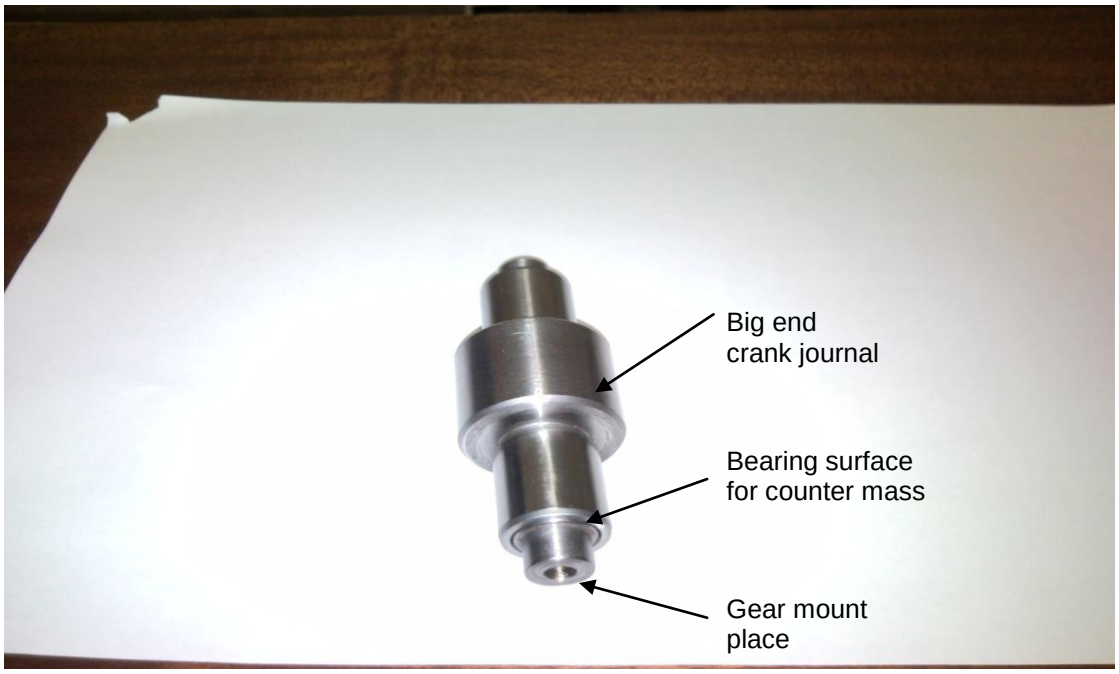

Figure 3.11: Prototype's big end journal

In the case of the prototype engine the connecting rod runs directly onto the crankshaft big end journal. The big end journal plays a double role; when the connecting rod rotates at the same time controls the extension and retraction of the connecting rod position. This will minimise any changes in the free space between the piston and cylinder head at TDC. The connecting rod is made from aluminium and the crankshaft journals from steel. The fact that there is no bearing between the crank journal and connecting rod is in contrast to the conventional method. This is customary for Briggs and Stratton engines normally used in lawnmowers, generators, compactors etc. For ease of manufacture and the fact that the engine is being designed as a prototype that will not be exposed to running for extensive working hours, the prototype followed the Briggs and Stratton engine design by not fitting bearings between the big end of the connecting rod and big end of the crankshaft journal.

The big end journal will be rotating at twice the speed of the crankshaft. This is due to the 1:2 control gear ratios. It is important that the big end journal balancing be improved to minimise out of balance forces. Space around the big end area is limited by maintaining most of the engine's original specifications. In order to balance the crankshaft big end journal, a mass can either be added or removed. The quickest way that the big end journal in the prototype could be statically balanced was to remove material from the outermost lobe of the eccentric (see figure 3.12).

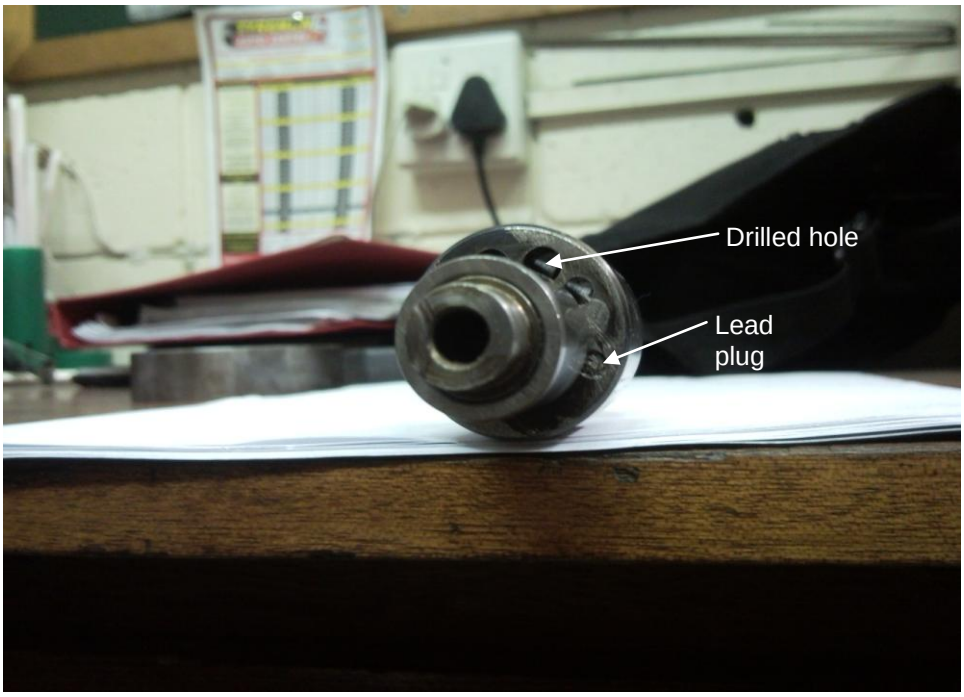

Figure 3.12: End view of the Prototype's big end journal

3.5.1.1 Finite Element Analysis on the big end crankshaft journal

The big end shaft diameters of the prototype had to be reduced to allow enough space for the eccentrics and bearings. The bulk of the forces exerted on the piston during the combustion stroke will be induced into these shafts. It was therefore necessary to determine whether the new shaft dimensions would be strong enough to handle the forces.

The first objective was to calculate the mean effective pressure (P_m).

The power developed in the cylinders by the expanding gasses is known as the indicated power (i.p.), and can be calculated from the following formula:

$$\text{i.p.} = \frac{P_m \times L \times A \times n \times E}{60} \quad \text{(Joel, 1996 : 577 - 578)}$$

Where :

P_m : Mean Effective Pressure

L : stroke length

A : piston area

n : number of cylinders

E : number of working cycles per minute

$\left(E = \frac{N}{2} \text{ for a four stroke engine, where N : speed} \right)$

The indicated power is equal to the engine rated power of 10hp (7.5 kW), the indicated mean effective pressure can thus be calculated. The maximum power of 10 hp is achieved at a speed (N) of 3600 rpm (see figure 3.13).

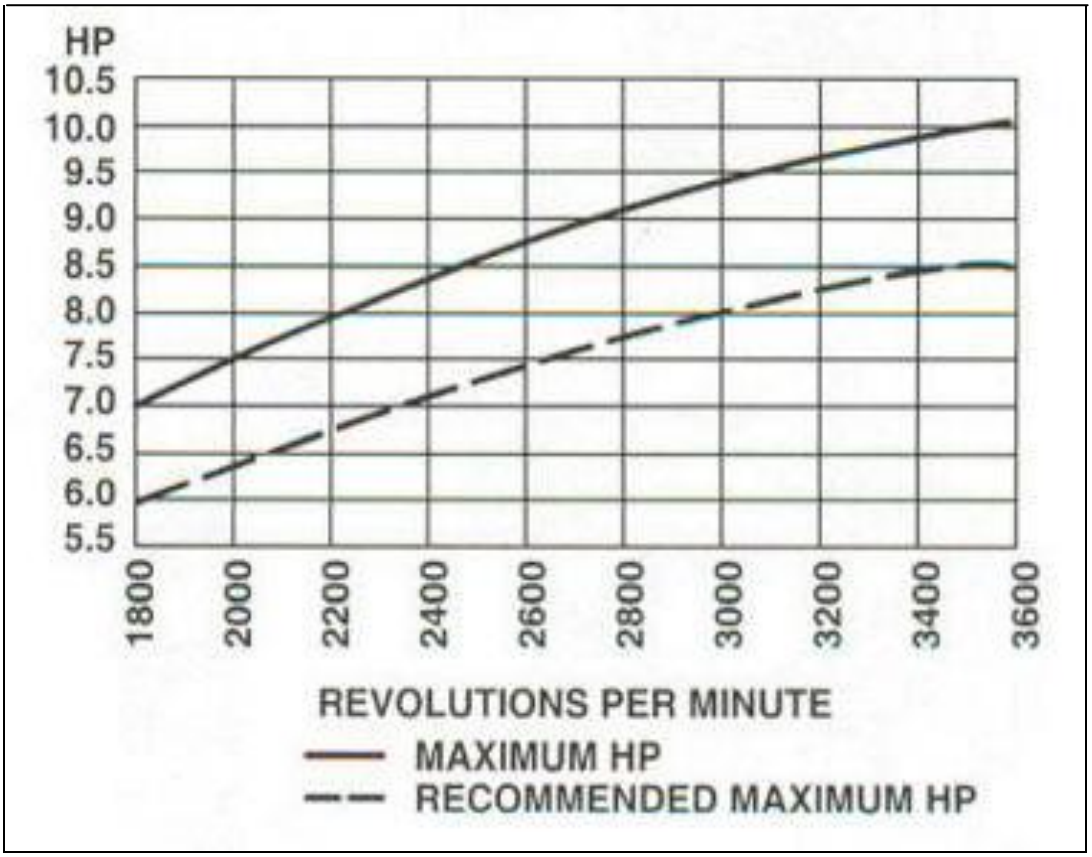

Figure 3.13: HP vs. Revolutions per minute

(Graph obtained from http://www.jackssmallengines.com/bs10intekpro.html)

From figure 3.13 we proceed to calculate P_m:

$$P_m = \frac{60 \times (\text{i.p.})}{L \times A \times n \times E}$$

$$P_m = \frac{60 \times 7500 \times 10^{-3}}{0.061722 \times \frac{\pi}{4} \times 0.079248^2 \times 1 \times \frac{3600}{2}}$$

$$P_m = 821.2\,\text{kPa}$$

Knowing the pressure exerted onto the profile of the eccentric and the pertinent dimensions, the force applied to it can be calculated as follows:

$$P_m = \frac{F}{A}$$ (Drotsky 1994)

$$P_m = \frac{F}{d \times L}$$

Where :

F : force
A : projected area of eccentric
d : diameter of eccentric
L : length of eccentric

$$\therefore F = P_m \times d \times L$$
$$F = 821.2 \times 10^3 \times 0.0317 \times 0.0262$$
$$F = 682.02\ N$$

The normal stress exerted by the force can be obtained from

$$\sigma = \frac{F}{A}$$ (Drotsky 1994)

Where :
σ : direct stress
F : force
A : projected area

The direct stress which is induced in the eccentric's profile can be calculated. Since the projected area to which the force is applied to calculate the direct stress is the same as the projected area to which the pressure is applied, means that the magnitude of the direct stress is equal to the magnitude of the pressure.

$$\therefore \sigma = P_m = 0.8212\,MPa\ (compressive)$$

The normal stress would be transmitted through the connecting rod to the eccentric at the big-end of the connecting rod. Half of this stress would be transmitted to each crank lobe from where it should be transmitted to the output shaft.

The most likely position of failure of the big-end would be where the side shafts steps next to the eccentric. Alternatively at where the shafts press fit into the crank lobes located at mains, since the dimensions of these components are smaller than the original crankshaft's sizes.

A Finite Element Analysis (FEA) was performed on the eccentric in order to ascertain the level of normal and shear stresses, maximum Von Misses stresses and maximum deflection of the component as to ensure that the actual modification on the engine "prototype" did not weaken it structurally. Also see sub heading 3.5.2.1 for the FEA on the counter mass lobes side shafts.

Outline of the method for the FEA on the eccentric:

Name and version number of the software:	Unigraphics NX 5.0.3.2
Type of analysis:	Linear static structural FEA
Element type:	Ten node tetrahedral
Element size:	4 mm

The 15 mm diameter shafts on either side of the eccentric's profile were fixed as they fit inside bearings situated in the crank lobes. The indicated mean effective pressure with a magnitude of 821.2 kPa was applied to the top half of the circumference of the eccentric's profile. This is the contact area between the connecting rod and eccentric during the expansion process of the piston.

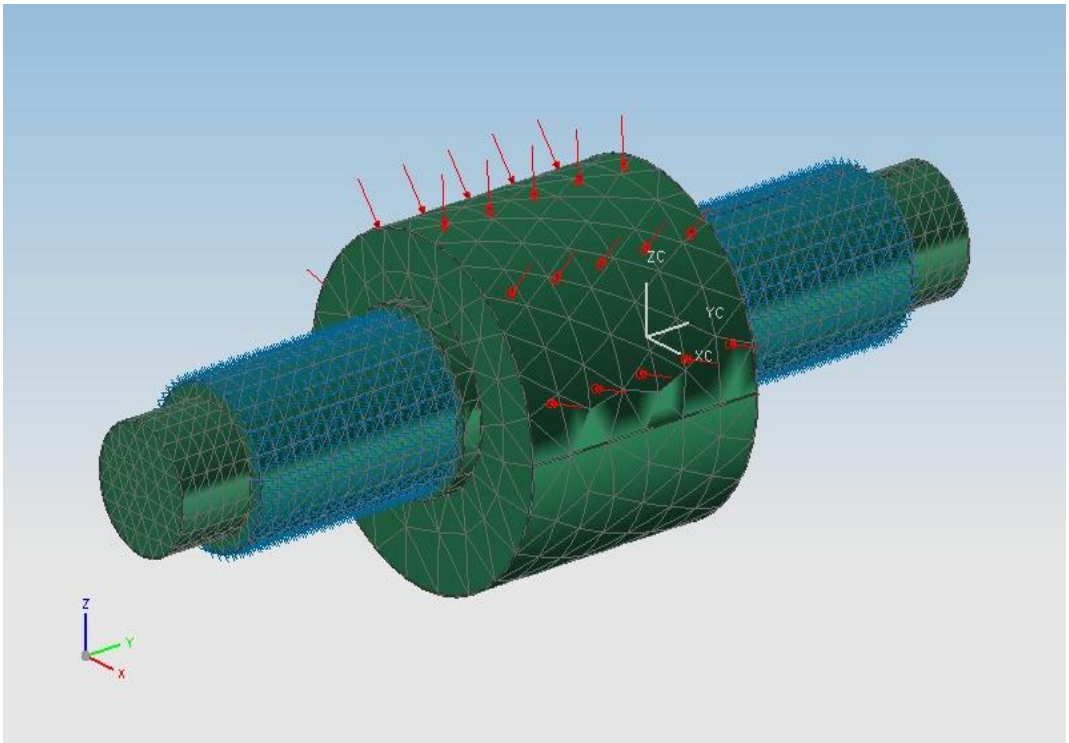

Figure 3.14: Eccentric with constraints and pressure applied

Figure 3.14 depicts the 'Fixed' constraints applied to the 15 mm diameter shafts and the indicated mean effective pressure of 821.2 kPa applied to the eccentric's profile.

To determine the optimum element size, the finite element analysis was repeated with different element sizes and the maximum shear stress for each case recorded. From the data a graph was produced as indicated in figure 3.15.

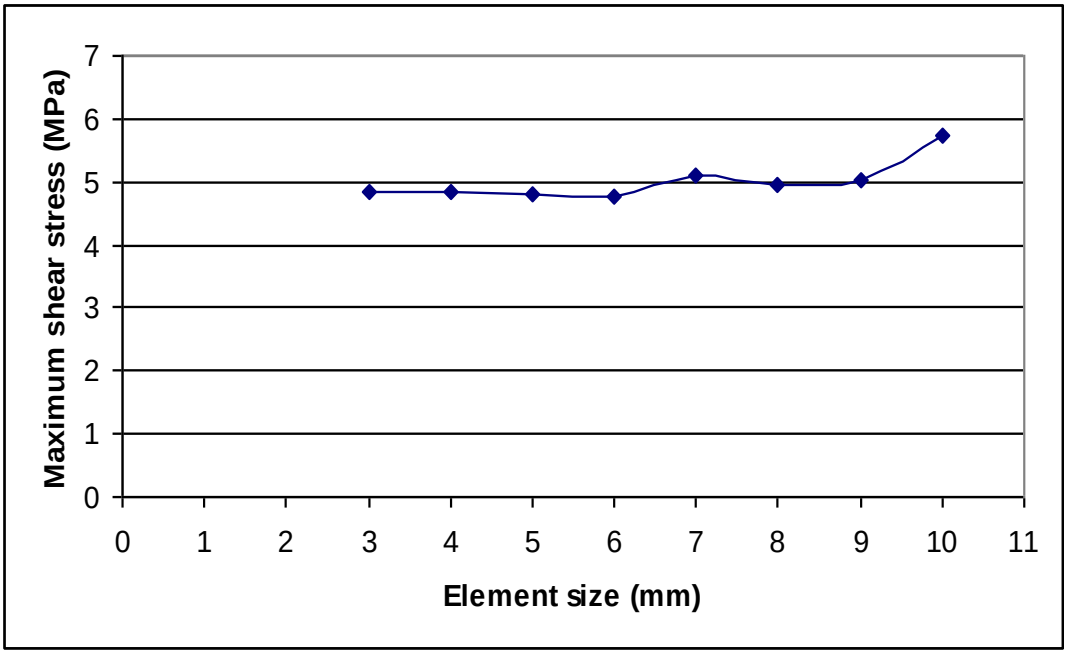

Figure 3.15: Maximum shear stress vs. element size for the eccentric

From figure 3.15 an element size of 4 mm was chosen (small element sizes require longer computational time). The maximum shear stress induced in the eccentric was found to be in the region of 4.5 MPa, which occurred on both sides of the eccentric's profile at the 15 mm diameter shafts (see figure 3.16).

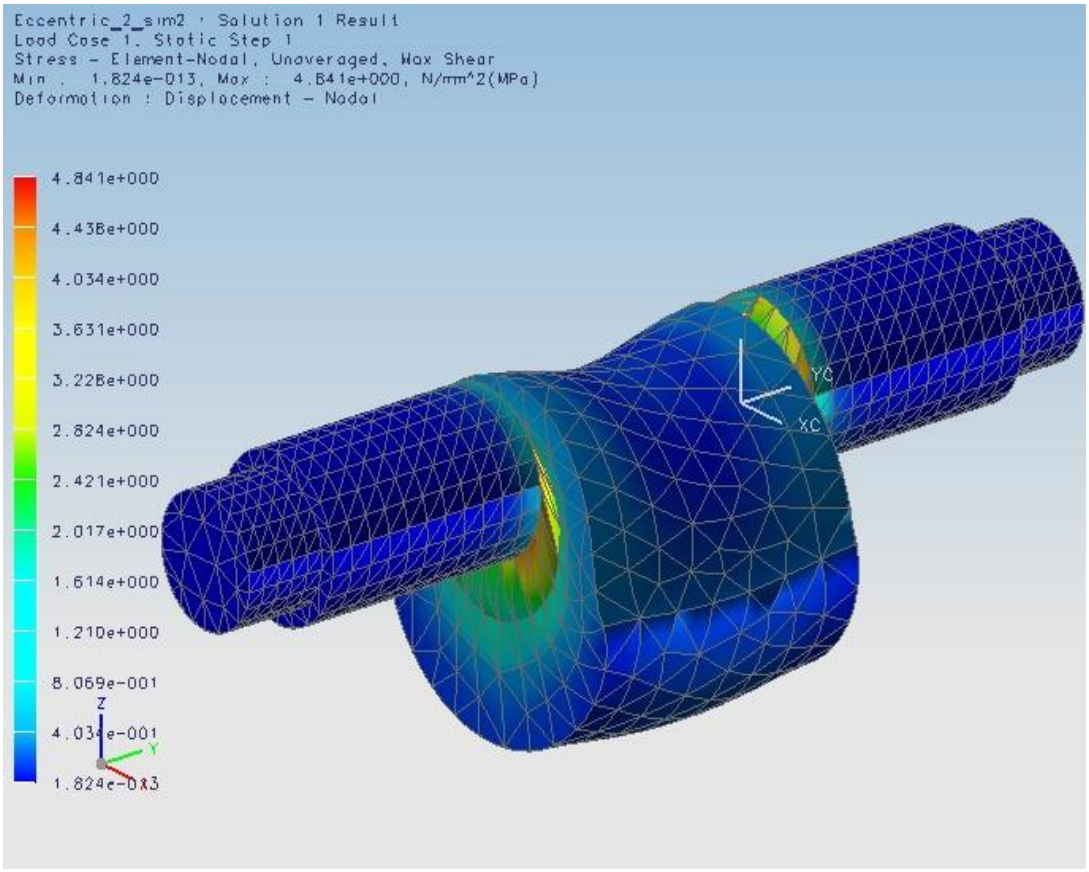

Figure 3.16: Maximum shear stress induced in the eccentric

The magnitude of the maximum shear stress induced in the eccentric is considerably less than the yield strength of the eccentric's material. According to Drotsky, J.G. 1994 the maximum shear stress for mild steel is 175 MPa.

The FEA results predicted that the eccentric situated in the connecting rod at the big-end would not shear.

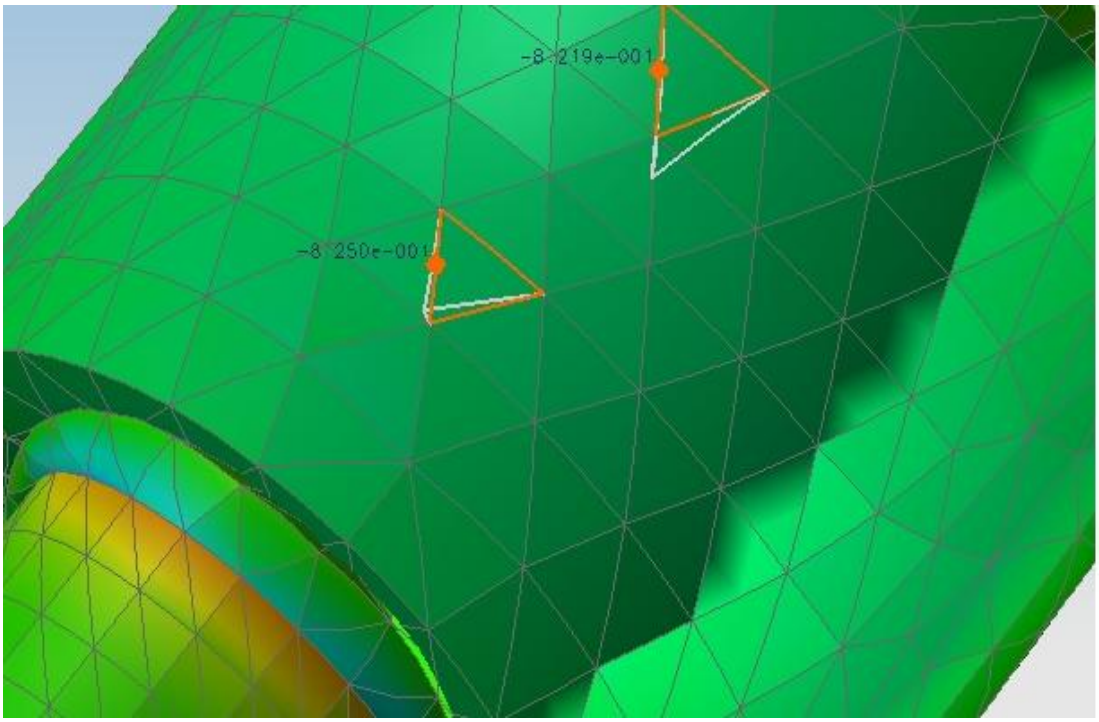

Figure 3.17: Direct stress induced in the eccentric's profile

The purpose of figure 3.17 is to show that the stress induced in the eccentric's profile obtained from the FEA simulation is in good agreement with the magnitude calculated earlier. Calculations indicated that the direct compressive stress induced in the eccentric's profile was 0.8212 MPa. The direct compressive stresses induced in the eccentric's profile resulting from the FEA were 0.825 MPa.

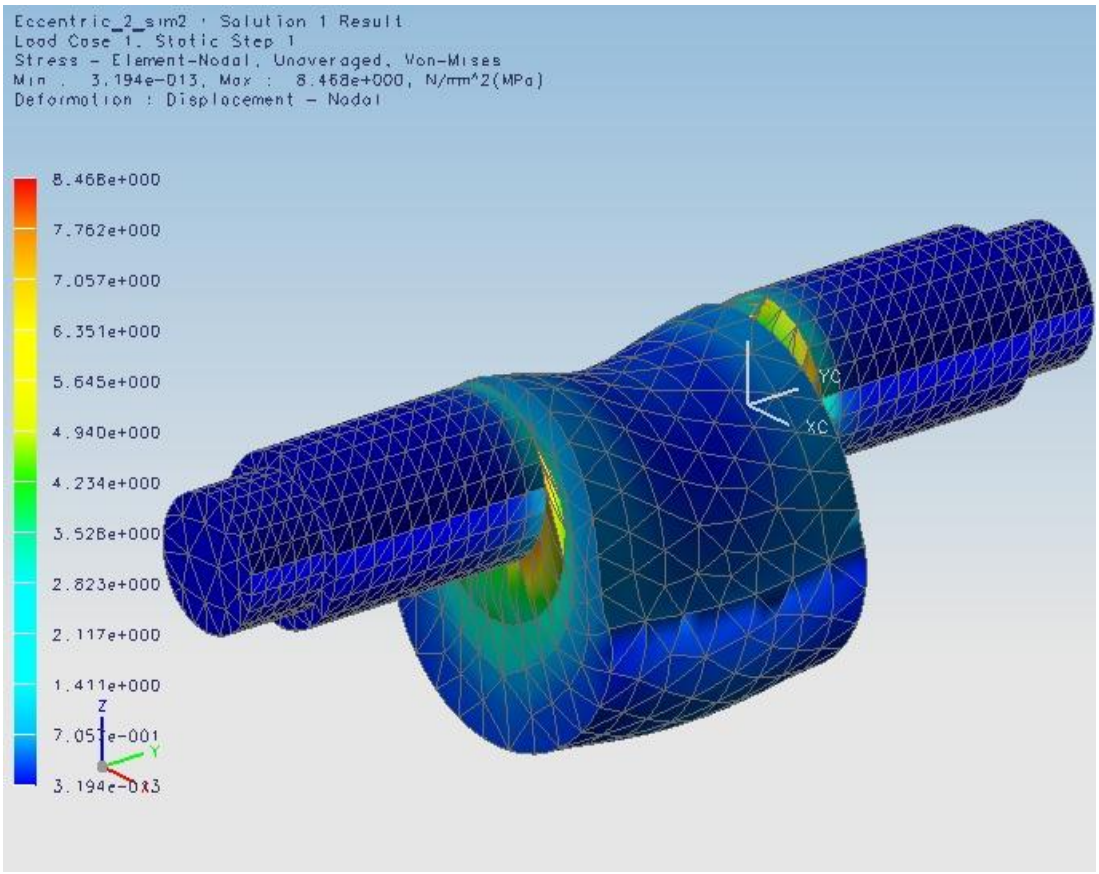

Figure 3.18: Maximum (Von-Mises) stress induced in the eccentric

Figure 3.18 depicts the Von Mises stresses that resulted from the FEA. It is seen that the maximum stress induced in the eccentric is in the region of 7.8 MPa under normal load conditions, which also occurred on both sides of the eccentric's profile at the 15 mm diameter shafts. This stress is very much below the yield strength of the eccentric's material.

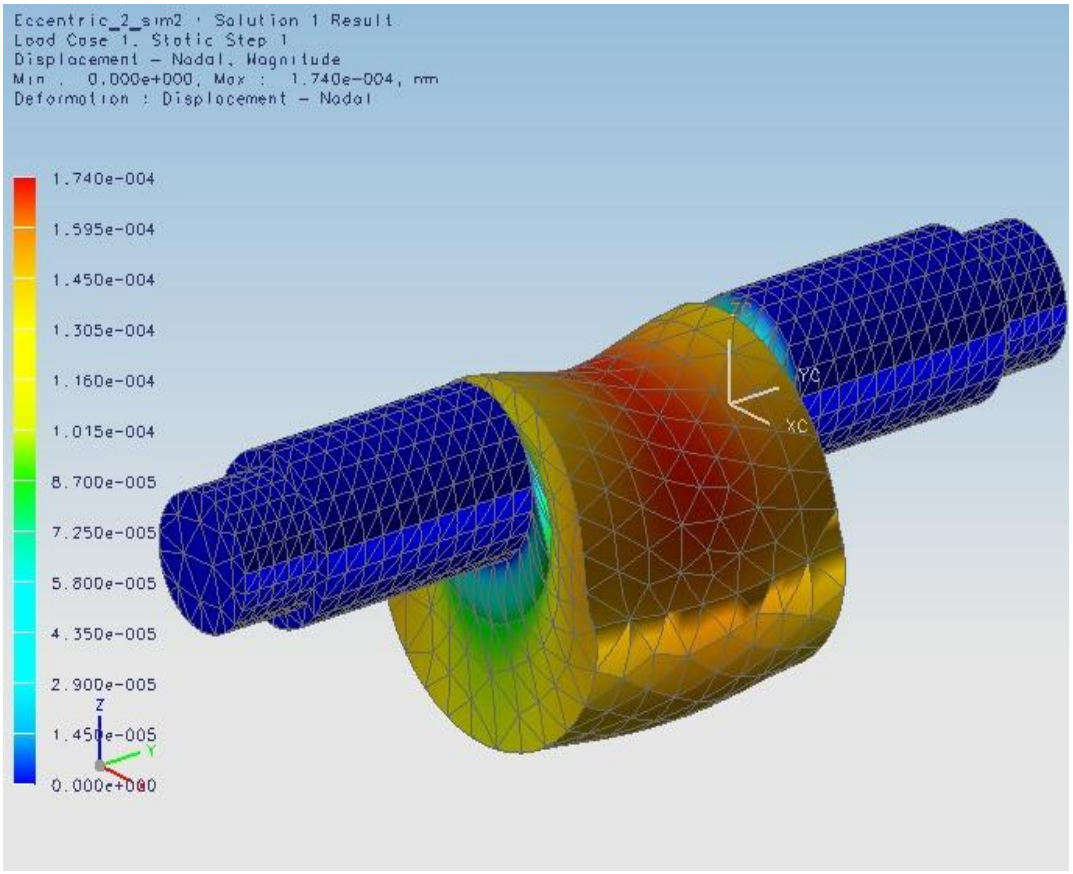

Figure 3.19: Maximum displacement of the eccentric

Figure 3.19 depicts the maximum displacement of the eccentric's profile as 0.000174 mm. The design clearance between the connecting rod's big end and the eccentric's surface is 0.02 mm. Seizing or bearing failure due to interference would be very unlikely to occur due to deformation.

In conclusion the results from the FEA analysis indicated that the modified eccentric would not fail either due to the stresses or deformation induced by the pressure caused by the engine's expansion process while the piston travels during the power stroke.

3.5.2 Crankshaft counter mass lobes and side shafts

The counter mass lobes in conventional engines are forged in unison with the big end journal and side crank shafts (see figure 3.7). These lobes support the big end journal and crank shafts. When balancing the crankshaft assembly mass can either be added or removed from the lobes. These lobes must always be in perfect alignment to prevent pinching and run-out on the crank shafts.

With the prototype design these counter mass lobes are separated from the big end journal and the side shafts are press fitted into the lobe (see figures 3.20 and 3.21). Furthermore, these side shafts are doweled to prevent slippage when transmitting torque. The big end journal rotates inside the needle bearings. The needle bearings are lightly press fitted into the counter mass lobes. It was important to get the counter mass close to the same mass as the original crankshaft counter mass.

This was achieved by machining away material at strategic positions to achieve the right balance (see figure 3.20).

The main journal shafts were press fitted and doweled into the counter mass lobes to form a rigid shaft that should be able to transmit the required torque.

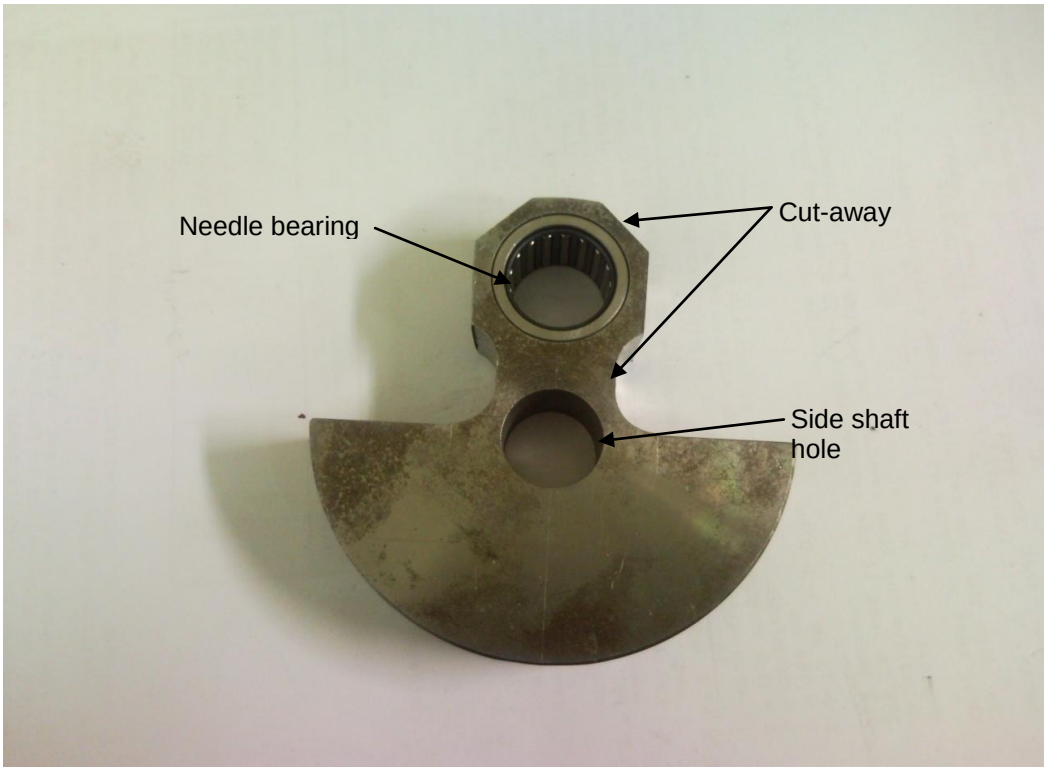

Figure 3.20: Counter mass lobe

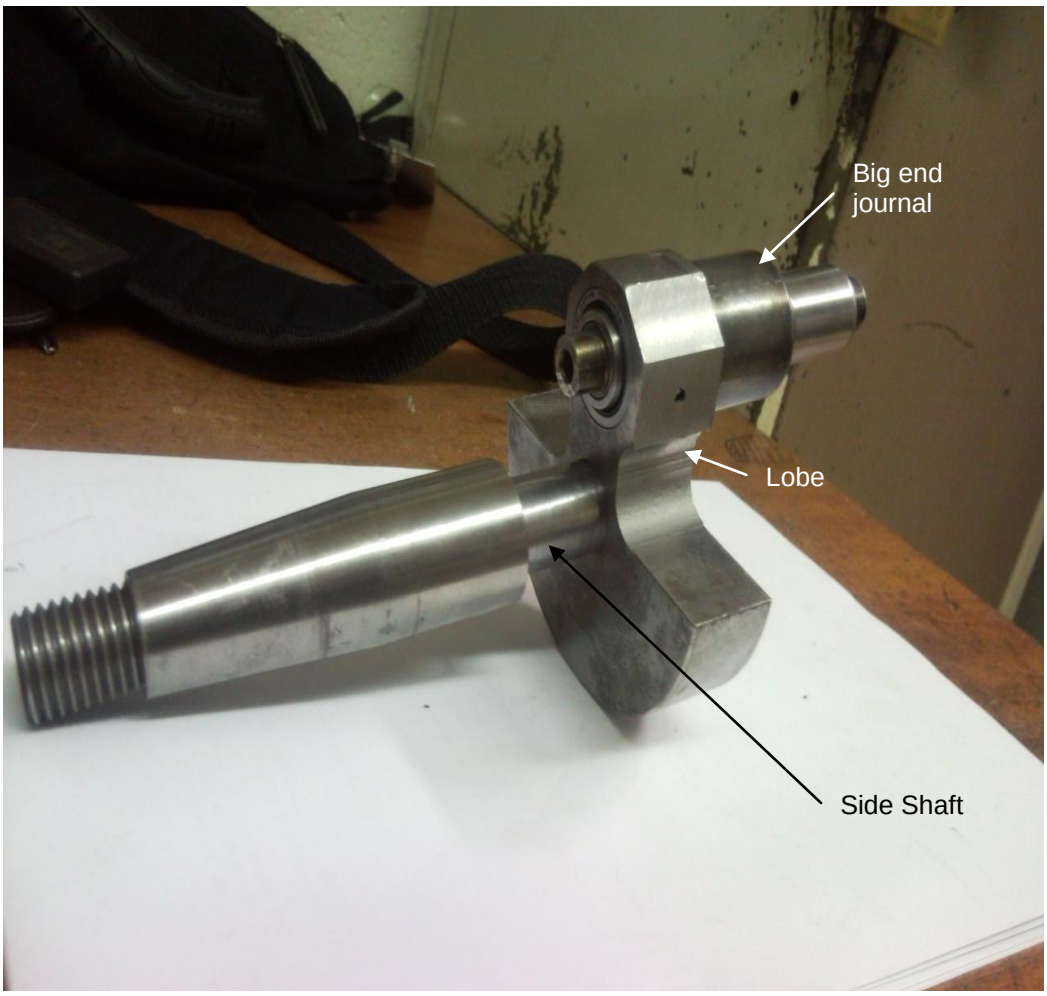

Figure 3.21: Counter mass lobe assembly (half crankshaft assembly)

3.5.2.1 Finite Element Analysis on the counter mass lobes side shafts

Just like with the big end shaft diameters of the prototype, the counter mass lobes side shafts had to be reduced to allow enough space for the eccentrics and bearings to operate within the engine housing. The same pressure exerted on the piston as determined earlier (P_m=0.8212 MPa compressive) during the combustion stroke would be induced into these side shafts.

Due to the crankshaft being symmetrical, half of the indicated mean effective pressure with a magnitude of 0.410 MPa was applied to the top half of the circumference of the section of the shaft situated inside the crank lobe.

The crankshaft being symmetrical, half of the “indicated” stress would be transferred through each crank lobe to the shafts which are press fitted into the crank lobes.

$$\therefore \sigma = \frac{1}{2} P_m = 0.4106 \text{MPa (compressive)}$$

Figure 3.22 depicts the “Fixed” constraint applied to the 16 mm diameter shaft as they are press fitted into the counter mass lobes. Half the indicated mean effective pressure of 0.4106 MPa applied to the section of the shaft situated inside the main bearing.

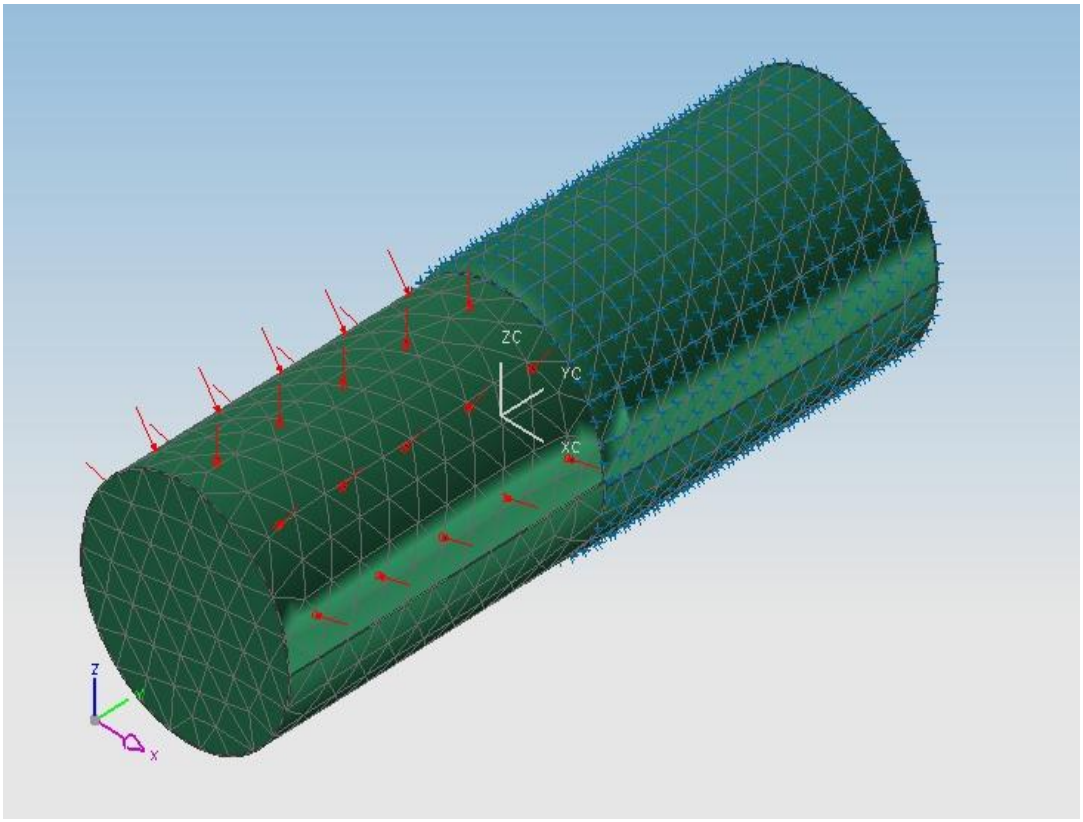

Figure 3.22: Shaft with constraint and pressure applied

To determine the optimum element size, the FEA was repeated with different element sizes and the maximum shear stress for each case was recorded. From the data a graph was produced as indicated in figure 3.23.

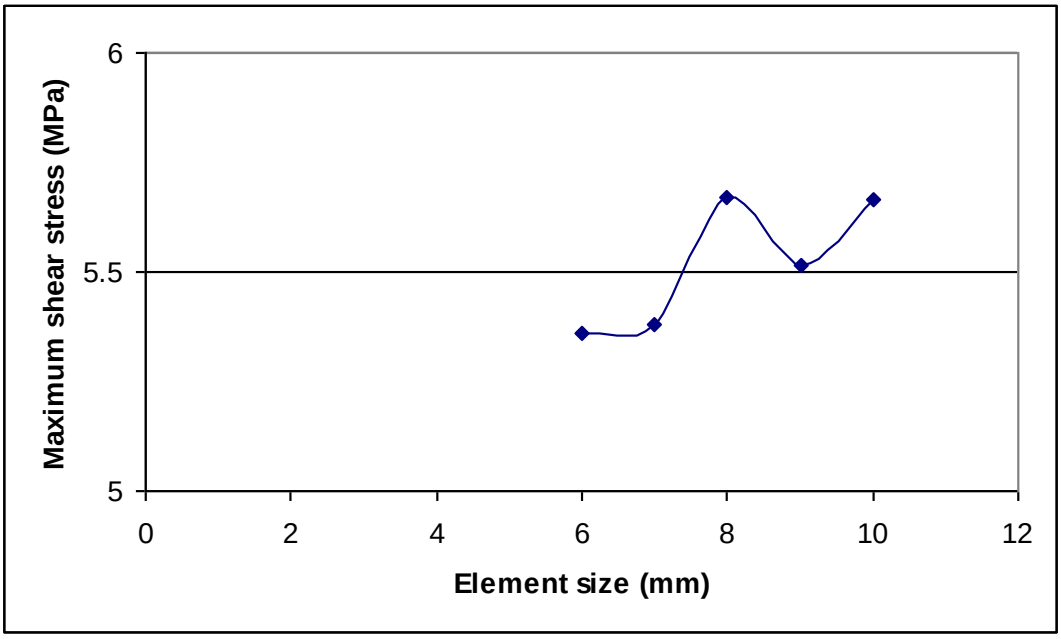

Figure 3.23: Maximum shear stress vs. element size for the main shafts

From the figure 3.23 an element size of 6 mm was chosen. The maximum shear stress induced in the shaft was found to be in the region of 4.92 MPa, which occurred on the vertical surface between the constrained section and section on which the pressure was applied (see figure 3.24).

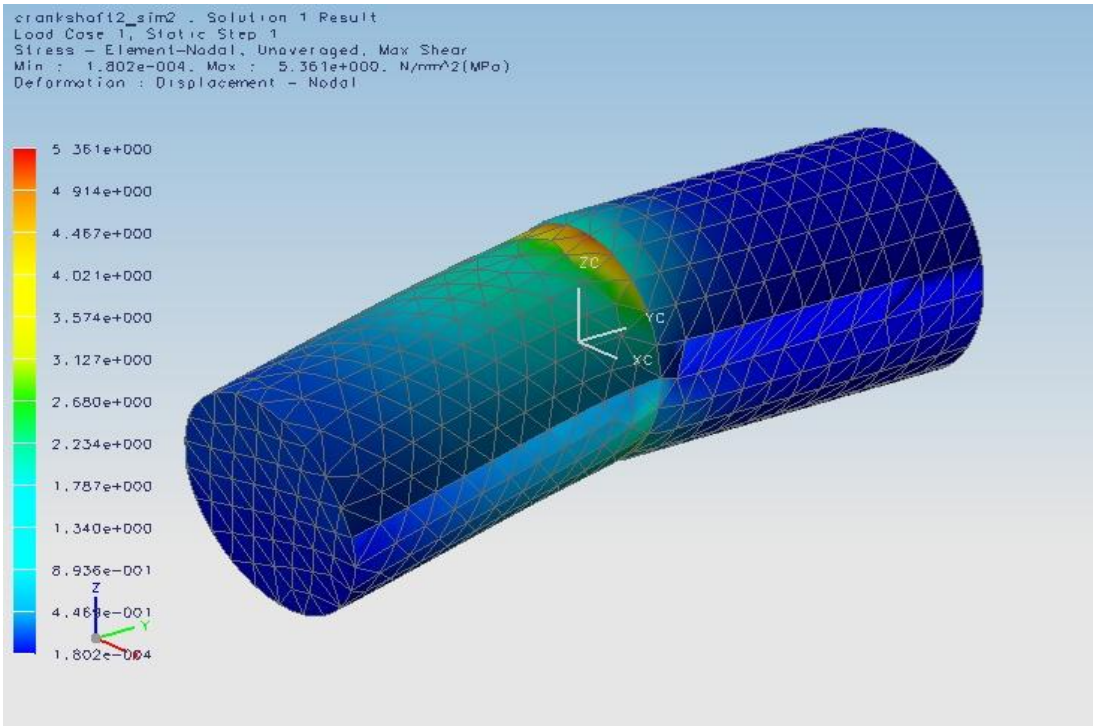

Figure 3.24: Maximum shear stress induced in the main shaft

The magnitude of the maximum shear stress (4.92 MPa) induced in the shaft is well within the limit of the yield strength the shaft's material (mild steel).

The FEA results predicted that the shaft situated in the crank lobe and mains bearing would not shear.

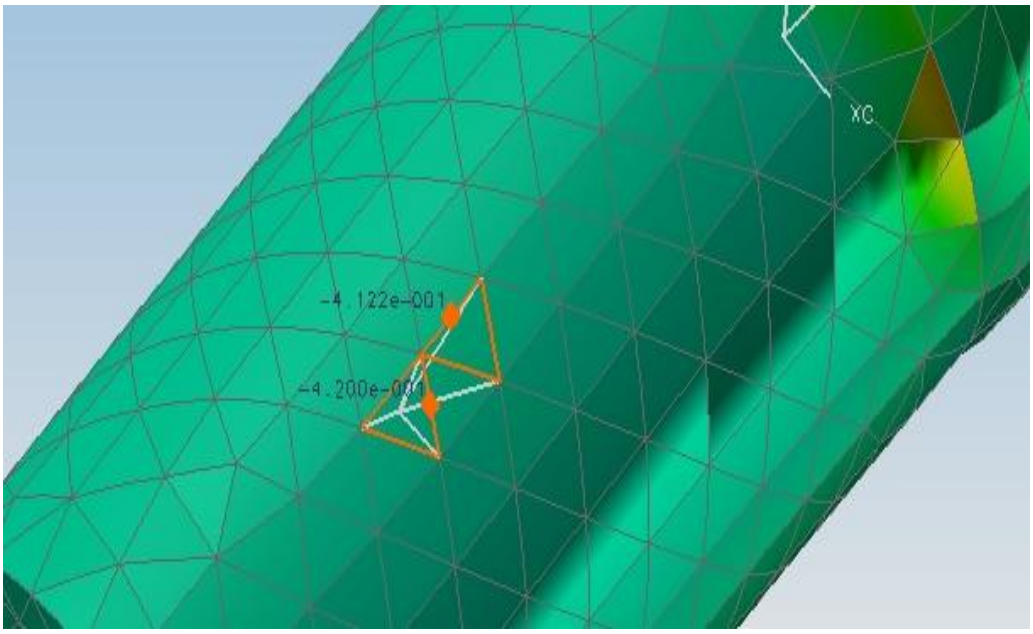

Figure 3.25: Direct stress induced in shaft

The purpose of figure 3.25 is to show that the stress induced in the shaft obtained from the FEA simulation is in good agreement with the magnitude calculated earlier. The direct compressive stress determined earlier (0.4106 MPa) is in agreement with the FEA results of 0.42 MPa.

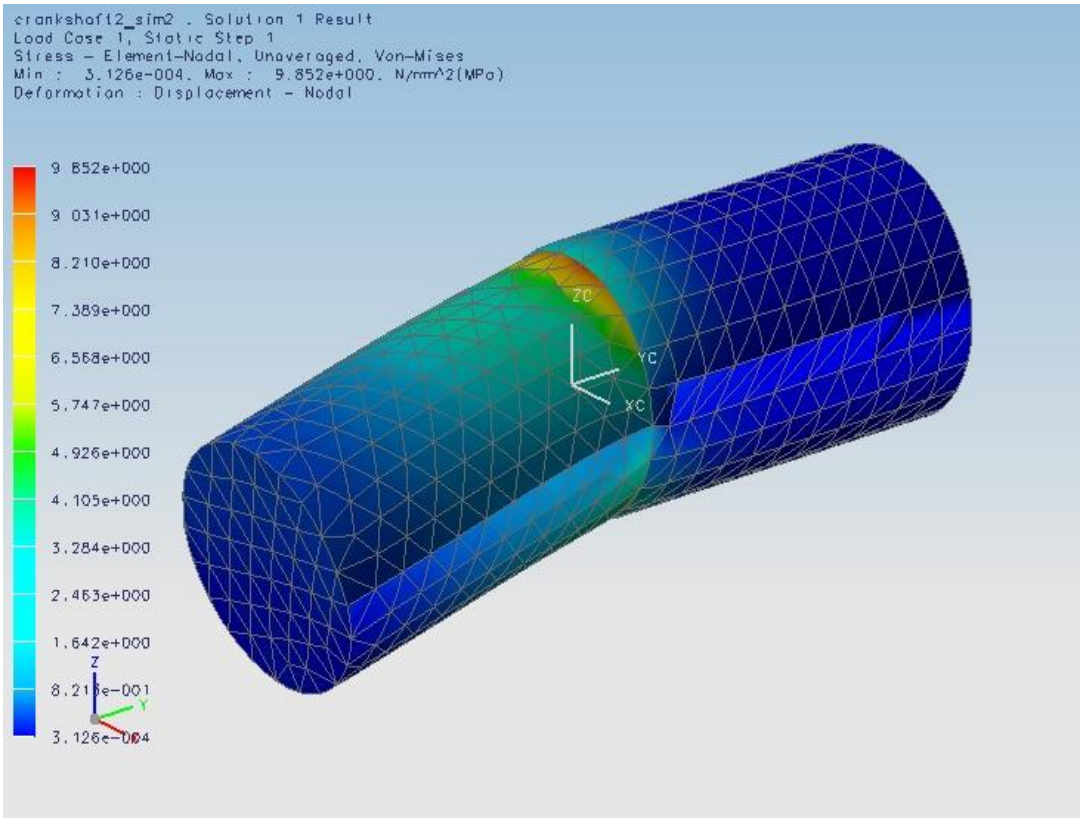

Figure 3.26: Maximum (Von-Mises) stress induced in the main shaft

Figure 3.26 depicts the Von Mises stresses that resulted from the FEA regarding. The maximum stress induced in the shaft is in the region of 9.5 MPa under normal static load conditions, which also occurred on the vertical surface between the constrained section and section on which the pressure is applied. This is much less than the yield strength (175 MPa) of the shaft's material (mild steel).

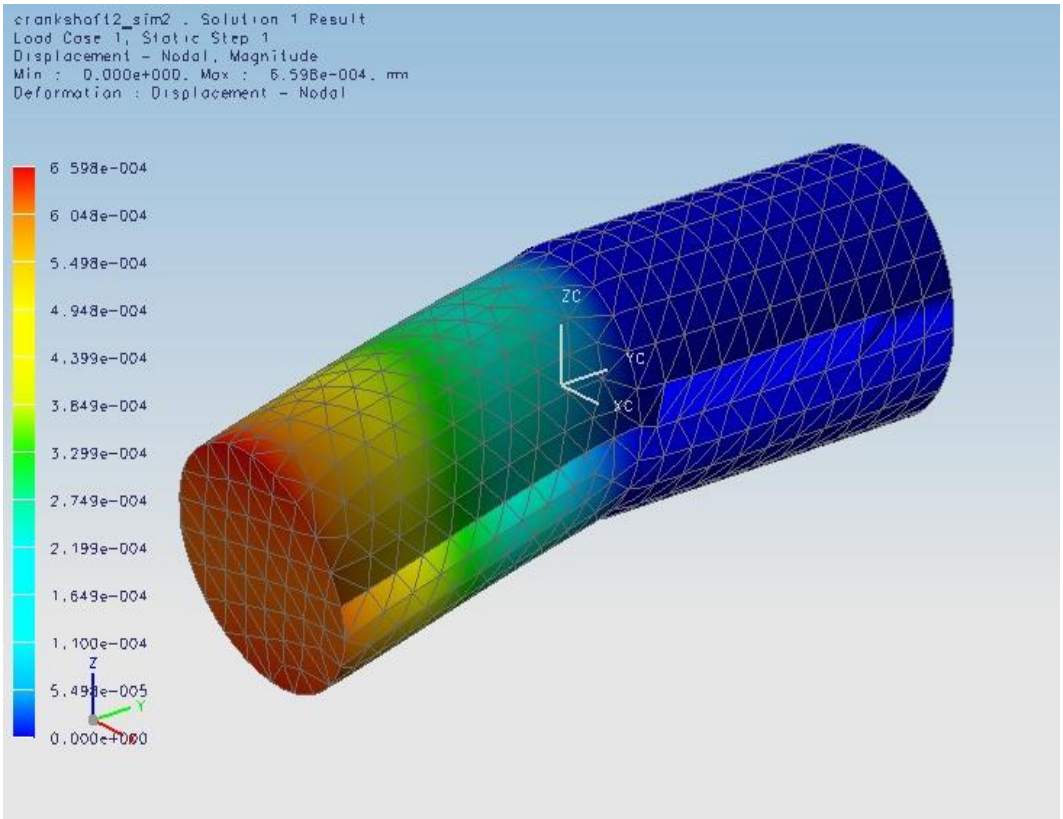

Figure 3.27: Maximum displacement of the shaft

Figure 3.27 depicts the maximum displacement of the shaft as 0.00066 mm. The design clearance between the crank main shaft and the bearing in the housing is 0.02 mm. Seizing or bearing failure due to interference would be very unlikely to occur.

In conclusion the results from the FEA analysis indicated that the modified main shafts would not fail either due to the stresses or deformation induced by the pressure caused by the engine's expansion process while the piston travels during the power stroke.

3.5.3 Crankshaft Housing/Engine Block

The crankshaft housing had to be machined on the inside to make space for the movement of the control gears (see figures 3.28 and 3.29). The existing main bearing bush was maintained for the eccentric 1 to rotate in.

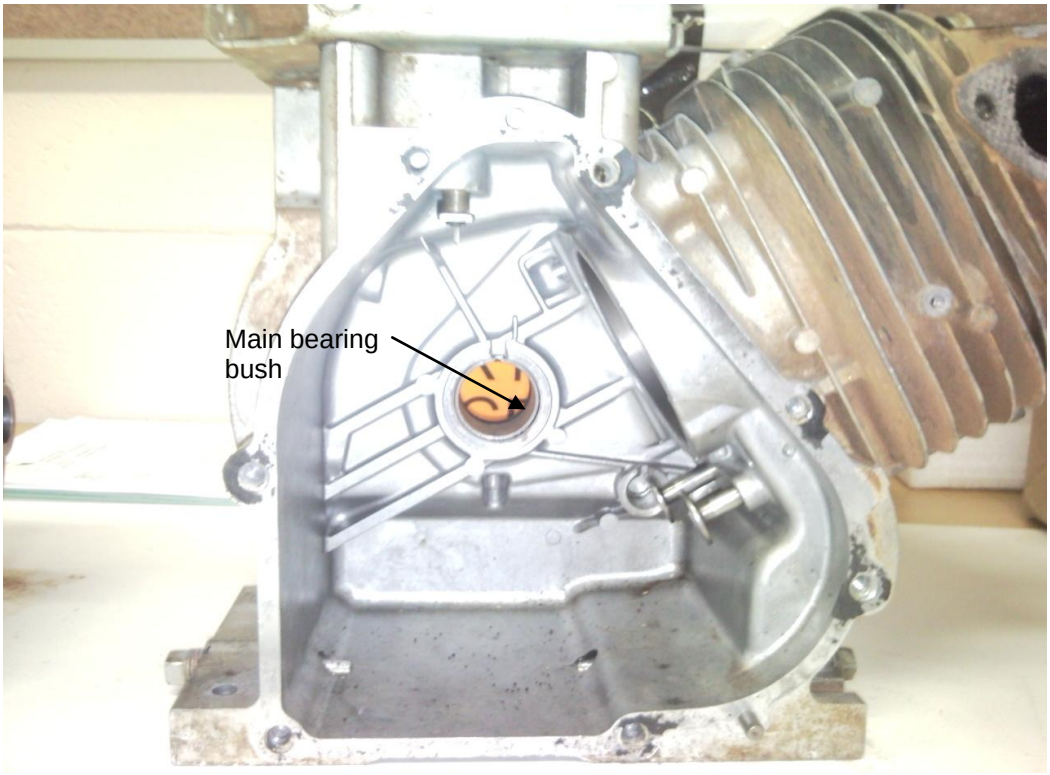

Figure 3.28: Standard crankshaft housing/engine block

Figure 3.29: Modified crankshaft housing/engine block

A new engine front cover was manufactured from steel plate as it was easier to fit the external components such as the timing sprockets, bearings, chain tensioner and gear rack guides (see figure 3.30).

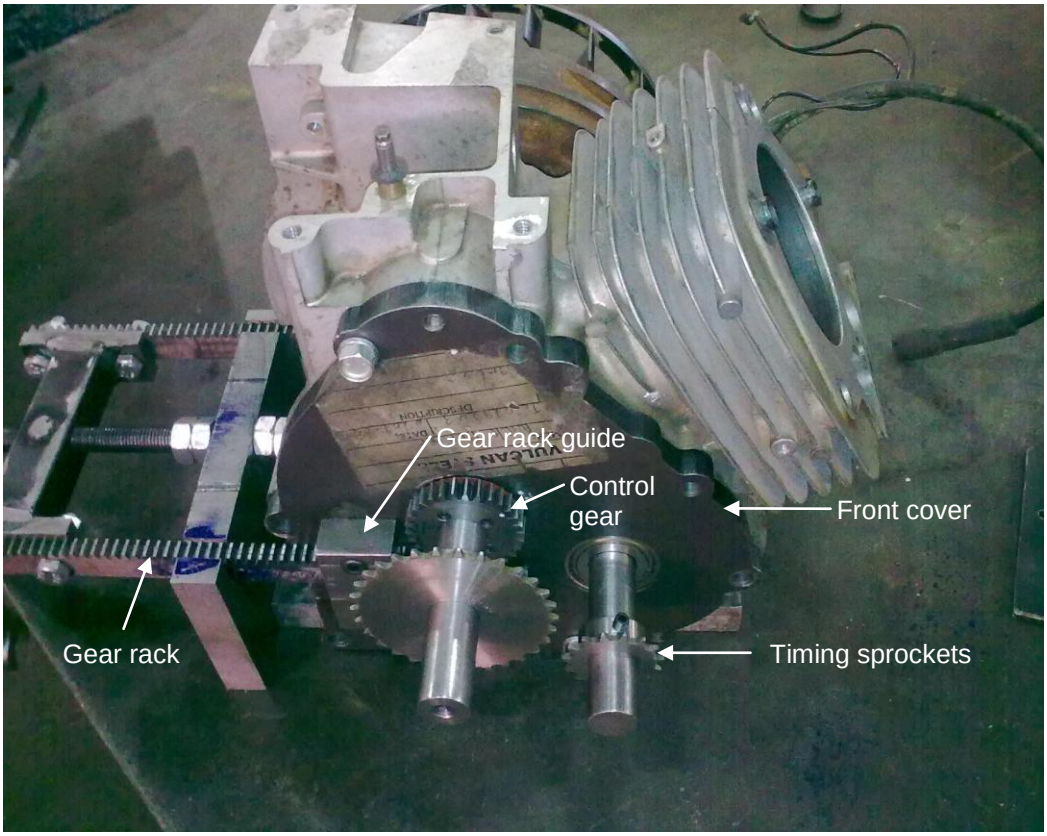

Figure 3.30: Modified crankshaft housing/engine block front cover

3.5.4 Engine Timing

The conventional internal combustion engine is a single piston four stroke spark ignition. Engine timing is managed by controlling the opening and closing of valves (valve timing) and spark ignition to the fuel mixture (ignition timing).

The different strokes are regulated by the valve train. The valve train consists of camshaft, cam followers, push rods, valves and valve lifters/rockers. The intake and exhaust valves have to operate at a specific angular position to the crankshaft thus allowing for the intake, compression, expansion and exhaust strokes to occur (see figure 3.31).

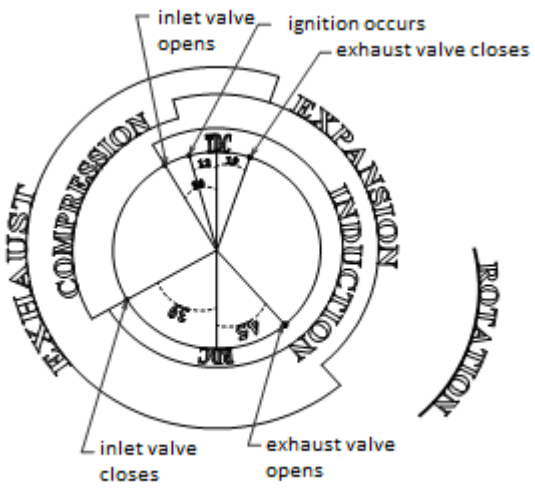

Figure 3.31: Four stroke cycles: Engine timing diagram
(Joel 1971)

During the combustion phase ignition is controlled by an induction coil or voltage transformer which generate the high voltage that causes the spark plug to operate.

In the standard engine the camshaft is driven by the crankshaft by means of a gear train (see figure 3.32). The camshaft rotates at half the crankshaft speed. This gear train is located on the inside of the engine.

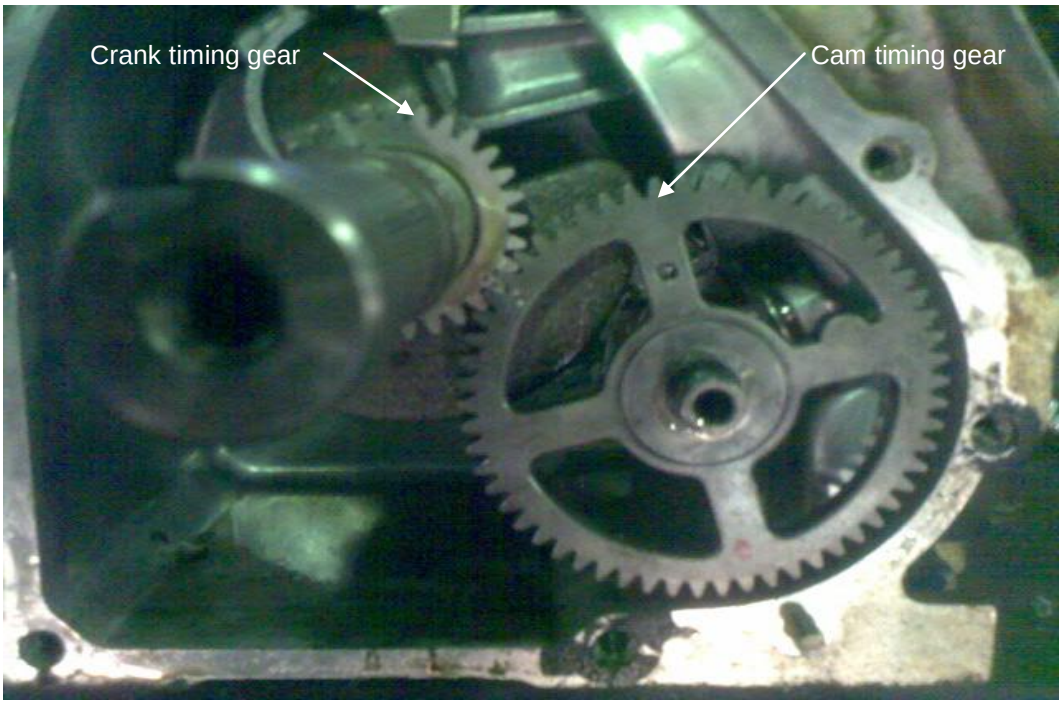

Figure 3.32: Standard engine cam control gears

The camshaft and crank timing gears had to be removed and the camshaft length extended to protrude through the new engine front cover. A new sprocket and chain drive system were introduced to facilitate with the timing process (see figure 3.33). A chain tensioner had to be introduced to ensure that the cam rotation direction is correct as well as maintaining the tension when changing the stroke length (see figure 3.34).

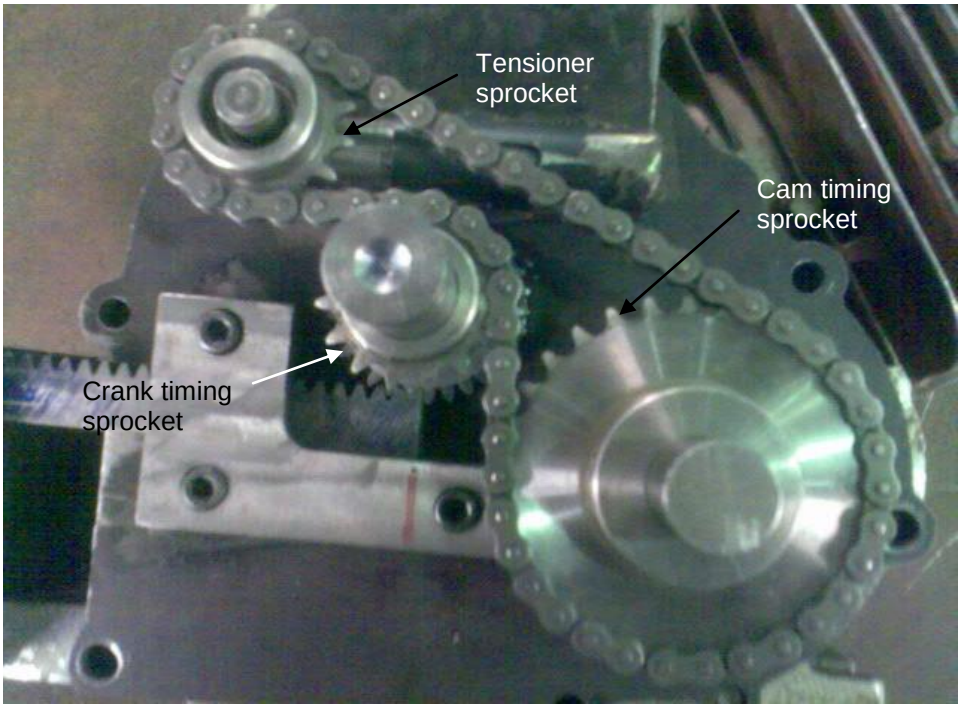

Figure 3.33: Modified engine timing sprockets

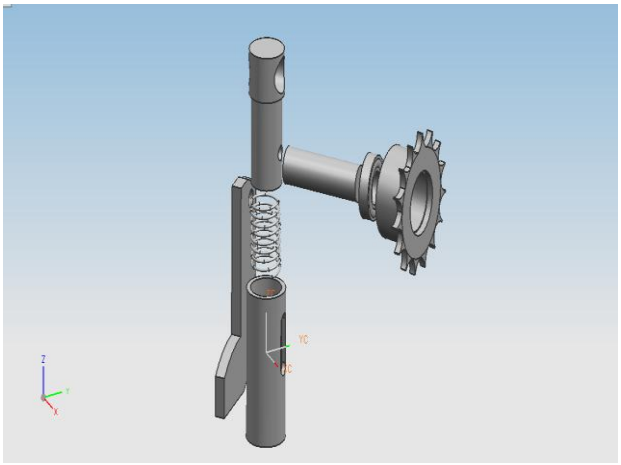

Figure 3.34: Exploded view of chain tensioner

Stone and Ball (2004) state that most spark ignition engines operate with a battery and coil or magneto. The spark plug central electrode operates in a temperature range of 350 °C to 700 °C. If the electrode gets too hot pre-ignition occurs and if operated too cold carbon deposits will build up. Carbon or residue build-up can slow down the combustion process. Ignition timing should occur before the piston reaches TDC position during the compression stroke. Ideally ignition timing should be varied for different speeds and engine loads. This is normally achieved by adding a spring load mechanism coupled to the vacuum operated diaphragm within the distributor.

The prototype has a fixed magneto type ignition system. The permanent magnet is fitted to the flywheel while the coil is connected to the engine housing. An adjustable bracket was manufactured to fit between the coil and engine housing. This allowed for fine tuning of the ignition process (see figure 3.35).

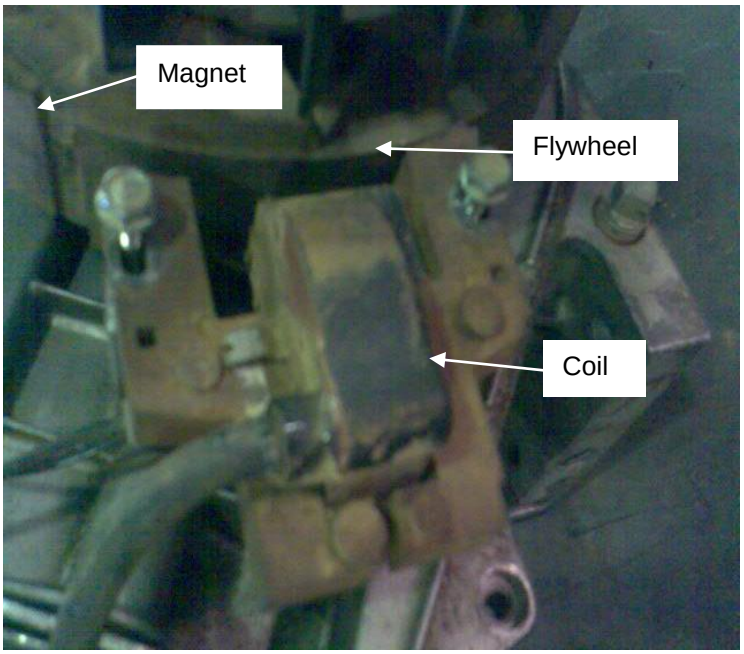

Figure 3.35: Ignition timing components

CHAPTER FOUR

Testing and Evaluation

4.1 Introduction

In order to evaluate the prototype's performance at different stroke levels it was necessary to conduct various tests. The tests included the setting up and running of the engine with the piston arm set for short and long strokes respectively.

4.2 Piston displacement measurement

To measure the piston displacement from TDC to BDC (swept volume) it was necessary to remove the cylinder head. Measurements were taken down the bore of the cylinder. A digital vernier calliper was used to record piston positions within the cylinder. The edge of the vernier scale was placed on the upper edge of the cylinder block (reference point for all measurements) and the vernier depth rod on the piston head. Care was taken ensuring vernier reference position to be the same for all readings taken. The distance measured from the upper edge of the cylinder block to the TDC position was corrected with the thickness of the head gasket (1 mm). This total distance was then also used to calculate the clearance volume within the cylinder block (see figures 4.1 and 4.2).

The crankshaft position was controlled by the gear rack. By marking and counting the number of teeth during its movement it gave an indication of the stroke position. The rack adjustment was carried out by loosening the grub screws and rotating the threaded bar. This allowed free linear travel of the control gear rack on either side of the engine. The side grub screws were re-tightened to avoid movement of the gear rack once the proper crank setting was achieved. The edge of the gear rack's guide plate was used as a fixed reference. The shifting of seven gear rack teeth from the fixed reference point determined the short and long stroke position (see figure 4.3).

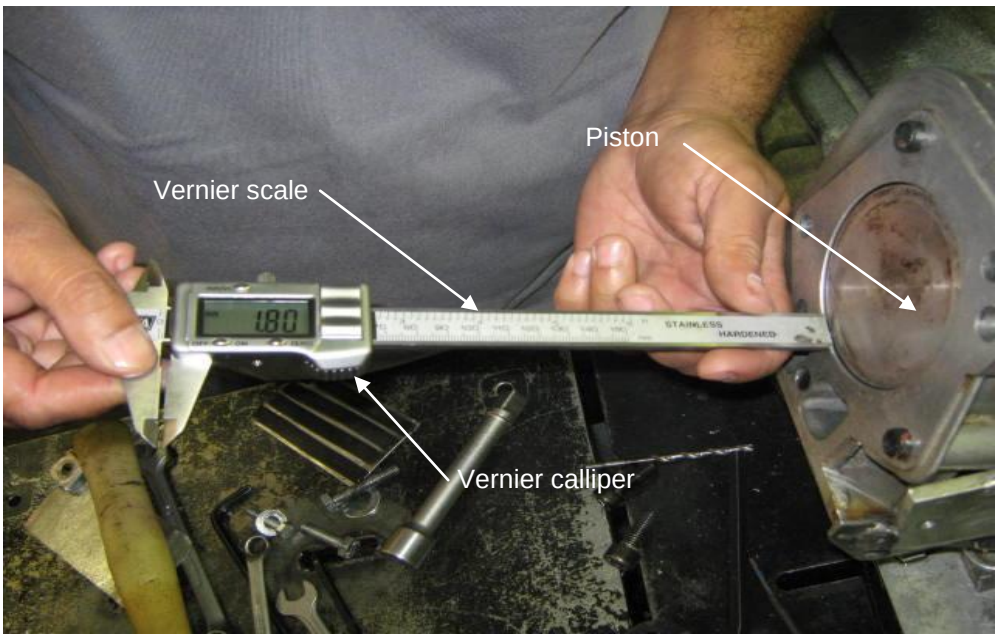

Figure 4.1: Piston displacement (TDC)

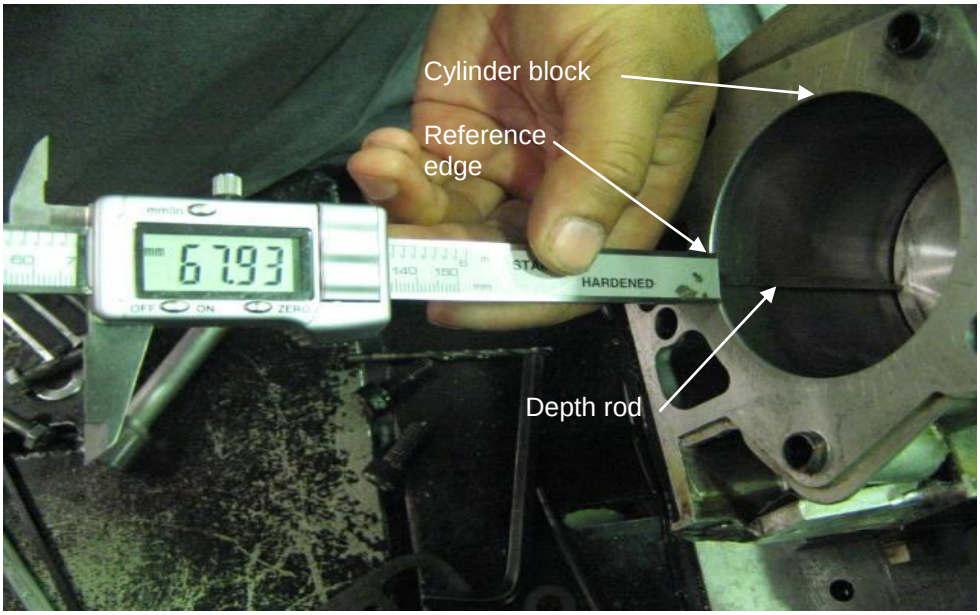

Figure 4.2: Piston displacement (BDC)

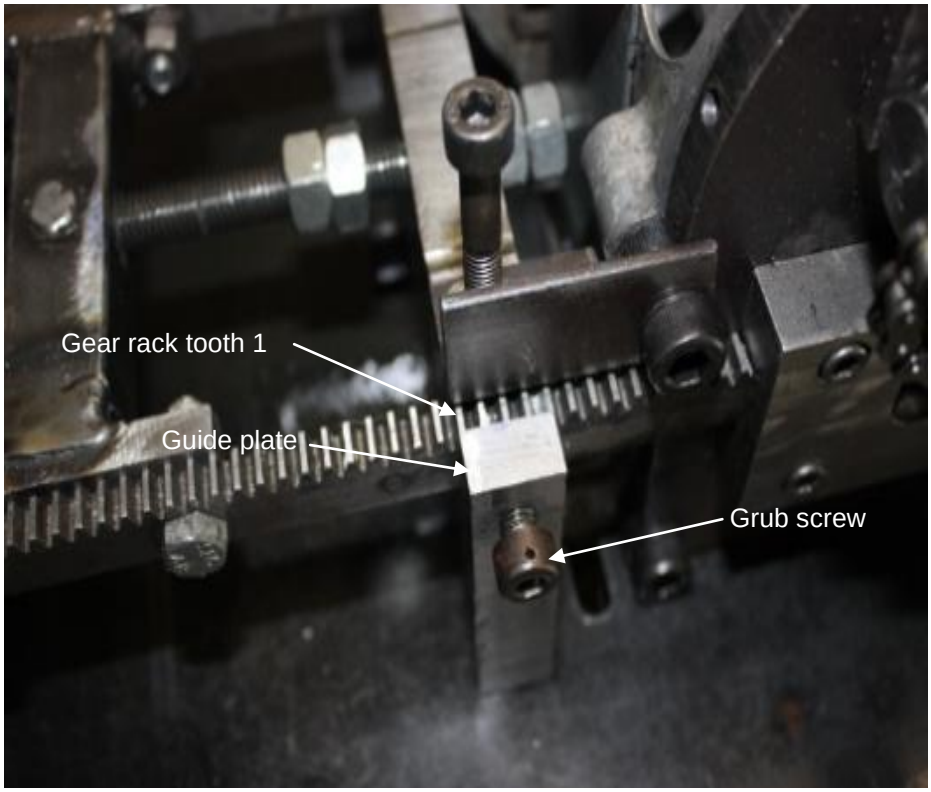

Figure 4.3: Crank position control gear rack

Measurements (in millimetres) were taken from the reference point to the TDC and BDC respectively. A number of tests were conducted to obtain an average on the swept distance (piston travel). Position gear tooth number 1 (see figure 4.3) is the longest stroke that could be achieved. Shifting the gear rack by seven and a half teeth towards the flywheel, it achieved the shortest stroke possible. These were the two extreme conditions that would be considered during testing. See table 4.1 for measurements.

Measuring procedure:

- Set the crank position to the desired stroke length by adjusting the gear rack teeth. Start with the “long stroke” position.
- Move the piston back to TDC and measure the clearance depth from the reference surface to the piston head surface.
- Rotate the crankshaft two times and obtain the measurements at each TDC stroke end position. This ensured a good average measurement.
- Move the piston down to the BDC and measure the depth from the reference surface to the piston head surface.
- Rotate the crankshaft two times and obtain the measurements at each BDC stroke end position to ensure a good average measurement.

- Adjust the stroke length and repeat the above steps until the last mark on the gear rack teeth is reached, which signified the shortest stroke achievable.

Table 4.1: Measurements for piston TDC and BDC

	Test 1			Test 2			Test 3	
Gear tooth no	TDC (mm)	BDC (mm)		TDC (mm)	BDC (mm)		TDC (mm)	BDC (mm)
0	0.53	70.46		0.46	70.55		0.45	70.55
1	0.22	70.22		0.13	70.23		0.30	70.30
2	0.12	70.02		0.15	70.01		0.07	70.00
3	0.40	69.32		0.32	69.52		0.37	69.47
4	0.65	69.06		0.77	69.08		0.72	68.94
5	1.27	68.33		1.19	68.50		1.26	68.49
6	1.75	67.38		1.76	67.91		1.86	67.74
7	2.19	67.03		2.13	67.45		2.33	67.48
7.5	2.49	67.38		2.40	67.32		2.46	67.30

The volume of the combustion chamber was measured by pouring water into the cavities until it was level with the cylinder head face. The amount of water collected is equal to the combustion clearance volume of the cylinder head (40 ml) (see figure 4.4.). The measurement of volume from the reference cylinder block edge position to the TDC position must be added to this clearance volume.

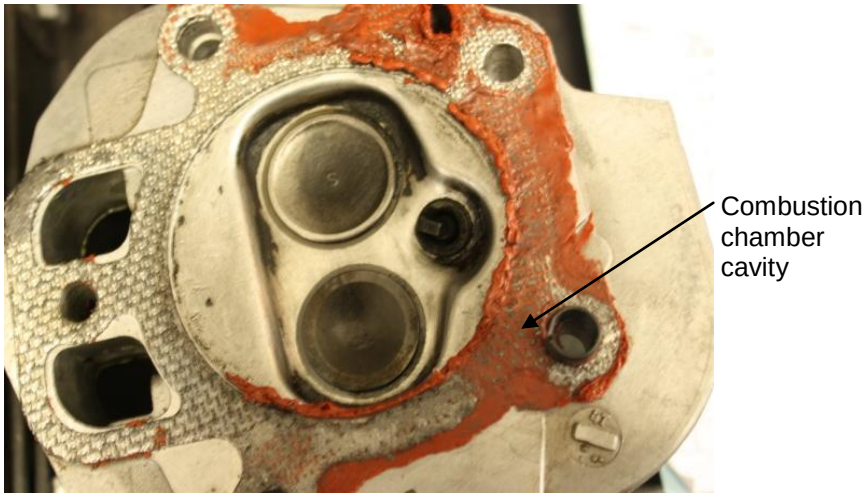

Figure 4.4: Cylinder head cavities

Method to calculate engine capacity:

Engine displacement = Area of cylinder x stroke length x number of cylinders.

Area of cylinder:

$$A = \frac{\pi d^2}{4}$$

$$A = \frac{\pi \times 0.079^2}{4}$$

$$\therefore A = 0.0049\, m^2$$

From table 4.1 and 4.2 the longest stroke length is at gear position “0” and shortest at “7.5”. The average long stroke length equals 70.04 mm and short stroke length equals 64.88 mm.

Engine capacity **long stroke**

$$Capacity = 0.0049 \times 0.07004 \times 1$$

$$Capacity = 343.2 \times 10^{-6}\ m^3$$

$$Capacity = 343.2\, cc$$

Engine capacity **short stroke**

$$Capacity = 0.0049 \times 0.06488 \times 1$$

$$Capacity = 317.91 cc$$

Table 4.2: Engine displacement data

Gear tooth no.	TDC Ave (mm)	BDC Ave (mm)	Swept length (mm)	Swept volume (m^3)	Clearance Volume Total (m^3)	CR	Engine Cap. (cc)
0	0.48	70.55	70.04	0.00034331	4.72545E-05	8.265	343.31
1	0.22	70.25	70.03	0.00034328	4.59637E-05	8.469	343.28
2	0.11	70.01	69.90	0.00034261	4.54572E-05	8.537	342.61
3	0.36	69.44	69.07	0.00033857	4.66826E-05	8.257	338.58
4	0.71	69.03	68.31	0.00033484	4.83982E-05	7.919	334.85
5	1.24	68.44	67.20	0.00032939	5.09797E-05	7.461	329.39
6	1.79	67.74	65.59	0.00032324	5.36757E-05	7.022	323.24
7	2.22	67.32	65.10	0.00031911	5.5767E-05	6.722	319.11
7.5	2.45	67.33	64.88	0.00031803	5.69108E-05	6.588	318.03

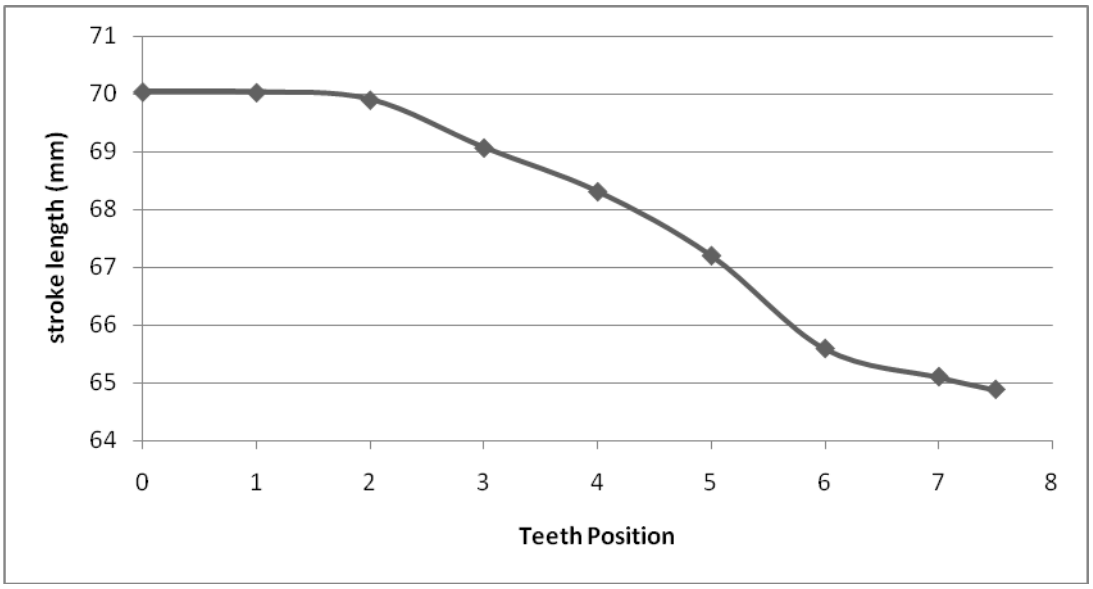

Figure 4.5: Stroke length vs teeth position

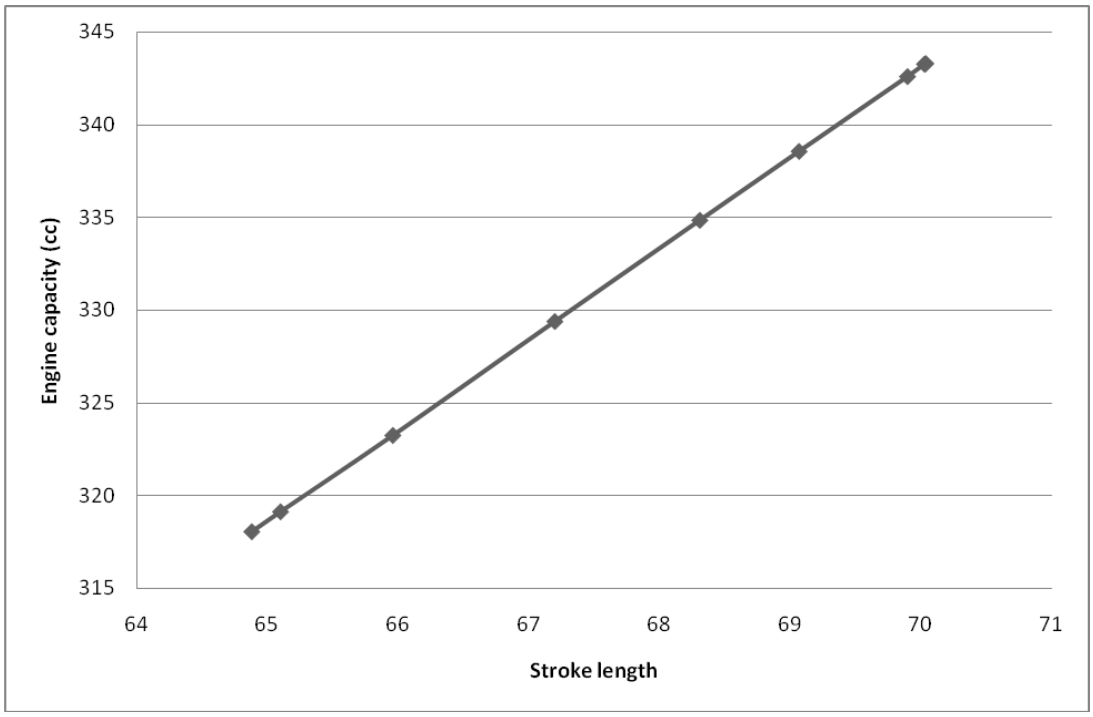

Figure 4.6: Stroke length vs Engine capacity

Adjusting the crank shaft position from the long stroke to the short stroke (using the gear rack teeth position) yielded a difference in stroke length of 5.16 mm. With this increase in stroke length the engine capacities increased by 25.29 cc (see figures 4.5, 4.6 and table 4.2).

4.3 Engine power absorption test

The engine was tested by driving it with an electric motor, sprockets and chain. By monitoring the power consumed by the electric motor it was possible to determine the power consumption characteristics of the engine. See figure 4.7 for test set-up.

The Nanovip power harmonic analyser was used to measure line voltage, current, power factor, frequency and power. The sample speed was limited by 2 samples per second. This was the only power analyser available at the time of the test.

A tacho-meter was used to measure the rpm of the electric motor and that of the engine.

The following specifications refer to the electric motor:

Power	2.2 kW
Phase	3
Voltage	380 V
Motor speed	1480 rpm

The following specifications refer to the drive train:

Small sprocket	13 teeth
Large sprocket	55 teeth
Ratio	1:4.23
Drive	chain

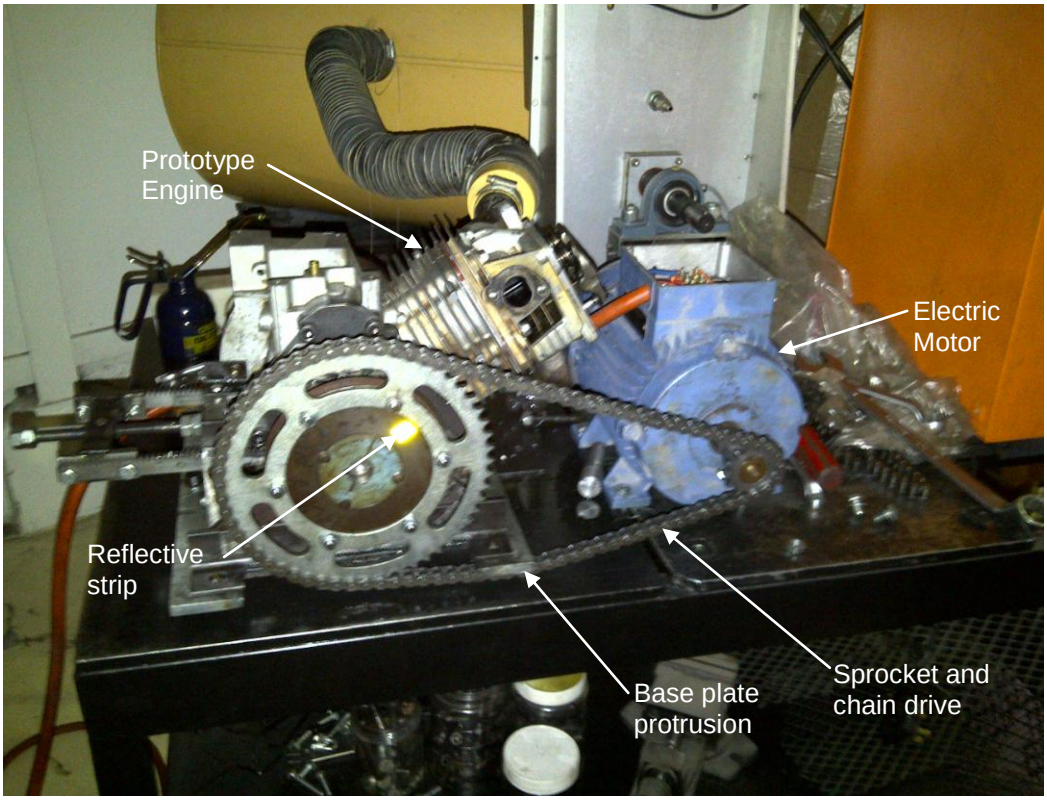

Figure 4.7: Engine test set-up

4.3.1 Electric motor and drive train test

The first test conducted was to determine the amount of power absorbed by the electric motor and drive train. The power harmonic analyser was connected to the wiring of the electric motor. A dummy shaft and bracketing to hold the larger sprocket in place were machined to allow rotation of the drive train without the engine connected (see figure 4.8).

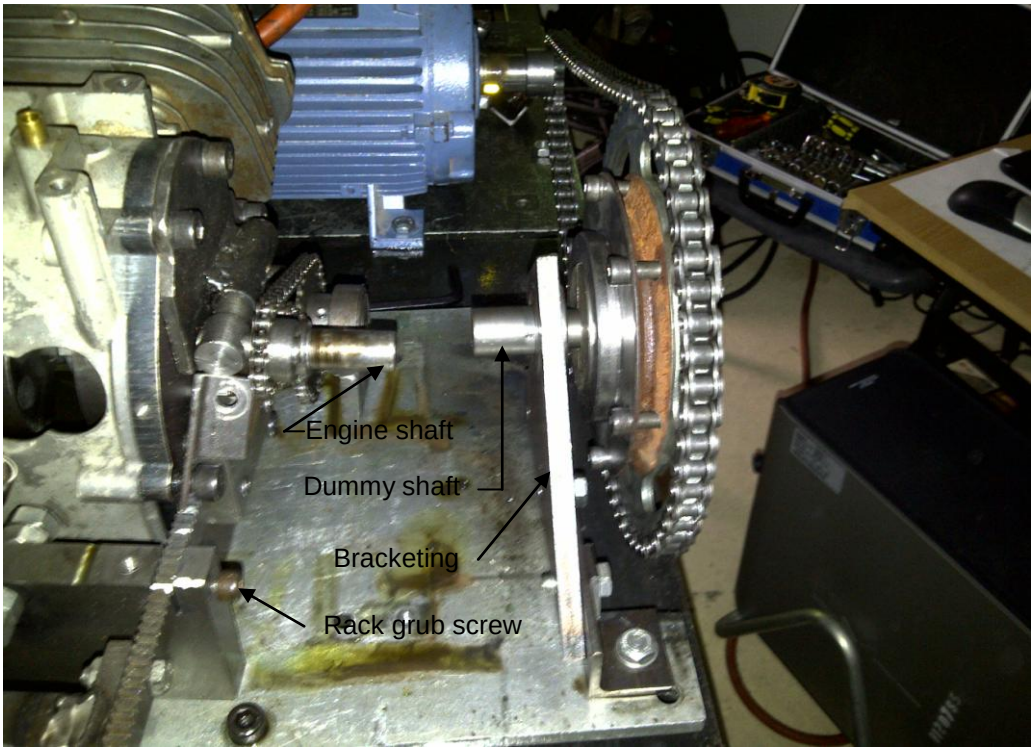

Figure 4.8: Motor and drive train set-up

The following data were recorded and used to calculate the power (see figure 4.9).

$Motor\ \ Speed = 1489\,rpm$

$Engine\ \ Speed = 352\,rpm$

$\sqrt{3} = 3 Phase\ Star\ Connection$

$V_L = Line Voltage = 390 V$

$I_L = Line Current = 2.12\ A$

$Cos\phi = Power\ Factor = 0.06$

$P = \sqrt{3} \times V_L \times I_L \times Cos\phi$

$P = 86 W$

(Formulae: Morley and Hughes 1994)

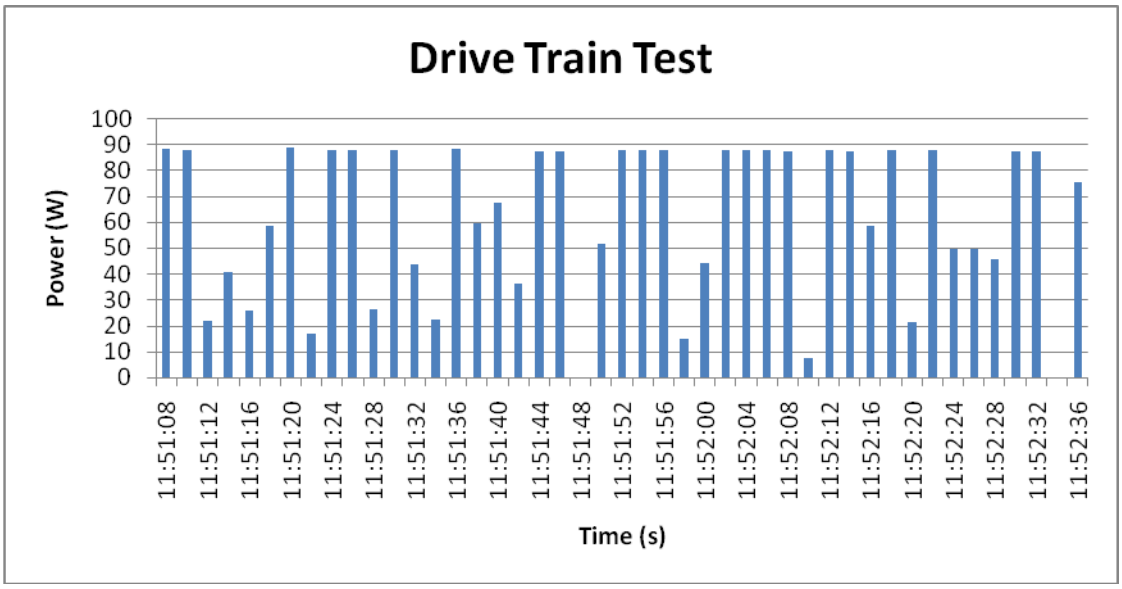

Figure 4.9: Motor and drive train test

A constant approximately 90 W peak power was noted. The dips on the graph can be attributed to chain flapping and the movement of the chain links over the small piece of base plate protrusion (see figure 4.7).

The power absorbed by the drive train was calculated to be 86 W, which is in good agreement with the peak data reflected in figure 4.9 and appendix B.

4.3.2 Spark plug removed

With the engine re-connected to the big sprocket and the spark plug removed measurements were taken to determine the losses in terms of power absorbed by friction of moving components and the restriction of air flow through the spark plug hole.

The following data were recorded and used for the calculation of power loss.

$Motor\ \ Speed = 1489\,rpm$

$Engine\ \ Speed = 352\,rpm$

$\sqrt{3} = 3 Phase\ Star\ Connection$

$\mathrm{V_L} = Line\,Voltage = 391.4\,V$

$\mathrm{I_L} = Line\,Current = 2.216\,A$

$\mathrm{Cos}\phi = Power\ Factor = 0.196$

$\mathrm{P} = \sqrt{3} \times \mathrm{V_L} \times \mathrm{I_L} \times \mathrm{Cos}\phi$

$\mathrm{P} = 294\,W$

(Formulae: Morley and Hughes 1994)

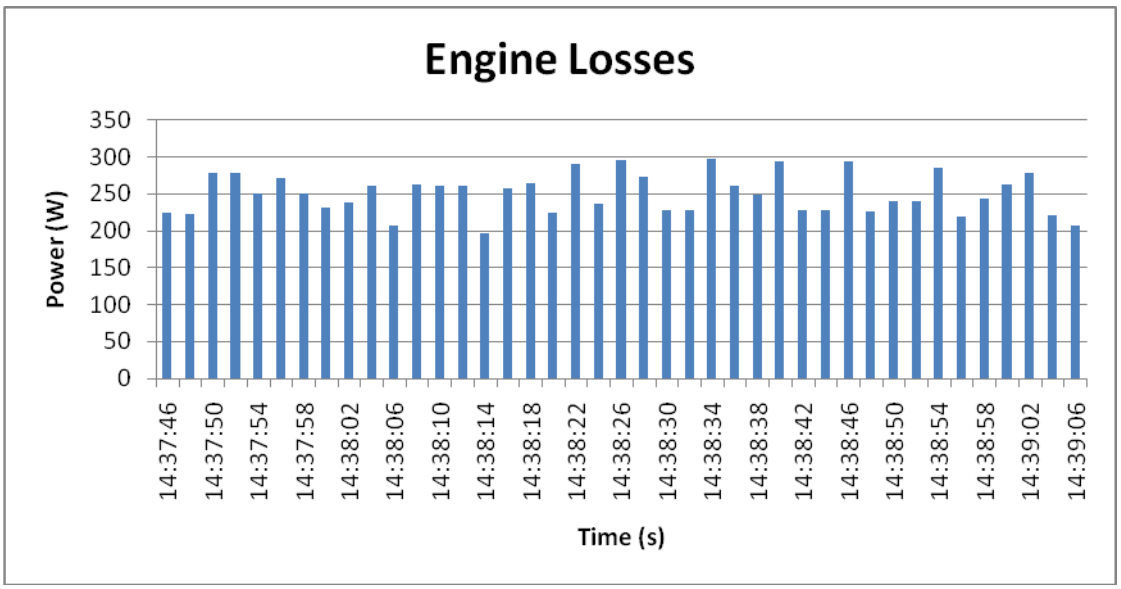

Figure 4.10: Motor, drive train and engine with spark plug removed

The peak power recorded was approximately 290 W. This peak power consumption attributed to the compression stroke. Dips in the graph can be attributed to the valves opening during the different strokes relieving more pressure than what occurred through the plug hole. The variance in the peak power was probably due to 2 samples taken per second; therefore stroke position readings were not consistently read during the recording of the data.

The peak power absorbed by the engine and drive train was calculated to be 294 W. This is in agreement with the peak data shown on the graph in figure 4.10. Engine power absorbed due to friction and air flow restriction at the spark plug hole is therefore calculated as 294-86=208 W.

4.3.3 Long stroke

With the engine set to operate at long stroke position, the peak power recorded was 1924 W. This peak power consumption was caused by the compression stroke. The slight variance in peak power on the graph can be attributed to only being able to record 2 samples per second. This meant that the chance of catching the maximum peak at the same time was limited. The lower dips in the graph can be attributed to the expansion, exhaust and suction strokes.

The following data were recorded and used for the calculation of power.

$Motor\ \ Speed = 1489\,rpm$

$Engine\ \ Speed = 352\,rpm$

$\sqrt{3} = 3 Phase\ Star\ Connection$

$V_L = Line\,Voltage = 386.9\,V$

$I_L = Line\,Current = 3.983\,A$

$Cos\phi = Power\ Factor = 0.721$

$P = \sqrt{3} \times V_L \times I_L \times Cos\phi$

$P = 1924\,W$

(Formulae: Morley and Hughes 1994)

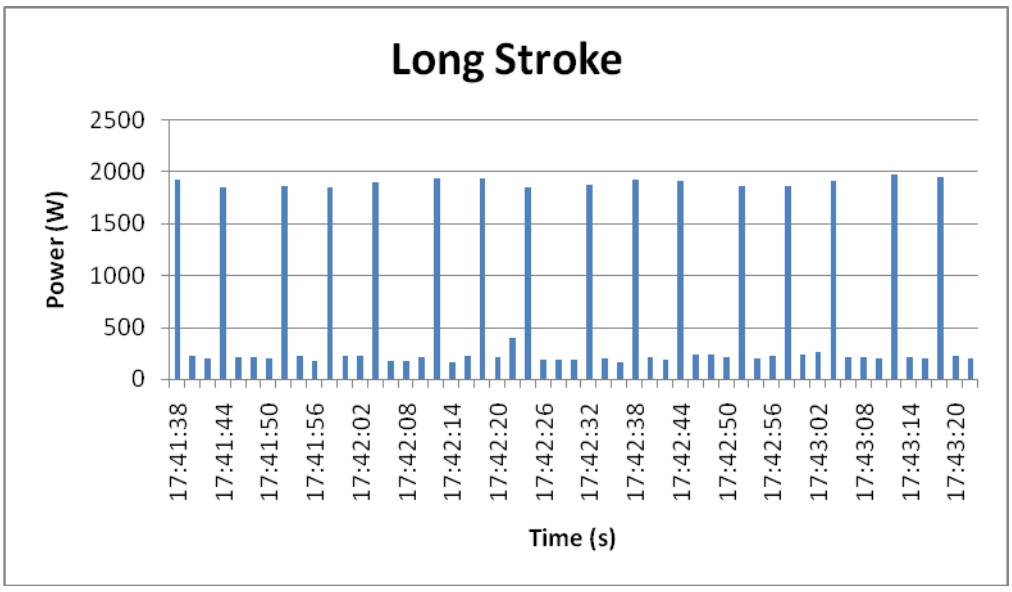

Figure 4.11: Extract of long stroke graph

The peak power absorbed by the engine (long stroke) and drive train was calculated to be 1924 W which compares well with the peak data reflected on the graph in figure 4.11. Engine power absorbed due to friction and air flow restriction 294-86=208 W. Max engine power absorbed (long stroke) to compress the air was; 1924-208=1716 W.

4.3.4 Short stroke

With the engine set to operate at short stroke position the peak power recorded was 1544 W. This peak power consumption was caused by the compression stroke. The slight variance in peak power on the graph can be attributed to the rate of only 2 samples per second, as stated before. The lower dips in the graph (figure 4.12) can be attributed to the expansion, exhaust and suction strokes.

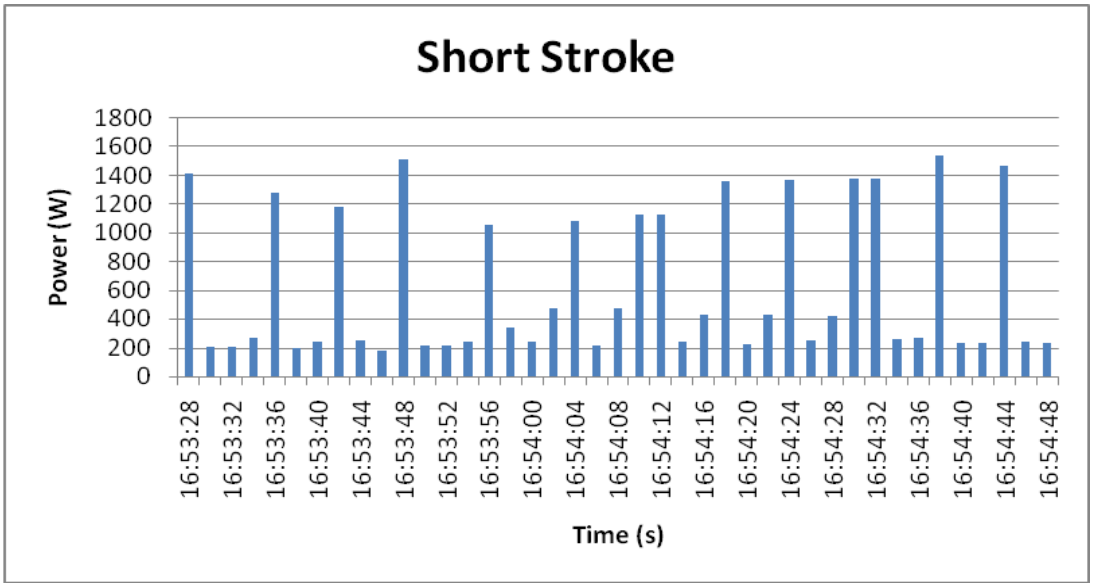

Figure 4.12: Extract of short stroke graph

The calculation of power was done using the following data:

$$P = \sqrt{3} \times V_L \times I_L \times Cos\phi$$

$$P = Power$$

$$\sqrt{3} = 3 Phase\ Star\ Connection$$

$$V_L = Line\ Voltage = 391.6\,V$$

$$I_L = Line\ Current = 3.434\,A$$

$$Cos\phi = Power\ Factor = 0.663$$

$$P = \sqrt{3} \times V_L \times I_L \times Cos\phi$$

$$P = 1544\,W$$

(Formulae: Morley and Hughes 1994)

The peak power absorbed by the engine (short stroke) and drive train was calculated. Engine power absorbed due to friction and air flow restriction 294-86=208 W. Engine power absorbed in compressing the air was 1544-208=1336 W.

4.4 Engine compression test

Compression tests were carried out for the long and short stroke conditions. Pressure transducers coupled to an oscilloscope were used to record the data. Two 0-16 bar pressure range transducers were used (see figure 4.13 and appendix C).

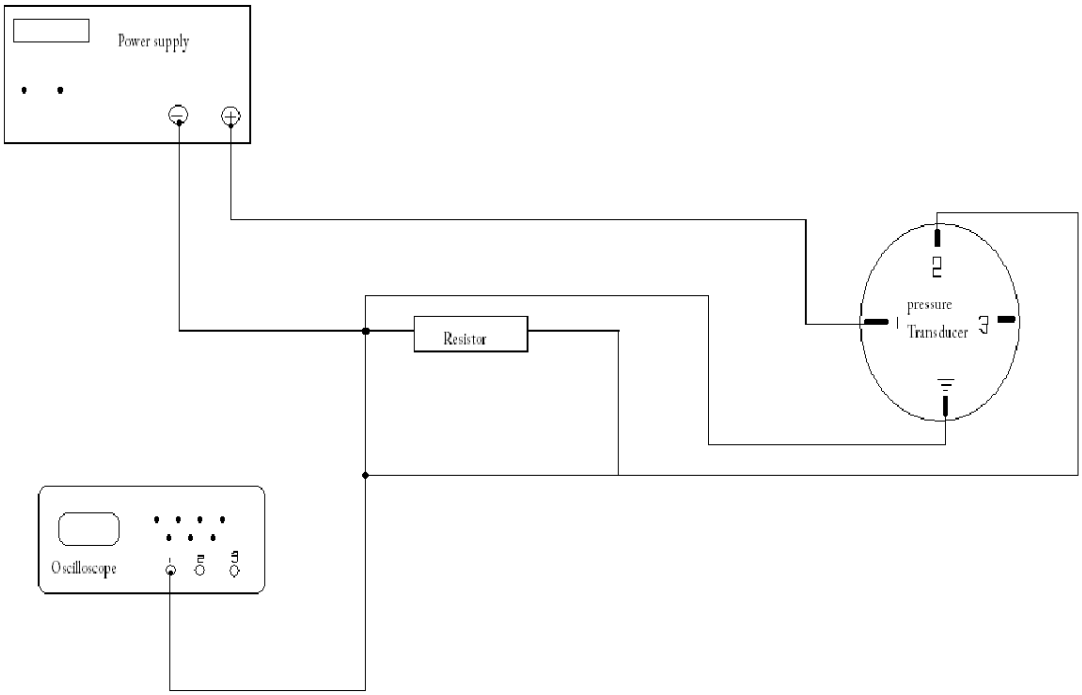

Figure 4.13: Pressure test equipment lay-out

A plug adaptor was manufactured that allowed the pressure transducer to be inserted into the spark plug hole (see figure 4.14).

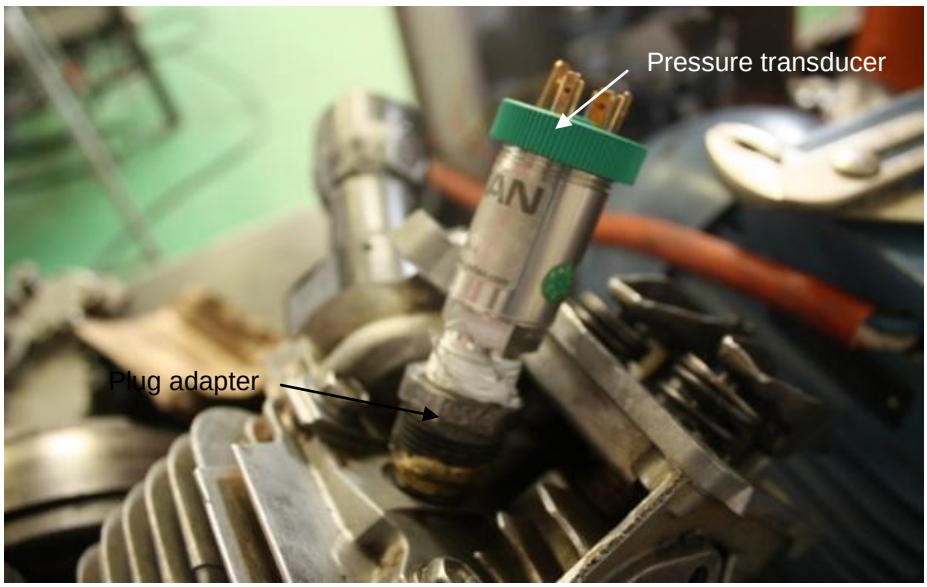

Figure 4.14: Pressure transducer plug

4.4.1 Engine pressure transducer test (long and short stroke)

Two 16 bar pressure transducers were used to record the level of pressure during tests. The tests were done with both transducers. The results were overlaid and are shown in figures 4.15 and 4.16. See appendix C for individual graphs. From the initial starting point (datum) to the apex shows the compression stroke. From the apex to the datum line represents the expansion stroke. The plateau shows the suction and exhaust strokes.

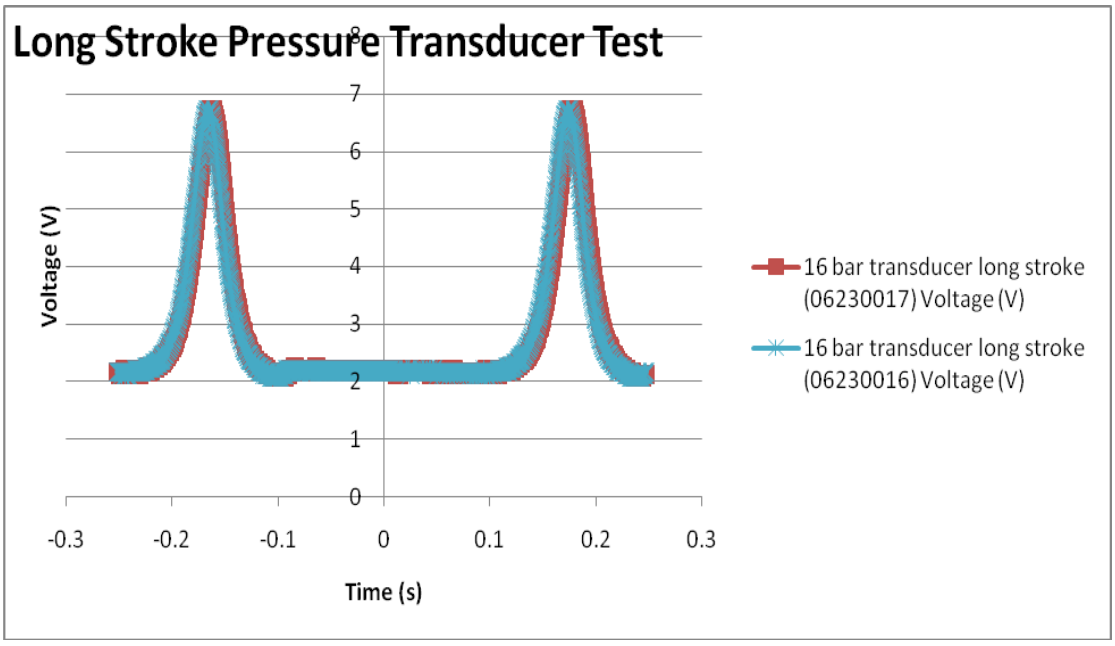

Figure 4.15: Long stroke pressure transducer test

Pressure range 0→16 bar = 4 → 20 mA

From the pressure: 16-0 =16 bar

From current range: 20-4 = 16 mA

Therefore pressure/ current ratio = (16/16) = 1 bar/mA

$$I = \frac{V}{R}$$

$$\Rightarrow I = \frac{6.72 - 2.16}{500}$$

$$\therefore I = 0.00912(A)$$

$$I = 9.12\,mA$$

$$P = \frac{16}{16} \times 9.12$$

$$\Rightarrow P_{gauge} = 9.12\,bar$$

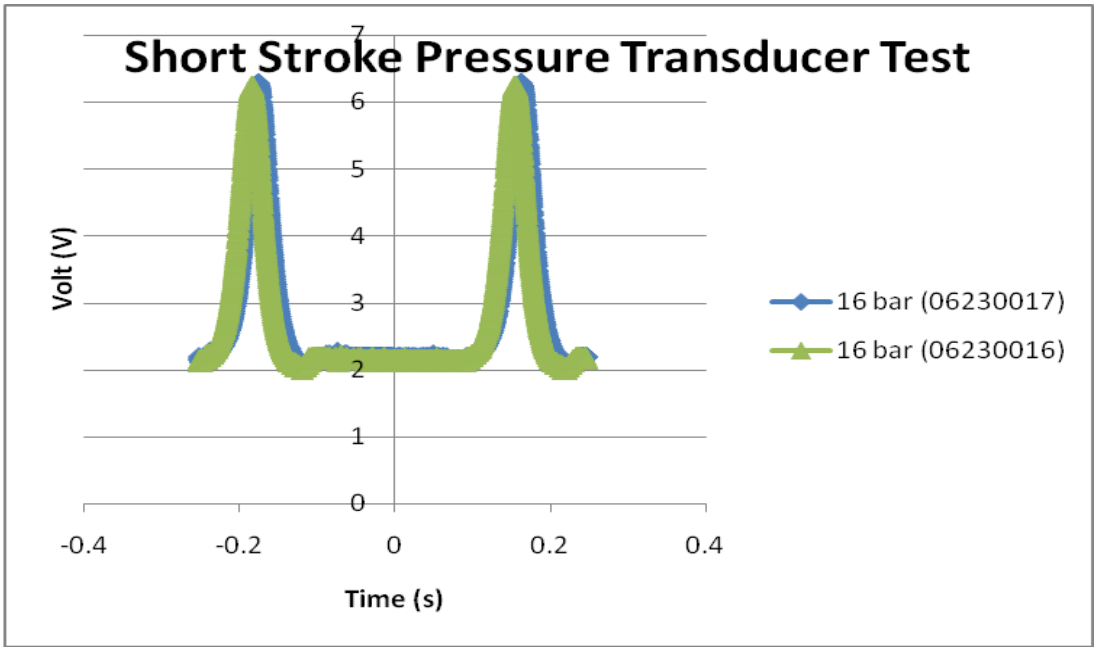

Figure 4.16: Short stroke pressure transducer test

Pressure range 0→16 bar = 4 → 20 mA

From the pressure: 16-0 =16 bar

From current range: 20-4 = 16 mA

Therefore pressure/ current ratio = (16/16) = 1 bar/mA

$$I = \frac{V}{R}$$

$$\Rightarrow I = \frac{6.28 - 2.16}{500}$$

$$\therefore I = 0.00824(A)$$

$$I = 8.24\,mA$$

$$P = \frac{16}{16} \times 8.24$$

$$\Rightarrow P_{gauge} = 8.24\,bar$$

An increase in compression of 0.88 bars from the short to long stroke is noted.

4.5 Engine temperature test

The temperature readings during compression were also determined when driving the engine with the electrical motor. The temperatures were measured by removing the spark plug and inserting a plug adapter that could accommodate a thermocouple. The tip of the thermocouple protruded into the hollow cavity of the plug adapter. A slight gap was allowed around the thermocouple probe to allow a small quantity of air to pass over the thermocouple, thus preventing stagnation pockets from forming during the compression stroke. Ideally one would want to measure instantaneous temperature at the peak of the compression stroke, but this was not possible with the available equipment at hand. The thermocouple probe was later replaced with a made up K-Type Chrome-Aluminium thermocouple without a sleeve/casing in an attempt to improve the accuracy of temperature readings. The made up K-Type thermocouple was calibrated with the standard thermocouple and a mercury thermometer. The standard thermocouple probe was connected to a Wika temperature indicator and the made up thermocouple was connected to a Pico data logger. The results were compared and found to be reasonably accurate comparable to each other (see figure 4.17, 4.18 and appendix D).

Figure 4.17: Thermocouple plug adapter

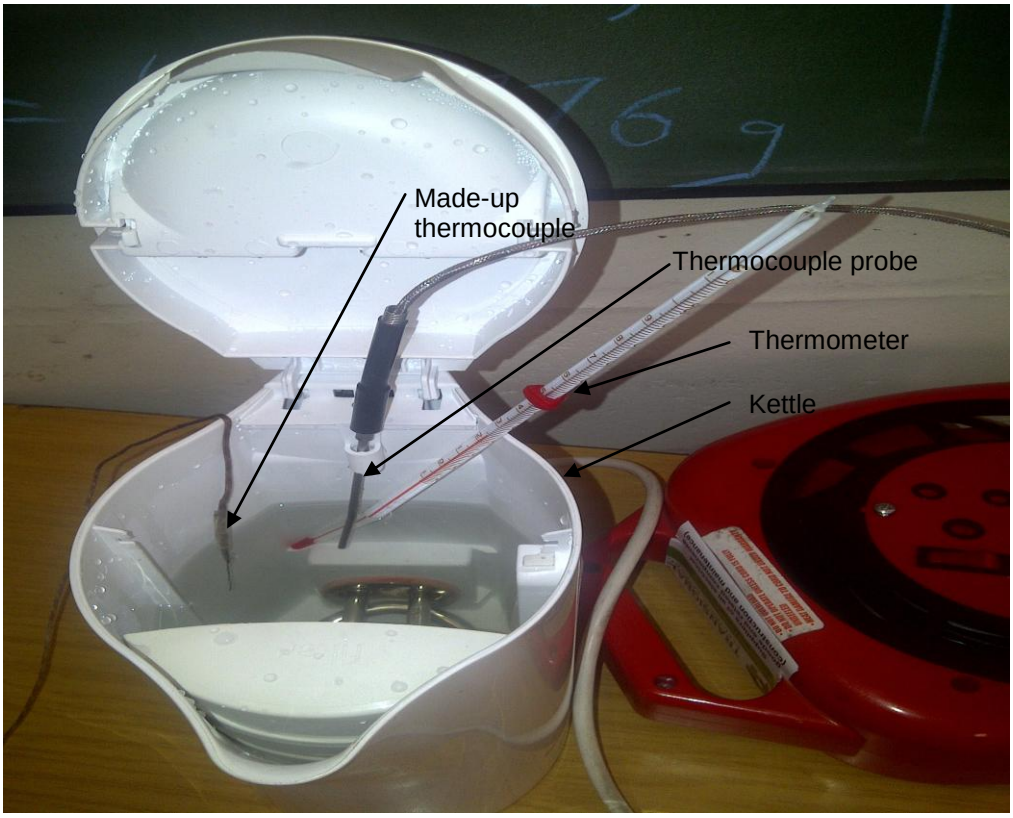

Figure 4.18: Calibration set-up

4.5.1 Engine temperature test (long and short stroke)

Long stroke

Ambient temperature = T1 = 27.98°C

Maximum temperature = T2 = 178.33°C

Ambient pressure absolute = P1 = 1.01325 bar

Maximum pressure absolute = P2 = 10.133 bar

Engine speed = 352rpm

Short stroke

Ambient temperature = T1 = 28.06°C

Maximum temperature = T2 = 167.5°C

Ambient pressure absolute = P1 = 1.01325 bar

Maximum pressure absolute = P2 = 9.493 bar

Engine speed = 352rpm

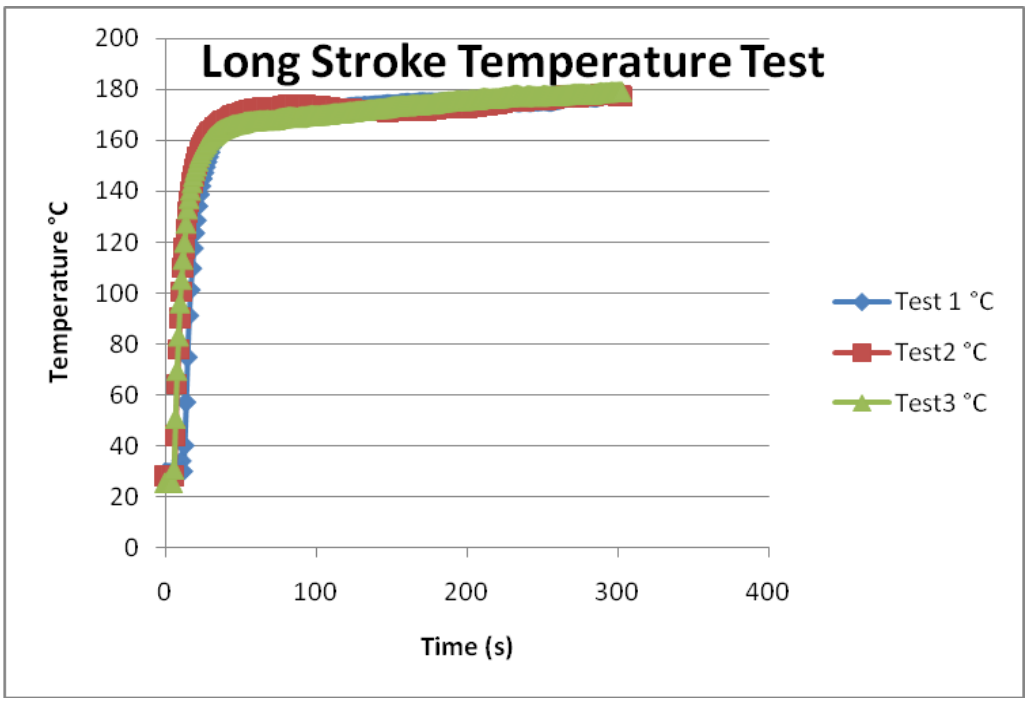

Figure 4.19: Test graph at long stroke

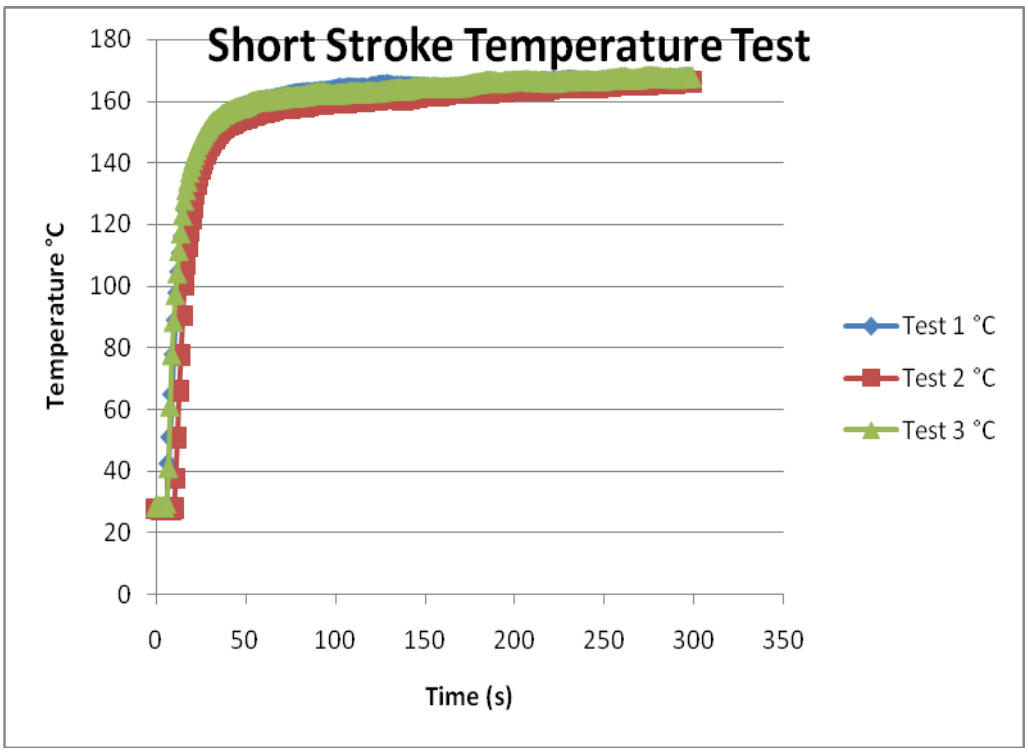

Figure 4.20: Test graph at short stroke

4.6 Determining air compression power

According to Joel (1996) in order to determine the air compression power it is necessary to plot a pressure vs volume graph. The area under the PV graph will determine the work done. By dividing the work done by the time taken will lead to the power. The Polytropic process $PV^n = C$ must be adhered to. The n value (Polytropic coefficient) will lie between 1 and 1.7; according to Joel it will most likely be within the range of 1.2 to 1.5.

Determine Polytropic coefficient (n value) for the **long stroke** conditions

$P_2 = 9.12 + 1.01325 = 10.133\,bar$

$P_1 = 1.01325\,bar$

$T_2 = 451.33\,K$

$T_1 = 300.98\,K$

$$\frac{T_2}{T_1} = \left(\frac{P_2}{P_1}\right)^{\frac{n-1}{n}}$$

$$\frac{451.33}{300.98} = \left(\frac{10.133}{1.01325}\right)^{\frac{n-1}{n}}$$

$$\ln(1.49953) = \frac{n-1}{n}\ln(10.00049)$$

$$0.17595n = n - 1$$

$$n = 1.2135$$

(Formulae: Rayner Joel 1996)

Determine n value for the **short stroke** conditions

$P_2 = 8.24 + 1.01325 = 9.25325\,bar$

$P_1 = 1.01325\,bar$

$T_2 = 440.5\,K$

$T_1 = 301.06\,K$

$$\frac{T_2}{T_1} = \left(\frac{P_2}{P_1}\right)^{\frac{n-1}{n}}$$

$$\frac{440.5}{301.06} = \left(\frac{9.25325}{1.01325}\right)^{\frac{n-1}{n}}$$

$$\ln(1.46316) = \frac{n-1}{n}\ln(9.1323)$$

$$0.1602n = n - 1$$

$$n = 1.191$$

(Formulae: Rayner Joel 1996)

From the calculations, the Polytropic coefficient n for the long stroke was found to be 1.214 and 1.205 for the short stroke. The n values will be used to construct the volume axis on the graph as the readings from the Oscilloscope presented the graph in volt vs time.

To convert the volts to pressure we have to take into account a conversion factor (see figure 4.21).

$1\,mA \equiv 10^5\ Pa$

$V = IR$

$V = 1\ mA \times 500\ \Omega$

$10^5\ Pa \equiv 0.5\ V$

$1V \equiv 20\ \ kPa$

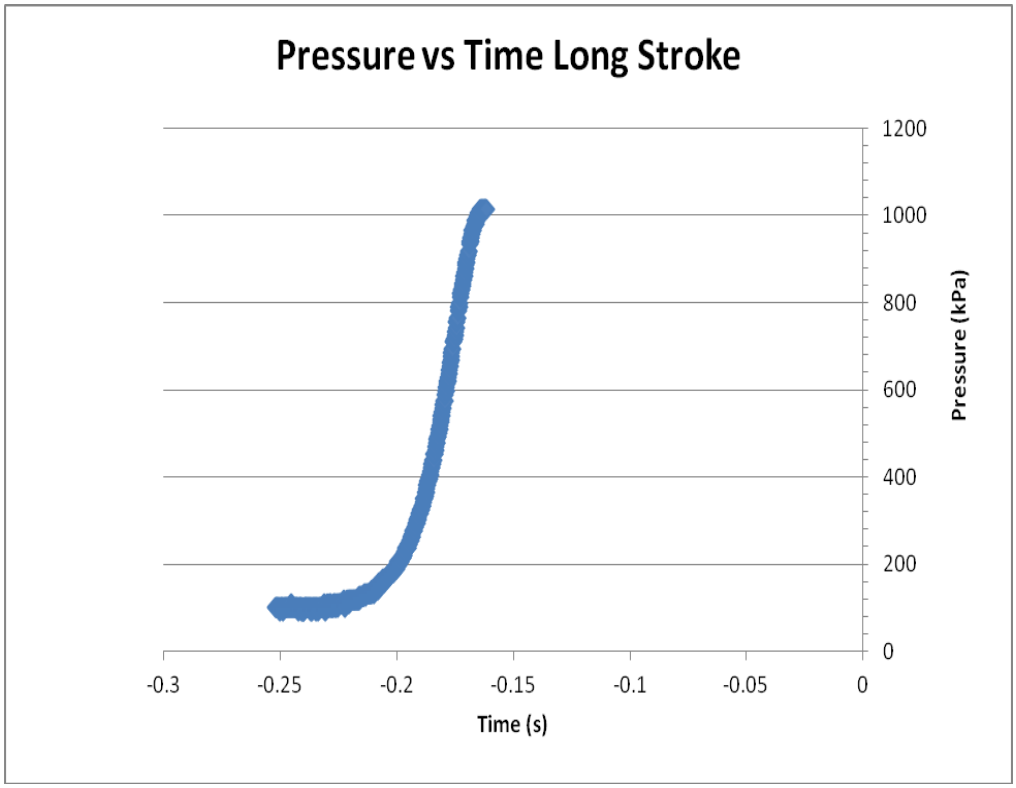

Figure 4.21: Compression (long stroke condition Pressure vs Time)

A maximum pressure of 10.13 bars (absolute) was noted during the compression stroke. The engine speed was 352 rpm.

Determine the power for the **long stroke** conditions

By using the expression $P_1 (V_1)^n = P_2 (V_2)^n$ (from Joel 1996) a relationship between the pressure and volume curve was established. See figure 4.22.

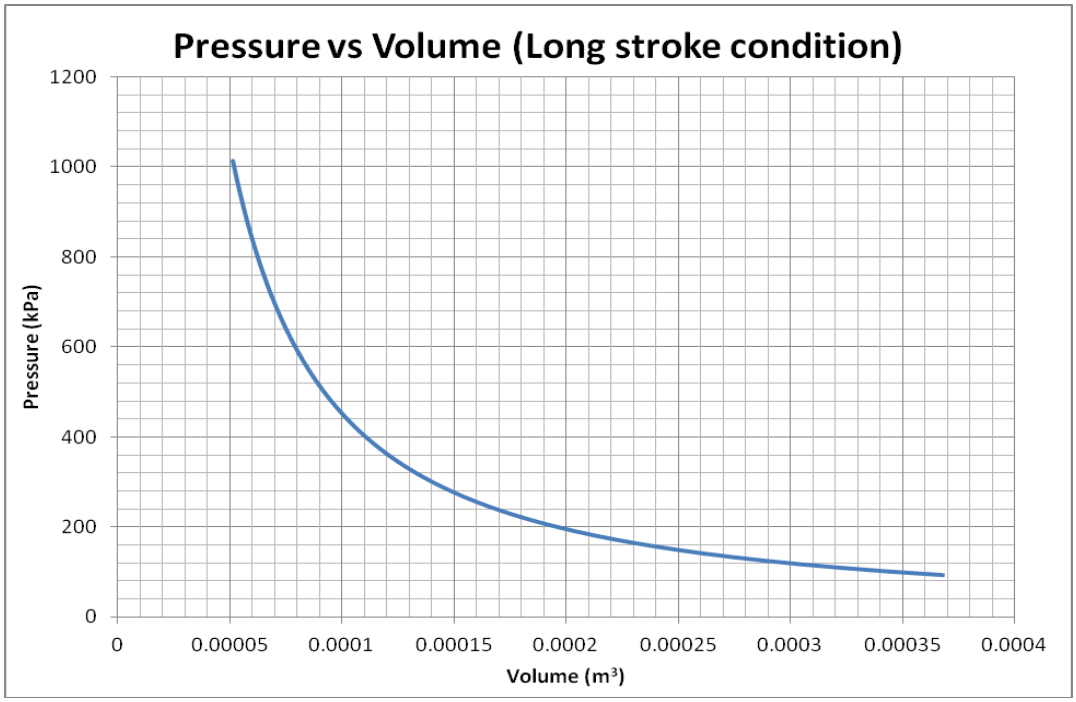

Figure 4.22: Compression (long stroke condition Pressure vs Volume)

A maximum pressure of 10.13 bar (absolute), clearance volume of 5.15×10^{-5} m^3 and swept volume of 34.33×10^{-5} m^3 was noted for the duration of the compression stroke. Two methods of determining the work done was employed, Joel Formulae and calculating the area under the graph.

$$Work\ \ Done\ (W) = \frac{P_2V_2 - P_1V_1}{n-1}$$

$$W = \frac{1013300 \times 5.148 \times 10^{-5} - 101325 \times 34.331 \times 10^{-5}}{1.2135 - 1}$$

$$W = 81.382\ Joules$$

(Formulae: Rayner Joel 1996)

The compression stroke occurs during every alternate revolution of the crankshaft.

$$Time\ to\ complete\ one\ revolution\ t_p = \frac{2\pi}{\omega}$$

$$\omega = \frac{2\pi N}{60}$$

$$\therefore t_p = \frac{60}{N}$$

$$t_p = \frac{60}{352}$$

$$t_p = 0.17\ s$$

$$Due\ to\ every\ alternate\ stroke\ \frac{1}{2}t_p$$

$$Actual\ \ t_p = 0.085\,s$$

$$Power\ \ (P) = \frac{J}{t}$$

$$P = \frac{81.382}{0.085}$$

$$P = 957.44\ Watts$$

The work done was calculated using Joel's formulae and amounted to 81.4 Joules while by measuring the area under the PV diagram the amount of work indicated was 85.4 Joules. Hence the theoretical power calculated amounts to 957.44 W, while using the area measuring method the power indicated was 1002 W. A difference of less then 5 % is noted between the two methods.

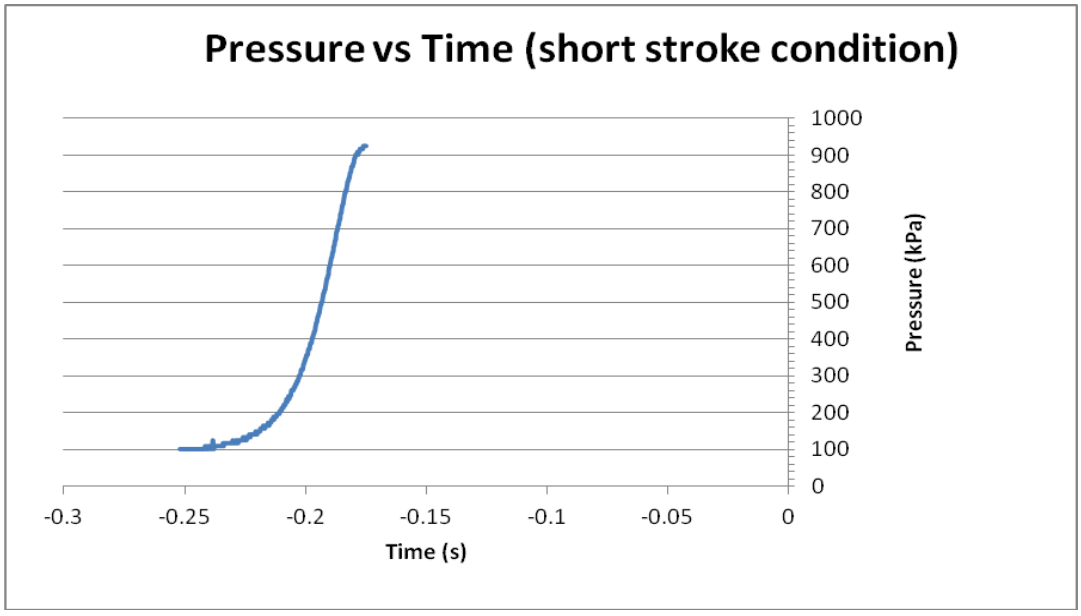

Figure 4.23: Compression (short stroke condition Pressure vs Time)

A maximum pressure of 9.25 bar (absolute) was recorded during the compression stroke. The engine speed was 352 rpm.

Determine the power for the **short stroke** conditions

Similarly to the long stroke condition using the expression $P_1 (V_1)^n = P_2 (V_2)^n$ (from Joel 1996) a relationship between the pressure and volume curve was established for the short stroke condition.

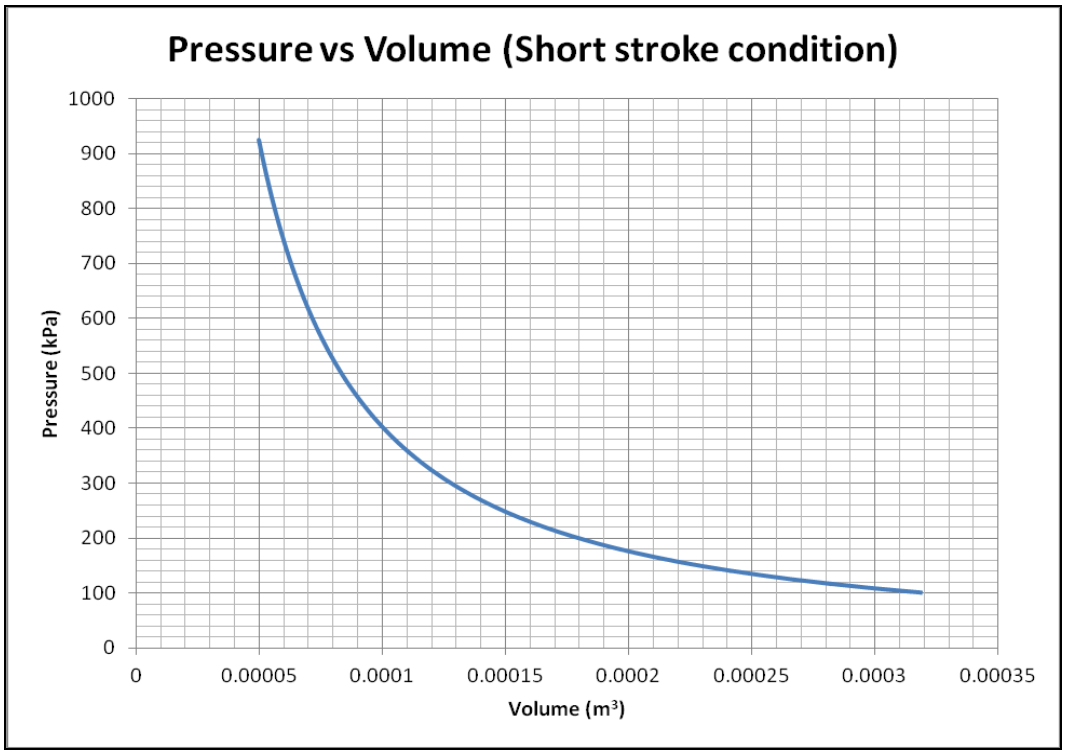

Figure 4.24: Compression (short stroke condition Pressure vs Volume)

A maximum pressure of 9.25 bar (absolute), clearance volume of 4.965×10^{-5} m^3 and swept volume of 31.803×10^{-5} m^3 were noted for the duration of the compression stroke. Two methods of determining the work done was employed, Joel Formulae and calculating the area under the pressure volume diagram.

$$Work\ Done\ (W) = \frac{P_2V_2 - P_1V_1}{n-1}$$

$$W = \frac{1013300 \times 4.965 \times 10^{-5} - 101325 \times 31.803}{1.19 - 1}$$

$$W = 71.832\,Joules$$

(Formulae: Rayner Joel 1996)

The compression stroke occurs during every alternate revolution of the crankshaft.

$$Time\ to\ complete\ one\ revolution\ t_p = \frac{2\pi}{\omega}$$

$$\omega = \frac{2\pi N}{60}$$

$$\therefore t_p = \frac{60}{N}$$

$$t_p = \frac{60}{352}$$

$$t_p = 0.17\ s$$

$$Due\ to\ every\ alternate\ stroke\ \frac{1}{2}t_p$$

$$Actual\ \ t_p = 0.085s$$

$$Power\ \ (P) = \frac{J}{t}$$

$$P = \frac{71.832}{0.085}$$

$$P = 845.1\ Watts$$

The work done was calculated using Joel's formulae and amounted to 71.8 Joules. By measuring the area under the PV diagram the amount of work done indicated 71.8 Joules. Hence the theoretical power calculated amounts to 845.1 W, while using the area measuring method the power indicated was 842.45 W. A difference of less then 1 % is noted.

CHAPTER FIVE

Conclusions

5.1 Design acquaint and shortcomings of the model

The initial concept (sketch on page 4) from Le Roux (2007) suggested an increase in stroke length by 100 %. From the model it was clear that this could be achievable however the connecting rod will need to be long and slender. This is unconventional and poses many problems such as buckling and excessive out of balance forces due to the extra weight of the longer connecting rods, and would have a negative impact on the life span of the engine. In general most combustion engines have a stroke length almost the same as the piston diameter; this is known as the 'squareness' ratio of the engine.

Le Roux (2007) suggested that the piston would return to its original TDC position during the different stroke changes. The model shows that this is not correct and that the piston TDC varies with the change in stroke.

The results from the analysis of the model clearly indicate that to increase the capacity of the internal combustion engine by almost 100% was over ambitious.

5.2 Re-design and prototype results

After the model stage a re-design was found to be necessary. Therefore a prototype engine was built by modifying an existing engine (Intek Briggs and Stratton 10HP engine). By changing the gear train and eccentrics, the excessive horizontal movement of the big end of the connecting rod, which was noted on the model, was greatly reduced. This allowed for a much smaller scale of the stroke change to be achieved.

A maximum change in stroke of approximately 6 mm was achieved by modifying the existing engine. This allowed for an increase of 8 % in stroke change, whilst maintaining most of the original engine "squareness" ratio.

Movement of the piston TDC position was minimised and by manipulating the eccentrics most of the stroke changes were concentrated at the BDC. This was significant as it proved that the engine could maintain a high combustion pressure during the various stroke changes.

After building the prototype the first test on completion was to fire up the engine. This procedure alone had many pit falls and failures, which are discussed below.

Attempt 1:

During the first attempt the key holding the flywheel to the crank shaft sheared. The cause of the failure was due to the shortening of the existing key and keyway. This was necessary to accommodate the gear rack passing between the flywheel and engine casing. The problem was solved by introducing a larger key and keyway and using stronger steel when manufacturing a new key.

Attempt 2:

During the second attempt to fire up, the hollow pin holding the side shaft in the crank lobe sheared (see figure 3.8). The side shaft was also press fitted with a 0.02mm interference fit. This was clearly not enough. The hollow pin was replaced with a solid pin which solved this particular problem.

Attempt 3:

During the third attempt failure occurred when the three M3 cap screws holding the control gear 3 to the eccentric sheared. At this stage the fault that was suspected was that the two counter mass lobes were misaligned. The cap screws were replaced and the counter mass lobes re-aligned.

Attempt 4:

On attempt number four there was some success and the engine managed to run for few seconds. It was noticed that a wobble occurred on the crankshaft ends. This was mainly due to the fact that the crank shaft ends were not supported in double shear. Consequently crank shaft end supports were introduced to keep the shafts steady.

Attempt 5:

After fixing the supports on the crank shaft ends movement on the gear rack was noticed. There was a continuous forward and backward oscillating movement of the gear rack. The rack movement was reduced by introducing grub screws on the sides of the gear rack guide plate.

Attempt 6:

Excessive smoking appeared and a residue of oil was noticed at the exhaust. Upon removing the cylinder head it was found that the top ring was travelling to the upper edge of the engine sleeve. It was then decided to introduce a shortened connecting rod. This concept did not work because after welding up of the connecting rod a slight pull (caused by welding) on the connecting rod caused seizure between the piston and the piston sleeve. It was then decided to use a standard connecting rod and limit the lift by means of controlling the eccentrics. This also meant a reduction in stroke length change.

Attempt 7:

The engine fired-up and ran for approximately 1 hour in both long and short stroke conditions. Catastrophic failure occurred when the three M3 cap screws holding the control gears to the eccentric sheared for the second time. This caused the destruction of the internal gears driving the big end eccentrics. Failure of the cap screws was caused by the continuous cyclic loading caused by the reciprocating motion of the piston assembly and the various speed fluctuations. The restriction of the vibration of the gear rack caused the unbalanced forces to transmit induced loads into the three M3 cap screws holding the control gear.

The gear train was repaired and five M3 screws were introduced. This was the maximum amount of screws that the space allowed. At this stage it was judged that any further attempts to run the engine by itself could lead to failure again. The engine ran for approximately 1 hour, which proved that the concept does work.

5.3 Prototype test results

Conclusive tests could not be performed during the short self run engine operating period (approximately 1 hour). To prevent further failure the engine was then driven by an electric motor, in other words it became an “air compressor”.

The engine capacity for the short stroke position was measured to be 318 cc and for the long stroke 343 cc. An increase of approximately 8% in engine capacity from short stroke to long stroke was noted.

The engine power tested when compressing air for the short stroke was found to be 1334 W and for the long stroke 1714 W. A power difference of approximately 28 % was noted.

It is clear from the results that the proposed type of mechanism for piston stroke adjustment can work and with a marginal increase in engine capacity a significant increase in power can be achieved.

CHAPTER SIX

Recommendations

6.1 It appears that it is possible and certainly feasible to embark on a design for a new engine, based on the concept competently demonstrated in this study.

6.2 The decision on a percentage improvement in capacity for the engine (from short stroke to long stroke) will determine the crankshaft and stroke variance dimensions. With the prototype produced in this work the space was limited and approximately 5 mm difference in stroke could be achieved.

6.3 Based on the above (6.2) one would design and build a housing (engine block) that would suit the crankshaft mechanism. More space should be allowed to build a rigid structure. With our prototype the space for securing the control gears to the eccentrics was limited. This resulted in continuous failure of the cap screws that secured the gears to the eccentrics at the main journals of the crankshaft.

6.4 Improve on the gear rack shifting mechanism by making it more robust. An automated and self locking mechanism can be introduced. On the prototype the use of grub screws to hold the rack firmly into position during normal engine operating conditions hampered the ability to change the stroke positions whilst the engine was running.

6.5 Introduce a variable ignition timing system. With the adjustment of the stroke length on the prototype the magneto shifted away from the pick-up. If designing for greater stroke changes the magneto and pick-up would shift away too far to transmit a proper signal.

6.6 With the adjustment of the stroke the crankshaft output shaft shifts respectively. A mechanism needs to be designed to centralise the output shaft.

6.7 Upon completion of the various modifications detailed above fuel consumption and load tests should obviously be carried out.

REFERENCES

Abenavoli, R.I., Naso, V., Rychter, T., Teodorzyk, A. 1990. *First experimental analysis of an internal combustion engine with variable stroke and compression ratio.* Proceedings of the 25th Intersociety Energy Conversion Engineering Conference. Pages 198-203, 12-17 Aug 1990.

Cengel, Y. A. & Boles, M. A. 1989. *Thermodynamics an Engineering Approach.* McGraw-Hill International Editions. 1st Edition

Crise G.W., Variable Displacement Internal Combustion Engine Having Automatic Piston Stroke Control, UNITED STATE PATENT, Patent Number 4,131,094, 1978.

Drotsky, J.G. 1994. *Strengths of Materials for Technicians.* Heinemann. 2nd Edition.

Gonzalez L.M., Variable Stroke Mechanism for Internal Combustion Engine, UNITED STATES PATENT, Patent Number 5,927,236, 1999.

Hannah, J. & Stephens, R.C. 1970. *Mechanics of Machines.* Great Britain: Edward Arnold. 3rd Edition.

Joel, R. 1996. *Basic Engineering Thermodynamics.* England: Longman. 5th Edition.

Litman, T. 2005. *Efficient vehicles versus efficient transportation. Comparing transportation energy conservation strategies.* Transport Policy, Volume 12, Issue 2, March 2005, Pages 121-129

Morley, A and Hughes, E 1994. *Principles of electricity.* England Longman. 5 th Edition

Nelson C.D., Variable Stroke Engine, UNITED STATES PATENT, Patent Number 4,517,931, 1985.

Ozcan H and Yamin J A.A., Performance and Emission Characteristics of LPG Powered Four Stroke SI engine under Variable Stroke Length and Compression Ratio, Energy Conversion and Management, Volume 49, Issue 5, May 2008, Pages 1193-1201

Pulkrabeck, W.W. 2004. *Engineering Fundamentals of the Internal Combustion Engine.* U.S.A, New Jersey: Pearson Prentice-Hall. 2nd Edition.

Romm, J. 2005. *The car and fuel of the future.* Energy Policy, Volume 34, Issue 17, November 2006, Pages 2609-2614

Ross, D. K. 2006. *Hydrogen storage: The major technological barrier to the development of hydrogen fuel cell cars.* The World Energy Crisis, Volume 80, Issue 10, August 2006, Pages 1084-1089

SAE, nd. *Mercedes-Benz launches cylinder cutout.* www.sae.org/automag/newenginereview/mercedes.htm, April 2010

Schecter MM, Simko AO and Levin MB, *Variable Displacement and Compression Ratio Piston Engine*, UNITED STATES PATENT, Patent Number 5,136,987, 1992.

South Africa. Department of Transport. No Date. *Moving South Africa:* http://www.transport.gov.za/projects/msa/msareport/msadraft82.html. 11 October 2007.

Stone, R. and Ball, J.K. 2004. *Automotive Engineering fundamentals.* Pennsylvania, USA: SAE International. 1st Edition.

Turrentine, T.S. and Kurani, K.S. 2007. *Car buyers and fuel economy.* Energy Policy, Volume 35, Issue 2, February 2007, Pages 1213-1223

Tobolt, W.K., Johnson, L. and Olive, S.W. 1989. *Automotive Encyclopedia.* Illinois: Goodheart-Willcox. 8th Edition.

van Basshuysen, R. & Schafer, F. 2006. *Modern Engine Technology from A to Z.* Pennsylvania, USA: SAE International. 1st Edition.

Yamin, J.A.A. & Dado, M.H. 2004. *Performance simulation of a four-stroke engine with variable stroke-length and compression ratio.* Applied Energy, Volume 77, Issue 4, April 2004, Pages 447-463

APPENDIX A:

Alternative Solutions

BRIEF DESCRIPTION OF EACH POSSIBLE SOLUTION:

Engine Housing:

Option one:

Design new engine housing.

Option two:

Modify an original engine housing to accommodate the new crankshaft configuration.

The existing Briggs and Stratton 10hp internal combustion engine was modified to construct the prototype.

Since the new crankshaft configuration will be wider than the original crankshaft the width of the engine housing will have to be increased.

The one side of the engine housing can be removed by unscrewing the bolts, and the other side forms part of the engine housing. To increase the width of the engine housing the fixed side has to be removed and by adding a spacer with gaskets, in a shape corresponding to the housing, to either side and replacing both ends a greater width can be achieved.

Mechanism to Rotate Both Eccentrics at Mains:

Option 1:

Rotating the eccentrics manually by making use of a slider mechanism similar to the principle used to which a vice clamp works.

By having a screw thread with a handle connected to both the racks that are fitted into slots on the base plate on which the engine will be mounted, the racks can be adjusted by turning the screw thread.

Option 2:

It can also be rotated by an electrical device.

Valve Timing:

Since the crankshaft is going to move radially up and down causing the position of the piston to vary according to this, the valve timing also needs to be adjusted. If this is neglected, the valves and other components of the engine will be damaged.

Option 1:

Using a chain and sprockets arrangement to open and close the valves. A restrainer/idler might be needed to keep the chain tensioned.

Option 2:

A gear situated on the camshaft will be in mesh with a gear on the crankshaft. Since the crankshaft can rotate radially up and down, the camshaft will also have to follow this principle. To achieve this, the camshaft will also have to be fitted within eccentrics.

CONCEPTUAL DESIGNS:

Engine Housing:

Option one:

Design a new engine housing. This option will be very time consuming and costly. Since this project is only for experimental use, it will not be wise to use this option.

Option two:

Modifying an existing engine housing will be more feasible and will be less time consuming than option one.

Mechanism to Rotate Both Eccentrics at Mains:

Option 1:

The slider mechanism is a simple way of achieving the need to rotate the eccentrics. Since this is only for experimental purposes, it will be more feasible than to use electrical devices.

Option 2:

Electrical devices might be more expensive and more complicated to incorporate into this design. For this reasons this option will not be used.

Valve Timing:

Option 1:

A chain and sprockets arrangement might not be the best option to use since chains have play which might lead to the valve timing going out of phase.

Option 2:

The gears will be in constant mesh and will ensure that the valve timing stays correct.

From investigating the setup mentioned in ‘Option 2’, it was found that it will not work, since the camshaft will not be in the correct position relative to the cam-followers.

Thus, option 1 will have to be used.

The aim of the project is to convert an original Briggs and Stratton 10 hp internal combustion engine into a variable stroke internal combustion engine for experimental purposes.

The conversion includes the following that needs to be done:

- New crankshaft configuration
- Crankshaft to be able to move radially about an off-set from the center of eccentrics at mains

- Modify engine housing to accommodate new crankshaft configuration, since it will be wider than the original one.
- Adjusting camshaft position to be able to provide changes made to the position of the piston, caused by the radial movement of the crankshaft and new position of the eccentric at the big-end of the connecting rod.

The starting point of the design was to measure the length of the original crankshaft. Taking the cylinder's centerline as the reference line, measurements were taken from this line to the outer surfaces of the crank lobes to determine the difference in length between the original crankshaft and new crankshaft. Also, on one side of the original crankshaft's crank lobe a gear is situated. Its thickness was also taken into account.

From the information gathered the increase in the width to either side from the cylinder's centerline was determined.

The engine housing was measured to determine the positions of the crankshaft, camshaft and holes through which the end caps will be fixed to the modified engine housing. Also, the inner profile of the engine housing was measured so that this shape can be cut into the end caps.

From all the information obtained the end caps could be designed.

By inspecting the modifications done so far concluded that the drive to be used for the valve timing needs to be fitted on the outside of the engine housing, since there is no available space inside. From this, it was clear that the camshaft must be extended.

The mechanism to turn the eccentrics at mains needed to be designed next. A gear will be fitted onto the outer surface of both eccentrics at mains which will be in mesh with a rack-spur that forms part of the mechanism. When the mechanism is moved linearly it will turn the eccentric at mains.

SOLID MODELS:

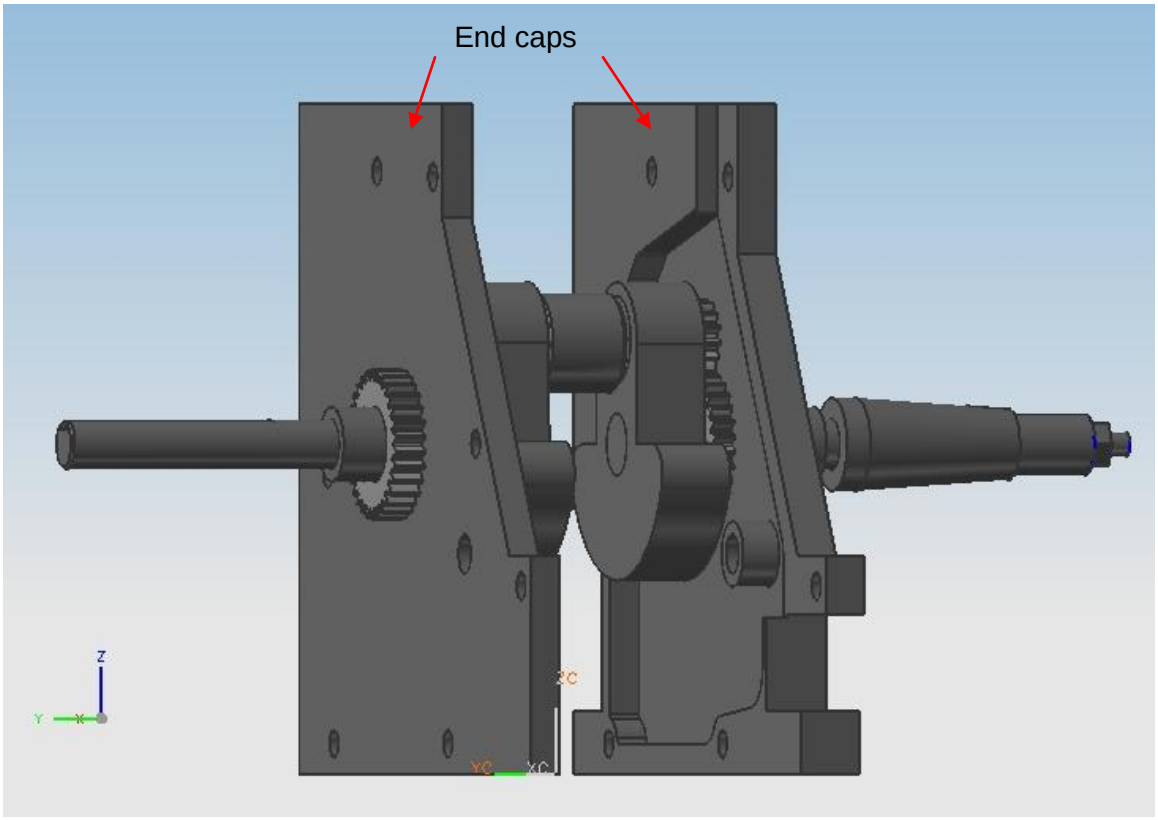

Figure A1: Rear view of component assembly

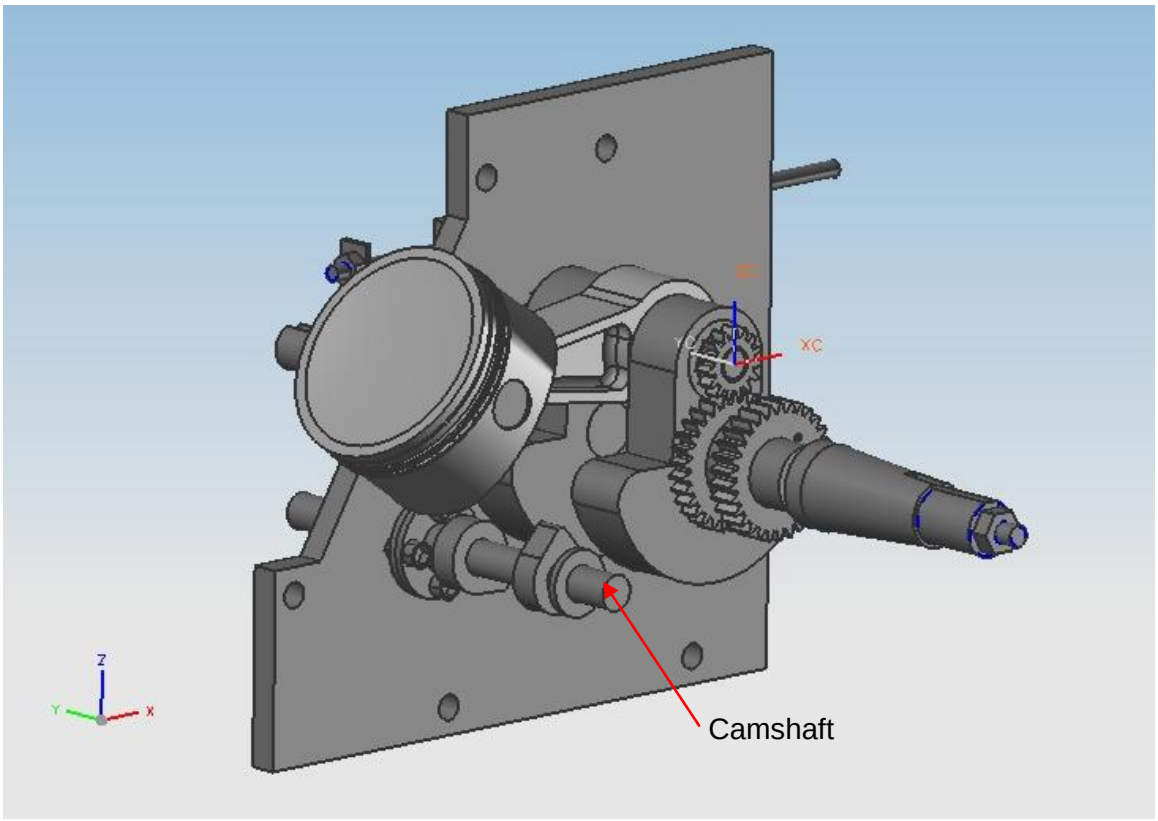

Figure A2: Partial view of assembled components

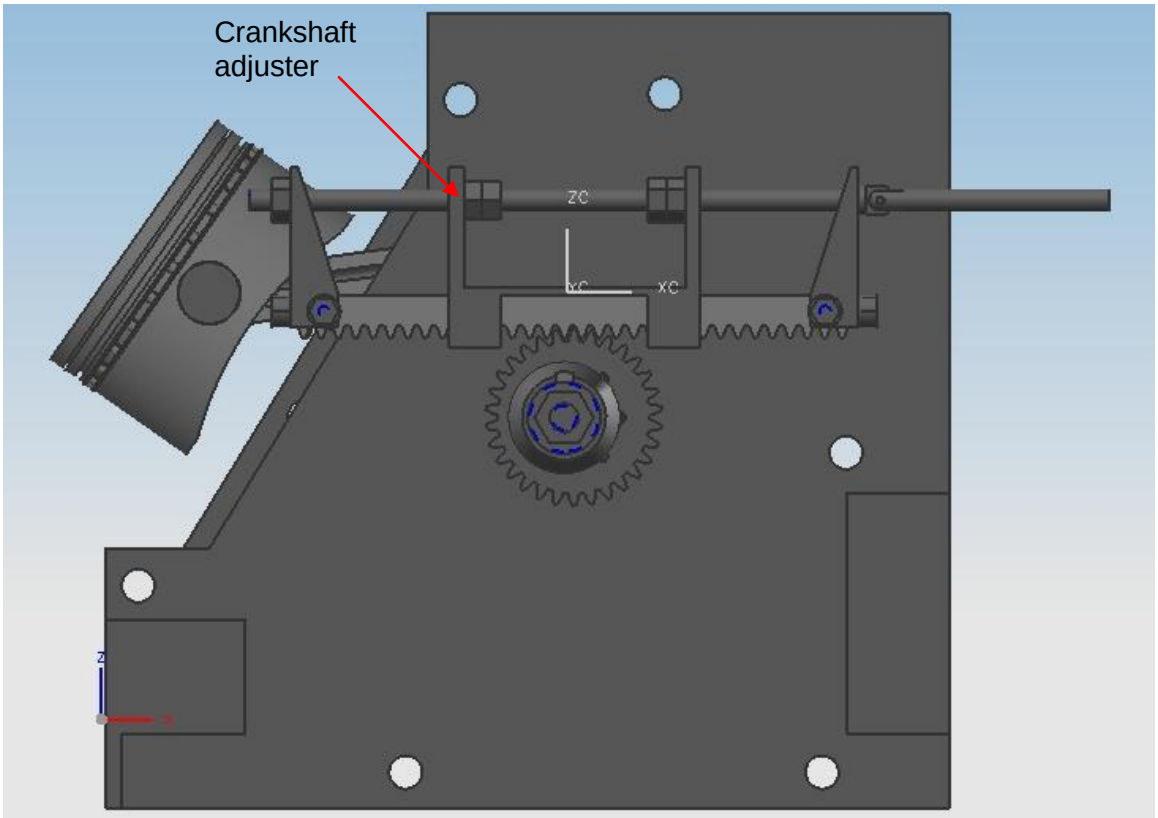

Figure A3: Side view of component assembly

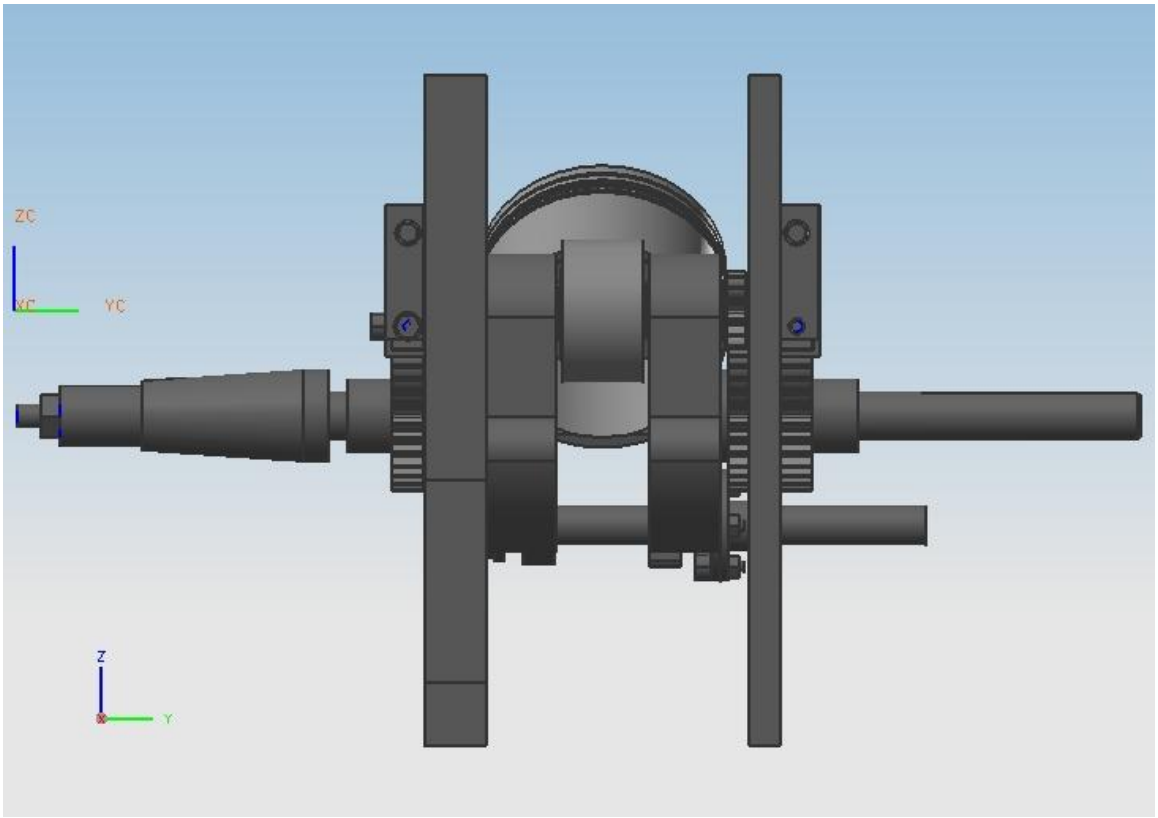

Figure A4: Front view of component assembly

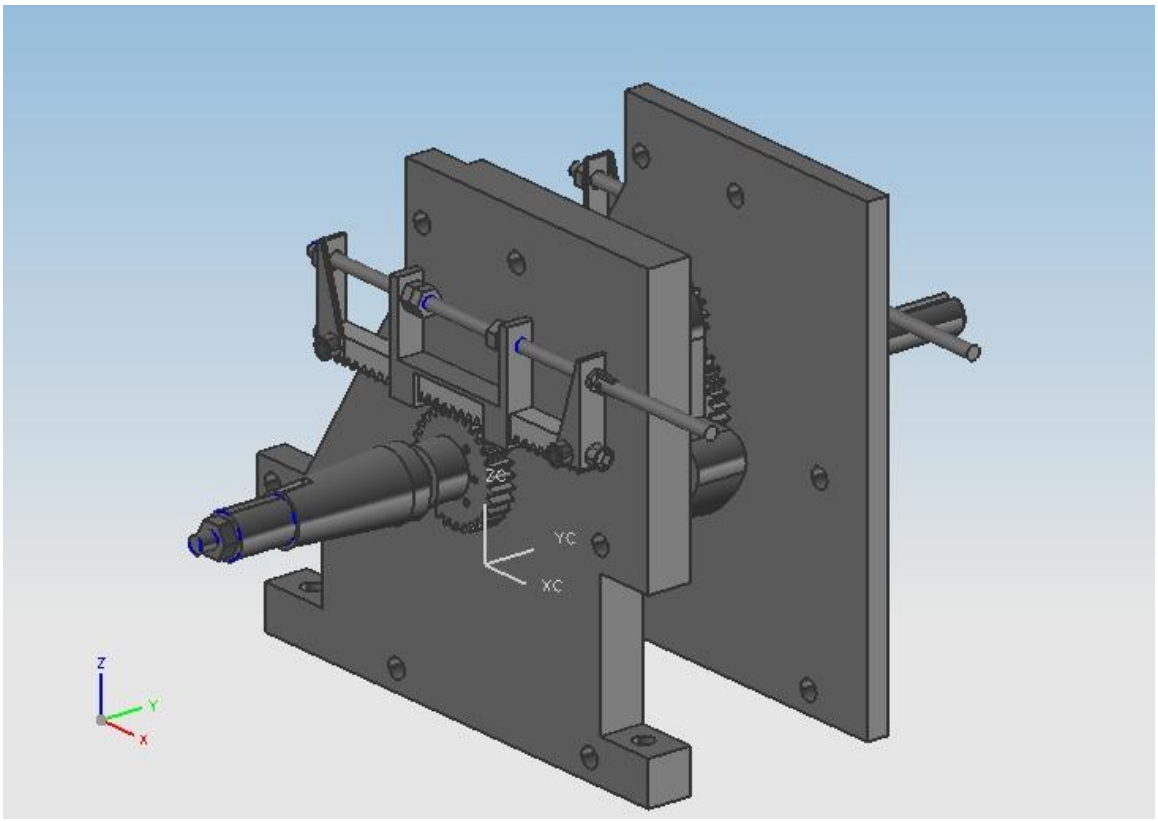

Figure A5: Isometric view of assembled components

APPENDIX B:

Power harmonic analyser data

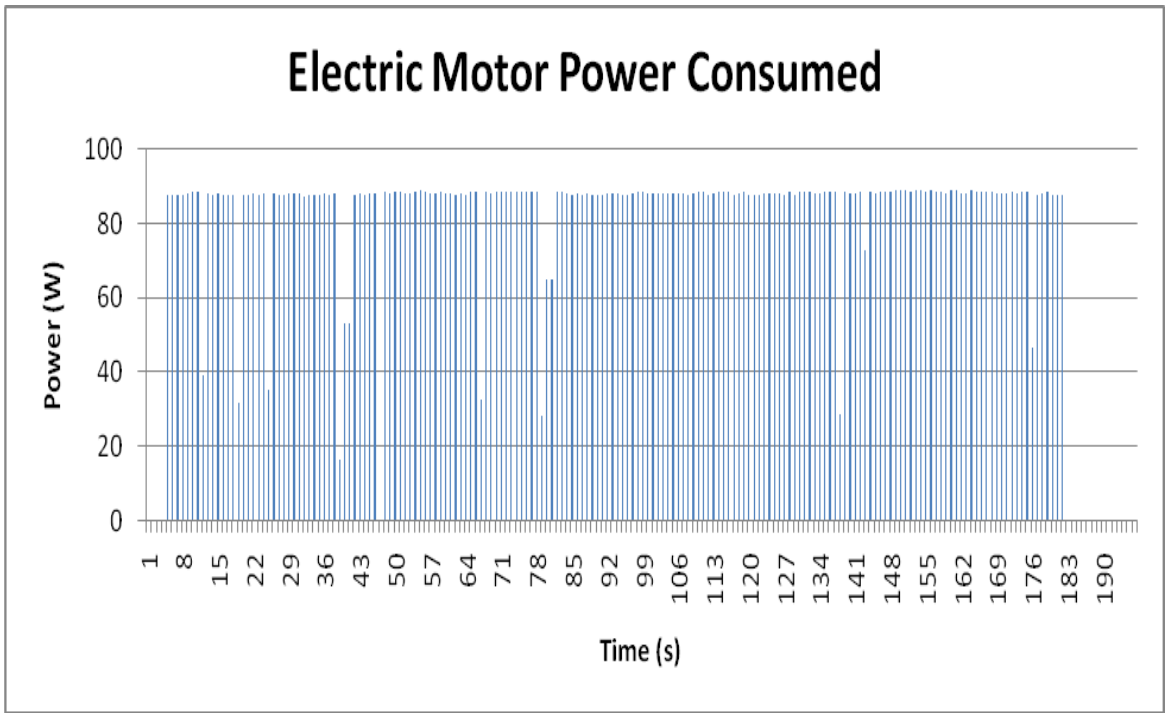

Figure B1: Extract power consumption test for electric motor only

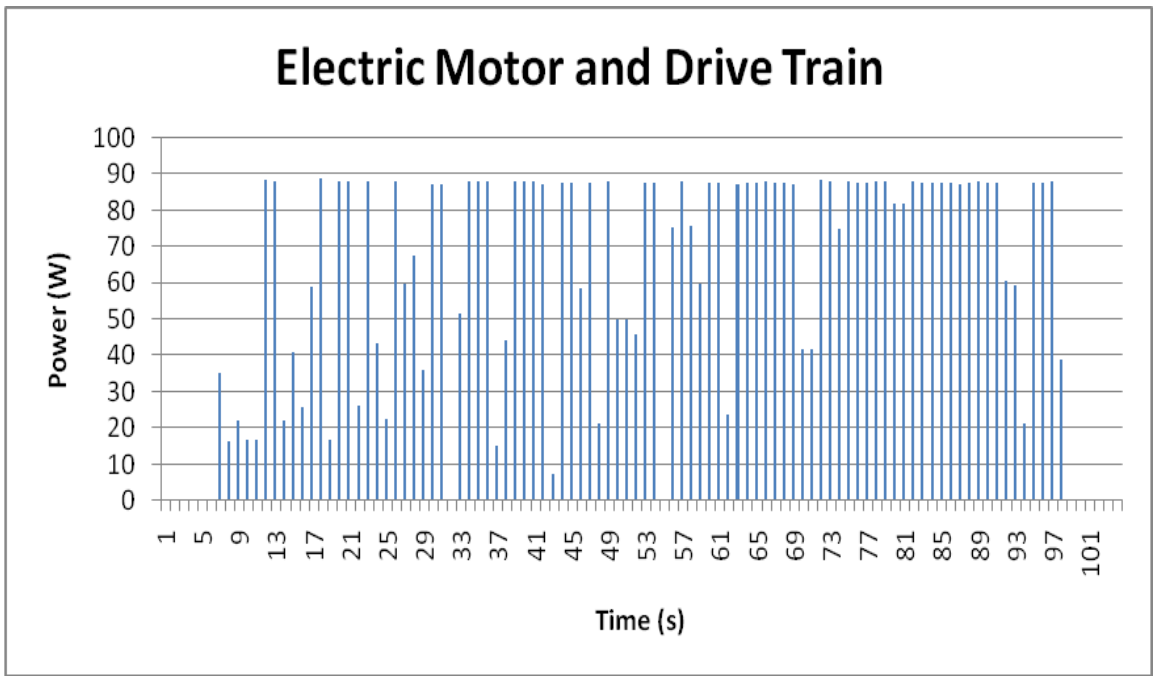

Figure B2: Extract power consumption test for electric motor and drive train

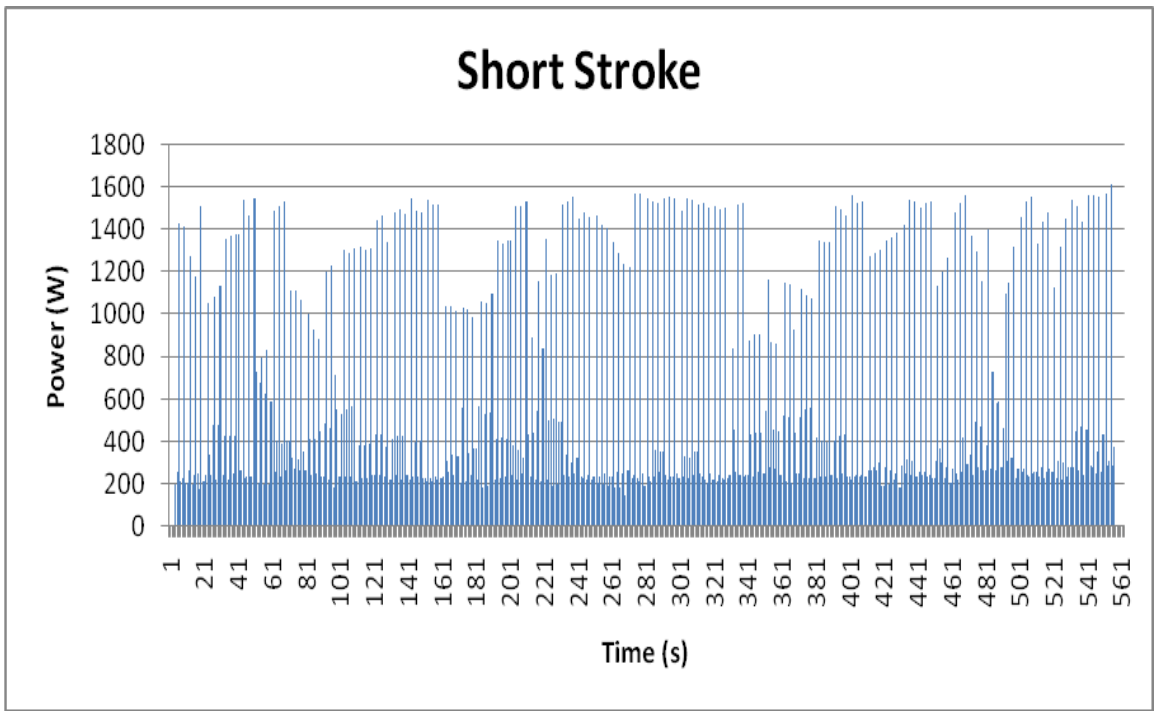

Figure B3: Extract power consumption test for short stroke

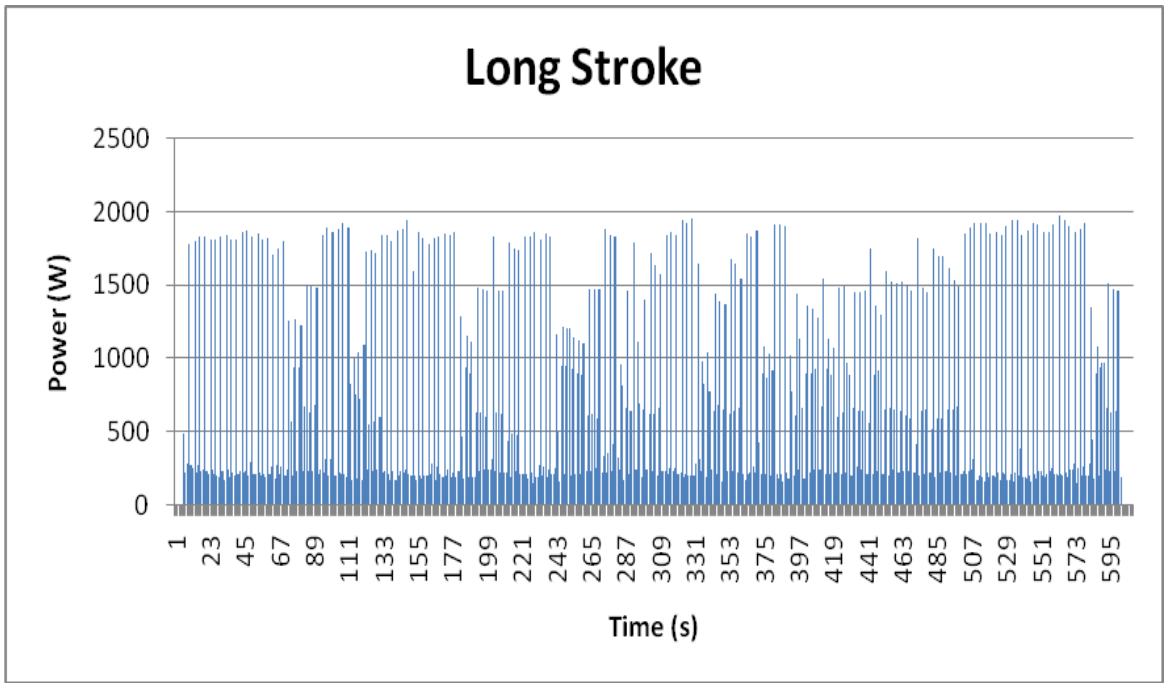

Figure B4: Extract power consumption test for long stroke

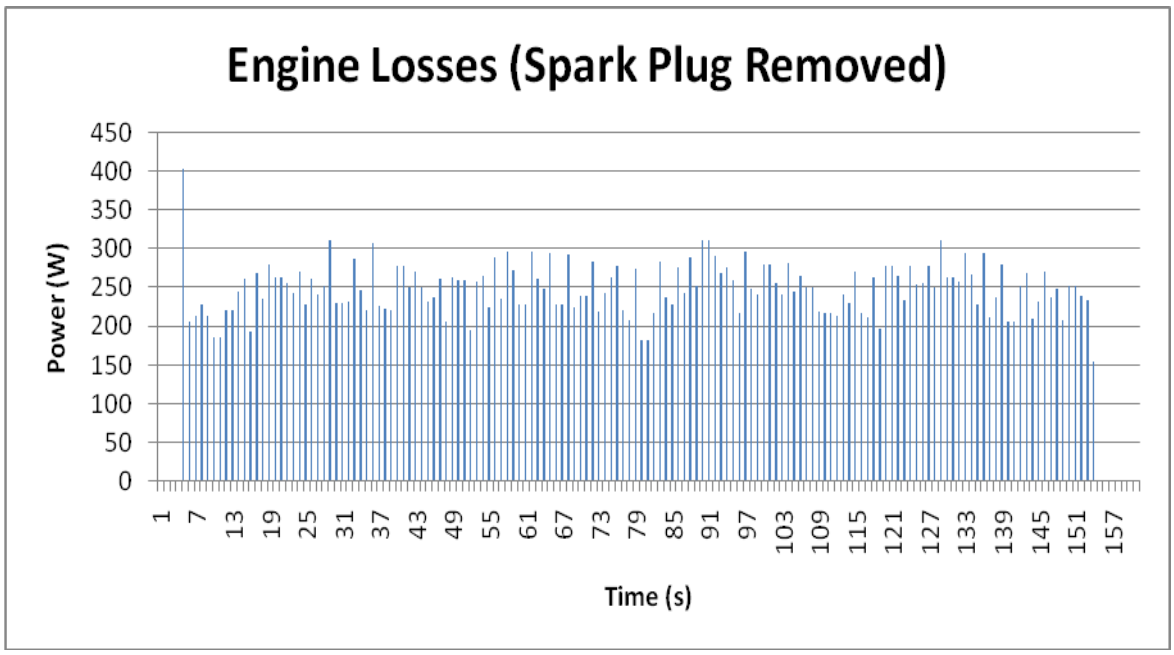

Figure B5: Extract power consumption test for engine with spark plug removed

APPENDIX C:

Pressure Readings

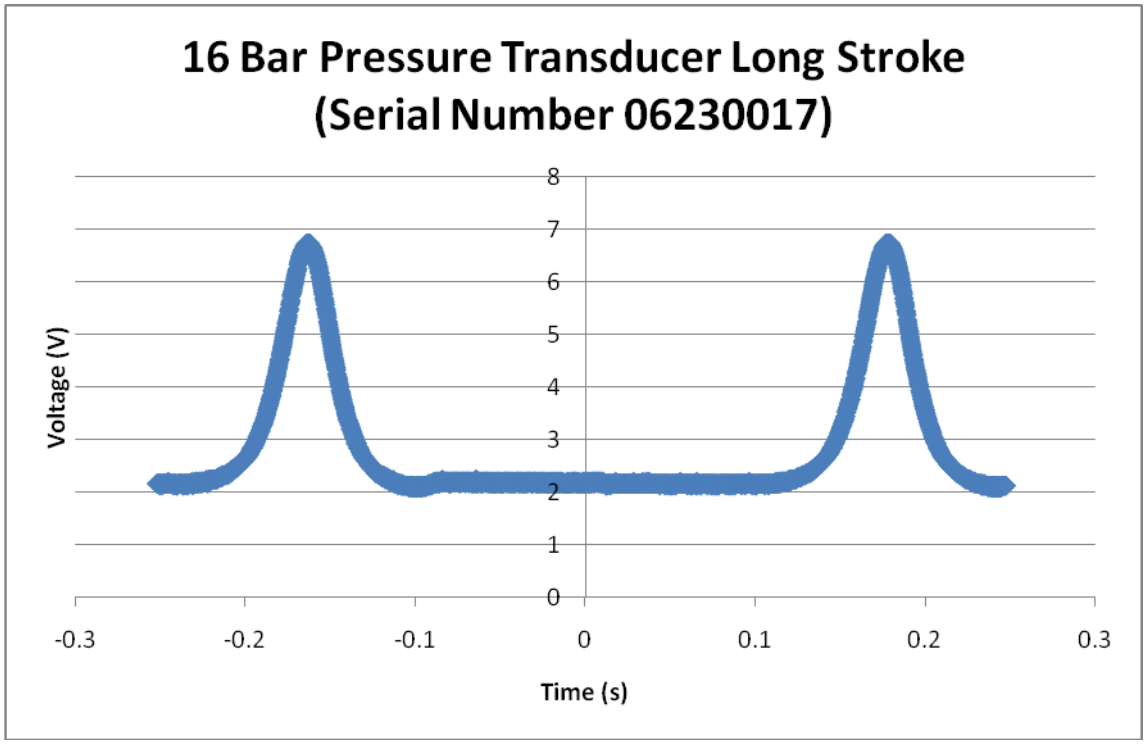

Figure C1: Extract pressure transducer test with serial number 06230017

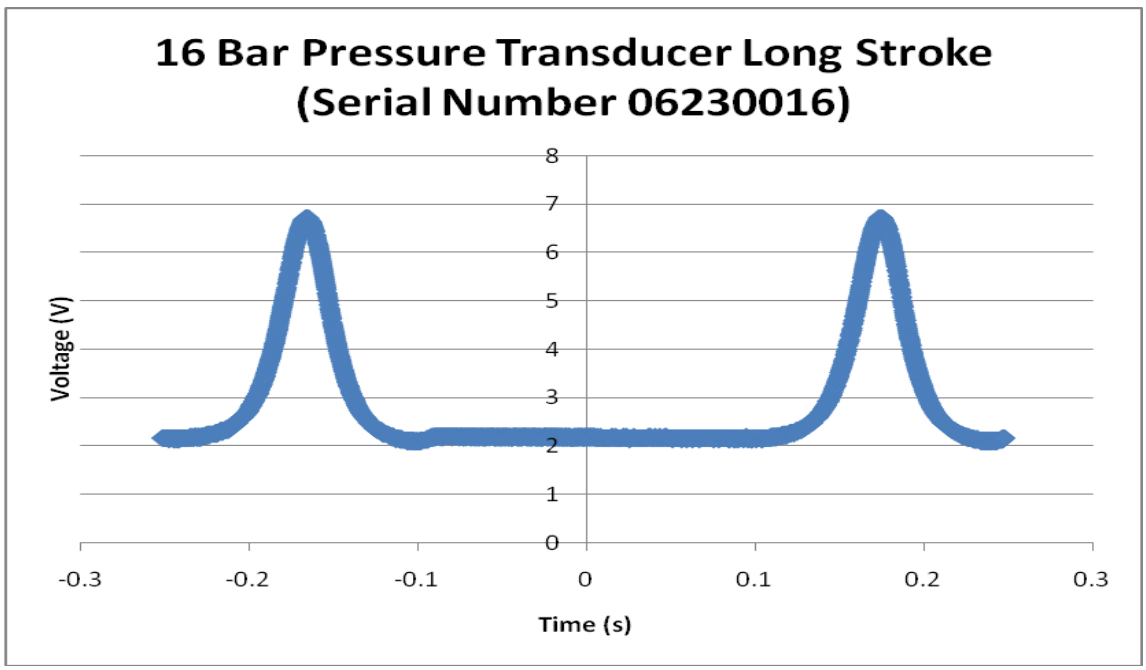

Figure C2: Extract pressure transducer test with serial number 06230016

APPENDIX D:

Temperature data

Book5.xlsx.Long Stroke.1.xlsx

	A	B	C
1	Time	Channel 1	Ambient
2	Seconds	°C	°C
3			
4			
5			
6	0	27.5	19.43
7	1	27.57	19.32
8	2	27.53	19.47
9	3	27.47	19.55
10	4	61.03	19.67
11	5	124.55	19.38
12	6	148.74	19.67
13	7	157.43	19.51
14	8	164.32	19.65
15	9	166.56	19.45
16	10	168.77	19.25
17	11	170.14	19.67
18	12	171.35	19.6
19	13	170.3	19.32
20	14	171.12	19.31
21	15	170.74	19.25
22	16	171.39	19.6

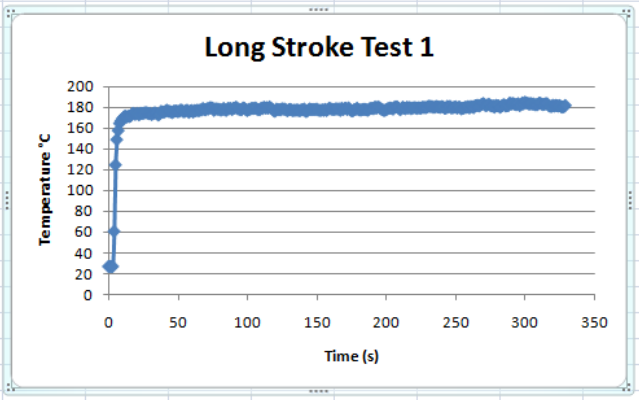

Figure D1: Extract of long stroke temperature test 1

Book6.xlsx.Long Stroke.2.xlsx

	A	B	C
1	Time	Channel 1	Ambient
2	Seconds	°C	°C
3			
4			
5			
6			
7	0	30.82	19.32
8	1	30.83	19.26
9	2	30.72	19.18
10	3	30.72	19.23
11	4	41.24	19.65
12	5	101.6	28.75
13	6	125.97	19.4
14	7	135.13	19.3
15	8	154.55	19.15
16	9	163.98	19.33
17	10	169.36	19.28
18	11	170.17	19.47
19	12	172.07	19.5
20	13	173.48	19.17
21	14	172.38	19.58

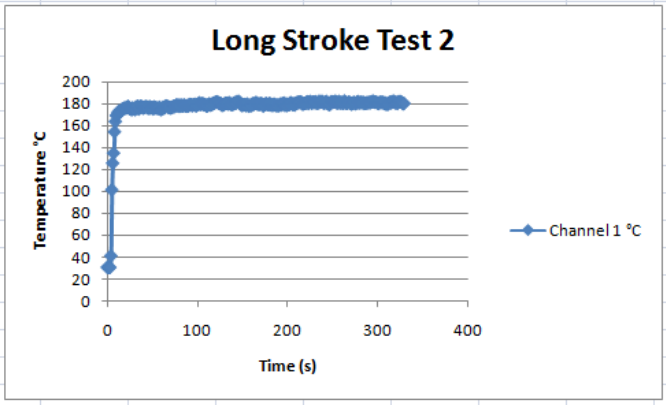

Figure D2: Extract of long stroke temperature test 2

Book7.xlsx. Long stroke.3.xlsx

	A	B	C
1	Time	Channel 1	Ambient
2	Seconds	°C	°C
3			
4			
5			
6	0	30.84	18.64
7	1	30.68	18.98
8	2	30.64	18.94
9	3	30.67	18.73
10	4	30.55	18.94
11	5	30.57	18.93
12	6	30.53	18.91
13	7	30.49	18.92
14	8	30.46	18.83
15	9	30.42	18.69
16	10	30.34	18.8
17	11	30.32	18.57
18	12	30.28	18.69
19	13	30.2	18.75
20	14	59.32	18.58
21	15	115.95	18.58
22	16	145.95	18.53

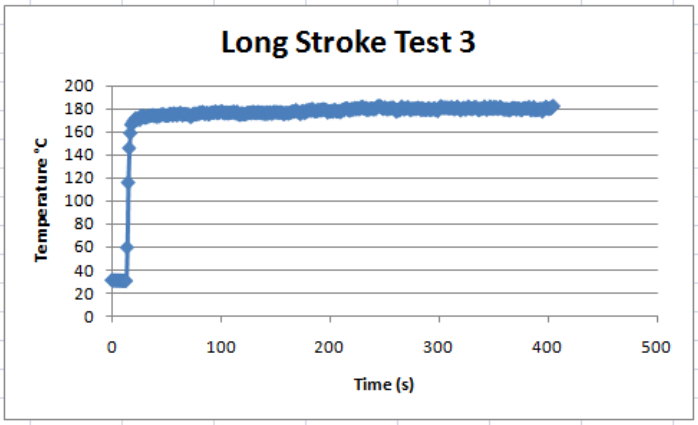

Figure D3: Extract of long stroke temperature test 3

Book3.xlsx.Short stroke.1.xlsx

	A	B	C
1	Time	Channel 1	Ambient
2	Seconds	°C	°C
3			
4			
5			
6	0	21.43	20.62
7	1	21.38	20.48
8	2	21.47	20.2
9	3	21.48	20.27
10	4	21.45	20.02
11	5	21.41	19.93
12	6	21.35	20.44
13	7	21.4	20.24
14	8	65.83	38.81
15	9	105.04	20.09
16	10	102.99	20.09
17	11	127.9	20.01
18	12	139.97	20.31
19	13	145.89	20.06
20	14	150.86	19.9
21	15	152.89	19.99
22	16	152.38	19.99

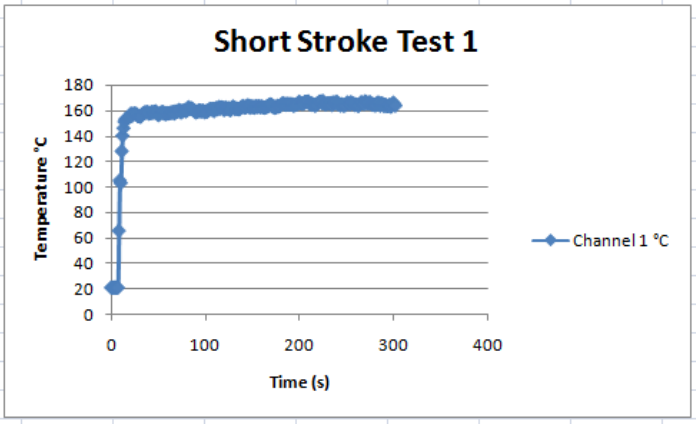

Figure D4: Extract of short stroke temperature test 1

Book4.xlsx. Short stroke.2.xlsx

	A	B	C
1	Time	Channel 1	Ambient
2	Seconds	°C	°C
3			
4			
5			
6			
7	0	26.92	19.66
8	1	26.79	19.84
9	2	26.74	19.79
10	3	26.78	19.83
11	4	26.75	19.65
12	5	28.83	19.65
13	6	44.14	19.66
14	7	107.32	19.64
15	8	137.04	19.57
16	9	145.82	19.56
17	10	151.73	19.55
18	11	154.54	19.52
19	12	157.39	19.48
20	13	158.33	19.6
21	14	157.59	19.59
22	15	159.11	19.59
23	16	160.12	19.47
24	17	160.48	19.58

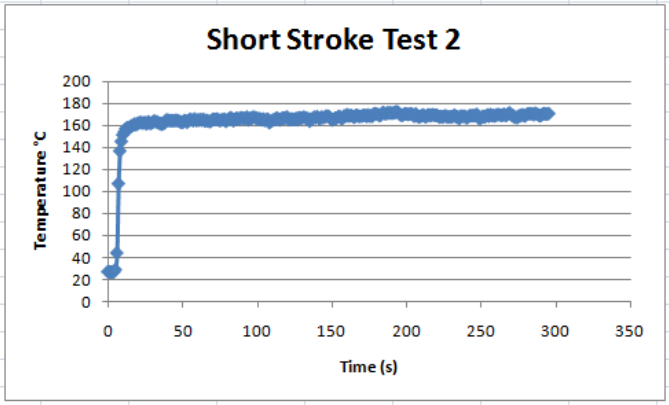

Figure D5: Extract of short stroke temperature test 2

Book1.xlsx. Short Stroke .3.xlsx

	A	B	C
1	Time	Channel 1	Ambient
2	Seconds	°C	°C
3			
4			
5			
6	0	40.68	23.1
7	1	40.42	23.22
8	2	40.28	23.34
9	3	40.22	23.17
10	4	40.02	25.4
11	5	73.3	23.72
12	6	123.14	23.6
13	7	136.55	23.17
14	8	148.38	23.13
15	9	155.28	23.15
16	10	157.73	23.24
17	11	160.83	23.39
18	12	162.85	23.53
19	13	163.71	23.82
20	14	164.87	23.68
21	15	165.29	23.61
22	16	166.12	23.43
23	17	166.45	23.36
24	18	167.48	23.21

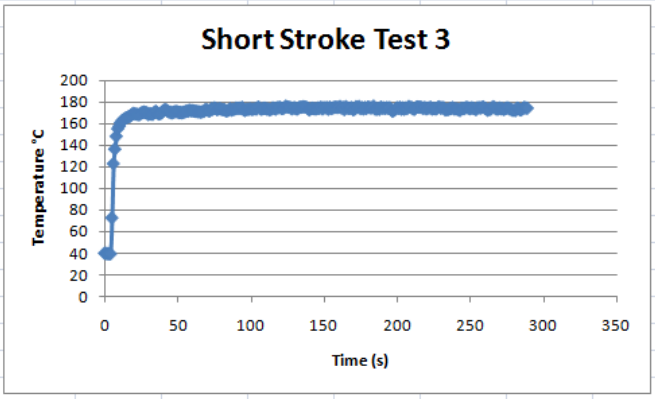

Figure D6: Extract of short stroke temperature test 3